

'Strongly correlated QCD' part of lecture course 'QCD' winter term 2017/2018

Jan M. Pawłowski¹ and Tilman Plehn¹

¹*Institut für Theoretische Physik, Universität Heidelberg*

These lecture notes are the ambitious attempt to combine the two QCDs of the two lecturers into one coherent document. It includes many aspects of perturbative and non-perturbative QCD, including the basic theoretical concepts we need to compute observables at hadron colliders.

CONTENTS

I. Basics	3
A. Yang-Mills theory	3
B. QCD	6
II. Strong chiral symmetry breaking	8
A. Spontaneous symmetry breaking and the Goldstone theorem	9
B. Spontaneous symmetry breaking, quantum fluctuations and masses*	10
C. Little reminder on the Higgs mechanism	13
D. Low energy effective theories of QCD	14
E. Strong chiral symmetry breaking and quark-hadron effective theories	17
F. Low energy quantum fluctuations	22
1. Quark quantum fluctuations	22
2. Mesonic quantum fluctuations	25
3. RG equation for the effective potential *	27
4. EFT couplings	28
III. Chiral phase transition	31
A. Mesons at finite temperature	31
B. Quarks at finite temperature	34
C. RG for the effective potential at finite temperature*	35
IV. Confinement	37
A. Order parameters for confinement	37
B. Confinement-deconfinement phase transition at finite temperature	41
1. Polyakov loop	41
2. Polyakov loop potential	44
V. Phase structure of QCD	54
1. Glue Sector	54
2. Matter sector	56
A. RG for the phase structure*	57
A. Feynman rules for QCD in the covariant gauge	59
B. Gribov copies	59
C. Some important fact of the background field approach	60
References	60

I. BASICS

The theory of strong interactions, quantum chromodynamics (QCD), has been developed on the basis of scattering experiments that showed an internal $SU(3)$ -symmetry and related charges much the same way quantum-electrodynamics (QED) shows the $U(1)$ -symmetry related to the electric charge. The corresponding gauge theory, $SU(3)$ Yang-Mills theory, is non-Abelian and hence self-interacting, i.e. the (quantized) pure gauge theory is already non-trivial, in contrast to the $U(1)$ -based QED.

A. Yang-Mills theory

We start by constructing the pure gauge part or Yang-Mills part of QCD as an $SU(3)$ gauge theory, fixing our conventions and repeating the main features known from the QFT II lecture. The weak $SU(2)$ -theory turns out to have the same qualitative features as QCD (asymptotic freedom and confinement), but is technically simpler. On the other hand, the $SU(2)$ gauge bosons in the Standard Model are massive, leading to a major modification of this theory. Instead, we will assume massless gauge bosons throughout this lecture. As for QED, the classical action of QCD can be derived from the gauge-invariant (minimal) extension of the action of a free spin-one particle. The requirement of invariance of physics under local $SU(N_c)$ or color rotations with $\mathcal{U} \in SU(N_c)$, combined with a minimal coupling, leads us from partial to covariant derivatives,

$$\partial_\mu \rightarrow D_\mu(A) = \partial_\mu - i g A_\mu. \quad (\text{I.1})$$

The gauge field A_μ in the adjoint representation is Lie-algebra-valued,

$$A_\mu = A_\mu^a t^a, \quad \text{with} \quad a = 1, \dots, N_c^2 - 1. \quad (\text{I.2})$$

The matrices t^a are the generators of $SU(N_c)$. In physical QCD the gauge group has eight generators, $a = 1, \dots, 8$, the Gell-Mann matrices. They are defined through

$$[t^a, t^b] = i f^{abc} t^c, \quad \text{tr}_f(t^a t^b) = \frac{1}{2} \delta^{ab}, \quad (\text{I.3})$$

where the coefficients f^{abc} are the structure constants of the Lie algebra. and tr_f is the trace in the fundamental representation. The covariant derivative (I.1) does not carry any indices. In the adjoint representation it links to $SU(N_c)$ indices and reads

$$D_\mu^{ab}(A) = \partial_\mu \delta^{ab} - g f^{abc} A_\mu^c. \quad \text{with} \quad (t_{\text{ad}}^c)^{ab} = -i f^{abc}. \quad (\text{I.4})$$

The covariant derivative D_μ with its two color indices then has to transform as a tensor under gauge transformations,

$$D_\mu(A) \rightarrow D_\mu(A^\mathcal{U}) = \mathcal{U} D_\mu \mathcal{U}^\dagger, \quad \text{with} \quad \mathcal{U} = e^{i\omega} \in SU(N_c), \quad (\text{I.5})$$

where $\omega \in su(N_c)$ is the corresponding Lie algebra element. The covariance of D under gauge transformations in (I.5) implies

$$A_\mu \rightarrow A_\mu^\mathcal{U} = \frac{i}{g} \mathcal{U} (D_\mu \mathcal{U}^\dagger) = \mathcal{U} A_\mu \mathcal{U}^\dagger + \frac{i}{g} \mathcal{U} (\partial_\mu \mathcal{U}^\dagger). \quad (\text{I.6})$$

From the first term we confirm that in a non-Abelian gauge theory the gauge boson A_μ carries the corresponding color charge. There are various notations on the market leading to factors i and $-$ in the Lie algebra relations above. In the present lecture notes we have chosen hermitian generators which leads to the factor $+1/2$ for the trace in (I.3). It also entails real structure constants f^{abc} in the Lie-algebra in (I.3).

In analogy to QED the field strength tensor is defined through the commutator of covariant derivatives, it is the curvature tensor of the gauge theory. Based on the definitions in (I.1) and (I.3) we find

$$F_{\mu\nu} = \frac{i}{g} [D_\mu, D_\nu] = F_{\mu\nu}^a t^a \quad \text{with} \quad F_{\mu\nu}^a = \partial_\mu A_\nu^a - \partial_\nu A_\mu^a + g f^{abc} A_\mu^b A_\nu^c. \quad (\text{I.7})$$

Defined as in (I.7) the field strength $F_{\mu\nu}$ also transforms covariantly (as a tensor) under gauge transformations,

$$\begin{aligned} F_{\mu\nu}(A^{\mathcal{U}}) &= \frac{i}{g} [D_{\mu}(A^{\mathcal{U}}), D_{\nu}(A^{\mathcal{U}})] \\ &= \frac{i}{g} \mathcal{U} [D_{\mu}(A_{\mu}), D_{\nu}(A_{\nu})] \mathcal{U}^{\dagger} = \mathcal{U} F_{\mu\nu}(A) \mathcal{U}^{\dagger} . \end{aligned} \quad (\text{I.8})$$

This allows us to define a gauge-invariant Yang-Mills (YM) action,

$$S_{\text{YM}}[A] = \frac{1}{2} \int_x \text{tr}_{\mathfrak{f}} (F_{\mu\nu} F_{\mu\nu}) = \frac{1}{4} \int_x F_{\mu\nu}^a F_{\mu\nu}^a , \quad (\text{I.9})$$

with $\int_x = \int d^d x$. Its gauge invariance follows from (I.8),

$$S_{\text{YM}}[A^{\mathcal{U}}] = \frac{1}{2} \int_x \text{tr}_{\mathfrak{f}} (\mathcal{U} F_{\mu\nu}(A) F_{\mu\nu}(A) \mathcal{U}^{\dagger}) = S_{\text{YM}}[A] , \quad (\text{I.10})$$

where the last equality holds due to cyclicity of the trace in color space. Clearly, the action (I.9) with the field strength (I.7) is a self-interacting theory with coupling constant g . It has a quadratic kinetic term and three-gluon and four-gluon vertices. This is illustrated diagrammatically as

$$S_{\text{YM}}[A] \propto \text{wavy line}^{-1} + \text{three-gluon vertex} + \text{four-gluon vertex}$$

This allows us to read off the Feynman rules for the purely gluonic vertices. The full Feynman rules of QCD in the general covariant gauge are summarized in Fig. 21 in Appendix A. As in QED we can identify color-electric and color-magnetic fields as the components in the field strength tensor,

$$\begin{aligned} E_i^a &= F_{0i}^a \\ B_i^a &= \frac{1}{2} \epsilon_{ijk} F_{jk}^a . \end{aligned} \quad (\text{I.11})$$

In contrast to QED these color-electric and magnetic fields are no observables, they change under gauge transformations. Only $\text{tr} \vec{E}^2$, $\text{tr} \vec{B}^2$ are observables.

A Yang-Mills theory can most easily be quantized through the path integral. Naively, the generating functional of pure YM-theory would read

$$Z[J] = \int dA \exp \left(-S_{\text{YM}}[A] + \int_x J_{\mu}^a A_{\mu}^a \right) . \quad (\text{I.12})$$

The fundamental problem is that it contains redundant integrations due to gauge invariance of the action, see (I.10). These redundant integrations are usually removed by introducing a gauge fixing condition

$$\mathcal{F}[A_{\text{gf}}] = 0 \quad (\text{I.13})$$

Commonly used gauge fixings are

$$\begin{aligned} \partial_{\mu} A_{\mu} &= 0 , & \text{covariant or Lorenz gauge ,} \\ \partial_i A_i &= 0 , & \text{Coulomb gauge ,} \\ n_{\mu} A_{\mu} &= 0 , & \text{axial gauge .} \end{aligned} \quad (\text{I.14})$$

The general covariant gauge has the technical advantage that it does not single out a space-time direction. This property reduces the possible tensor structure of correlation functions and hence simplifies computations. The Coulomb gauge and the axial gauge single out specific frames. At finite temperature (and density) this might be useful as the temperature singles out the thermal rest frame. In that case the Coulomb gauge and the temporal or Weyl gauge

$(n_\mu = \delta_{\mu 0})$ are used often.

Gauge fields that are connected by gauge transformations are physically equivalent, i.e. their actions agree. They lie in so-called gauge orbits, $\{A^\mathcal{U}, \mathcal{U} \in SU(N)\}$, and fixing a gauge is equivalent to choosing a representative of such an orbit $A \rightarrow A_{\text{gf}}$, up to potential (Gribov) copies. The occurrence of Gribov copies and how to handle them is discussed in Appendix B. To keep things simple we ignore them for the time being and continue with the construction of the QCD Lagrangian.

The path integral measure dA introduced in (I.12) can be split into an integration over physically inequivalent configurations A_{gf} and the gauge transformations \mathcal{U} ,

$$dA = J dA_{\text{gf}} d\mathcal{U} \quad (\text{I.15})$$

In (I.15) J denotes the Jacobian of the transformation $A \rightarrow (A_{\text{gf}}, \mathcal{U})$, and we include $d\mathcal{U}$ as the Haar measure of the gauge group, see e.g. [1]. The coordinate transformation (I.15) and the computation of the Jacobian J are done using the Faddeev-Popov quantization, [2]. To separate the integral (I.12) into the two parts shown in (I.15) we insert a very convoluted unity into the path integral,

$$1 = \int d\mathcal{U} \delta[\mathcal{F}[A^\mathcal{U}]] \Delta_{\mathcal{F}}[A] = \Delta_{\mathcal{F}}[A] \int d\mathcal{U} \delta[\mathcal{F}[A^\mathcal{U}]] \Leftrightarrow \Delta_{\mathcal{F}}[A] = \left(\int d\mathcal{U} \delta[\mathcal{F}[A^\mathcal{U}]] \right)^{-1}, \quad (\text{I.16})$$

where $\Delta_{\mathcal{F}}[A]$ is gauge-invariant due to the property $d(\mathcal{U}\mathcal{V}) = d\mathcal{U}$ of the Haar measure. For the path integral this gives us

$$\int dA e^{-S_{\text{YM}}[A]} = \int dA d\mathcal{U} \delta[\mathcal{F}[A^\mathcal{U}]] \Delta_{\mathcal{F}}[A] e^{-S_{\text{YM}}[A]}. \quad (\text{I.17})$$

Let us now consider a general observable \mathcal{O} , like e.g. $\text{tr}F^2(x) \text{tr}F^2(0)$. Observables are necessarily gauge invariant and local. The expectation value of \mathcal{O} is defined as

$$\langle \mathcal{O} \rangle = \frac{\int dA \mathcal{O}[A] e^{-S_{\text{YM}}[A]}}{\int dA e^{-S_{\text{YM}}[A]}} = \frac{\int dA d\mathcal{U} \delta[\mathcal{F}[A^\mathcal{U}]] \Delta_{\mathcal{F}}[A] \mathcal{O}[A] e^{-S_{\text{YM}}[A]}}{\int dA d\mathcal{U} \delta[\mathcal{F}[A^\mathcal{U}]] \Delta_{\mathcal{F}}[A] e^{-S_{\text{YM}}[A]}}, \quad (\text{I.18})$$

where we have simply inserted (I.16) into the path integral. In (I.18) all terms are gauge invariant except for the δ -function. Hence we can absorb the \mathcal{U} -dependence via $A \rightarrow A^{\mathcal{U}^\dagger}$. Then the (infinite) integral over the Haar measure decouples in numerator and denominator, and we arrive at

$$\langle \mathcal{O} \rangle = \frac{\int dA \delta[\mathcal{F}[A]] \Delta_{\mathcal{F}}[A] \mathcal{O}[A] e^{-S_{\text{YM}}[A_{\text{gf}}]}}{\int dA \delta[\mathcal{F}[A]] \Delta_{\mathcal{F}}[A] e^{-S_{\text{YM}}[A_{\text{gf}}]}}.$$

To compute the Jacobian $\Delta_{\mathcal{F}}[A]$ we apply a coordinate transformation to the δ -distribution

$$\delta[\mathcal{F}[A^\mathcal{U}]] = \frac{\delta[\omega - \omega_1]}{|\det \frac{\delta \mathcal{F}}{\delta \omega}|} \equiv \frac{\delta[\omega - \omega_1]}{|\det \mathcal{M}_{\mathcal{F}}[A]|} \quad \text{with} \quad \mathcal{U} = e^{i\omega}, \quad (\text{I.19})$$

combined with a gauge fixing condition in the form (I.13)

$$\mathcal{F}[A_{\text{gf}} = A^{\mathcal{U}(\omega_1)}] = 0. \quad (\text{I.20})$$

Using the definition (I.16) this leads to

$$\Delta_{\mathcal{F}}[A] = |\det \mathcal{M}_{\mathcal{F}}[A_{\text{gf}}]| \quad \text{with} \quad \mathcal{M}_{\mathcal{F}}[A] = \left. \frac{\delta \mathcal{F}}{\delta \omega} \right|_{\omega=0} [A]. \quad (\text{I.21})$$

Here A_{gf} is the solution with the minimal distance to $A = 0$. The inverse Jacobian $\det \mathcal{M}_{\mathcal{F}}$ of the ansatz (I.15) is called the Faddeev-Popov determinant. For its computation we consider an infinitesimal gauge transformation $\mathcal{U} = 1 + i g \omega$ where we have rescaled the transformation with the strong coupling g for convenience. Such a rescaling gives global factors of powers of $1/g$ that drop out in normalized expectation values. Then, the infinitesimal variation of the

covariant gauge $\partial_\mu A_\mu = 0$ follows as

$$\mathcal{F}[A^\mu] = \partial_\mu A^\mu = \partial_\mu A_\mu - \partial_\mu D_\mu \omega + O(\omega^2) \stackrel{!}{=} 0. \quad (\text{I.22})$$

This gives us the Faddeev-Popov matrix

$$\mathcal{M}_{\mathcal{F}}[A] = -\frac{\delta \partial_\mu D_\mu \omega}{\delta \omega} = -\partial_\mu D_\mu \frac{\delta \omega}{\delta \omega} = -\partial_\mu D_\mu \mathbf{1}. \quad (\text{I.23})$$

We assume that $-\partial^\mu D_\mu$ is a positive definite operator and we arrive at

$$\Delta_{\mathcal{F}}[A] = \det \mathcal{M}[A] = \det (-\partial_\mu D_\mu). \quad (\text{I.24})$$

A useful observation is that determinants can be represented by a Gaussian integral. In regular space such a Gaussian integral reads

$$\int_x e^{-\frac{1}{2} x^T M x} = \frac{(2\pi)^n}{\sqrt{\det M}}. \quad (\text{I.25})$$

We want to use this relation to replace the Faddeev-Popov determinant (I.24) in the Lagrangian. It turns out that the usual form does not give a useful action or Lagrangian. However, we can instead use two anti-commuting Grassmann fields C and switch the sign in the exponent to

$$\det \mathcal{M}_{\mathcal{F}}[A] = \int dc d\bar{c} \exp \left\{ \int d^d x d^d y \bar{c}^a(x) \mathcal{M}_{\mathcal{F}}^{ab}(x, y) c^b(y) \right\}. \quad (\text{I.26})$$

Finally we slightly modify the gauge by introducing a Gaussian average over the gauges

$$\delta[\mathcal{F}[A^\mu]] \rightarrow \int dC \delta[\mathcal{F}[A^\mu - C]] \exp \left\{ -\frac{1}{2\xi} \int_x C^a C^a \right\}. \quad (\text{I.27})$$

In summary, and restricting ourselves to the covariant gauge we then arrive at the generating functional for our Yang-Mills theory

$$Z[J_A, J_c, \bar{J}_c] = \int dA dc d\bar{c} e^{-S_A[A, c, \bar{c}] + \int_x (J_A \cdot A + \bar{J}_c \cdot c - \bar{c} \cdot J_c)}. \quad (\text{I.28})$$

The action including a general gauge fixing term and the Faddeev-Popov ghosts c^a is

$$S_A[A, c, \bar{c}] = \frac{1}{4} \int_x F_{\mu\nu}^a F_{\mu\nu}^a + \frac{1}{2\xi} \int_x (\partial_\mu A_\mu^a)^2 + \int_x \bar{c}^a \partial_\mu D_\mu^{ab} c^b, \quad (\text{I.29})$$

where $\int_x = \int d^d x$ and the Landau gauge is achieved for $\xi = 0$. Note that the ghost action implies a negative dispersion for the ghost, related to the determinant of the positive operator $\mathcal{M}_{\mathcal{F}} = -\partial_\mu D_\mu$. However, this is a matter of convention, we might as well use a positive dispersion, the minus sign drops out for all correlation functions which do not involve ghosts, and only those are related to scattering amplitudes. The source term with all indices reads

$$\int_x (J_A \cdot A + \bar{J}_c \cdot c - \bar{c} \cdot J_c) \equiv \int_x (J_{A,\mu}^a A_\mu^a + \bar{J}_c^a c^a - \bar{c}^a J_c^a). \quad (\text{I.30})$$

The Feynman rules derived from (I.29) are summarized in Appendix A.

B. QCD

After briefly sketching the gauge part of QCD we now add fermionic matter fields. As before we start with the classical action, now given by the Dirac action of a quark doublet,

$$S_{\text{Dirac}}[\psi, \bar{\psi}, A] = i \int_x \bar{\psi} (\not{D} + m_\psi + \mu\gamma_0) \psi, \quad (\text{I.31})$$

where the Dirac matrices are defined through

$$\{\gamma_\mu, \gamma_\nu\} = 2\delta_{\mu\nu} \quad (\text{I.32})$$

In (I.31), the fermions carry a Dirac index defining the 4-component spinor, gauge group indices in the fundamental representation of $SU(3)$, as well flavor indices. The latter we will ignore as long as we only talk about QCD and neglect the doublet nature of the matter fields in the Standard Model. The Dirac operator \mathcal{D} is diagonal in the flavor space as is the chemical potential term. The mass term depends on the current quark masses related to spontaneous symmetry breaking of the Higgs sector of the Standard Model. The up and down current quark masses are of the order 2 – 5 MeV whereas the current quark mass of the strange quark is of the order 10^2 MeV. The other quark masses are of order 1 – 200 GeV. In low energy QCD this has to be compared with the scale of strong chiral symmetry breaking $\Delta m \approx 300$ MeV. This mass scales are summarized in Table I.

Generation	first	second	third	Charge
Mass [MeV]	1.5-4	1150-1350	170×10^3	
Quark	u	c	t	$\frac{2}{3}$
Quark	d	s	b	$-\frac{1}{3}$
Mass [MeV]	4-8	80-130	$(4.1-4.4) \times 10^3$	

TABLE I: Quark masses and charges. The scale of strong chiral symmetry breaking is $\Delta m \approx 300$ MeV as is Λ_{QCD} . This entails that only $2 + 1$ flavours have to be considered for most applications to the phase diagram of QCD.

Evidently, for most applications of the QCD phase diagram we only have to consider the three lightest quark flavors, that is up, down and strange quark, to be dynamical. The current quark masses of up and down quarks are two order of magnitude smaller than all QCD infrared scales related to Λ_{QCD} . Hence, the up and down quarks can be considered to be massless. This leads to the important observation that the physical masses of neutrons and protons — and hence the masses of the world around us — comes about from strong chiral symmetry breaking and has nothing to do with the Higgs sector.

In turn, the mass of the strange quark is of the order of Λ_{QCD} and has to be considered heavy for application in low energy QCD. The three heavier flavors, charm, bottom and top, are essentially static they do not contribute to the QCD dynamics relevant for its phase structure even though in particular the c -quark properties and bound states are much influenced by the infrared dynamics of QCD. In summary we will consider the $N_f = 2$ and $N_f = 2 + 1$ flavor cases for the phase structure of QCD, while for LHC physics all flavors are relevant.

Again in analogy to the Yang-Mills action we describe the quantized theory using its generating functional. The full generating functional of QCD is the straightforward extension of the Yang-Mills version in (I.28). The quark fields are Grassmann fields because of their fermionic nature and we are led to the generating functional

$$Z[J] = \int d\Phi e^{-S_{\text{QCD}}[\Phi] + \int_x J \cdot \phi}, \quad (\text{I.33})$$

As a notation we have introduced super-fields and super-currents

$$\begin{aligned} \Phi &= (A, c, \bar{c}, \psi, \bar{\psi}) & J &= (J_A, J_c, \bar{J}_c, J_\psi, \bar{J}_\psi) \\ d\Phi &= \int dA dc d\bar{c} d\psi d\bar{\psi} & J \cdot \Phi &= J_A \cdot A + \bar{J}_c \cdot c - \bar{c} \cdot J_c + \bar{J}_\psi \cdot \psi - \bar{\psi} \cdot J_\psi. \end{aligned} \quad (\text{I.34})$$

The gauge-fixed action S_{QCD} in (I.33) in the Landau gauge is given by

$$S_{\text{QCD}}[\Phi] = \frac{1}{4} \int_x F_{\mu\nu}^a F_{\mu\nu}^a + \frac{1}{2\xi} \int_x (\partial_\mu A_\mu^a)^2 + \int_x \bar{c}^a \partial_\mu D_\mu^{ab} c^b + i \int_x \bar{\psi} (\mathcal{D} + m_\psi + \mu\gamma_0) \psi. \quad (\text{I.35})$$

The action in (I.35) is illustrated diagrammatically as

For physical observables the gauge dependence entering through the last two graphs in the first line, the ghost terms, is cancelled by the hidden gauge fixing dependence of the inverse gluon propagator. The Feynman rules are summarized in Appendix A.

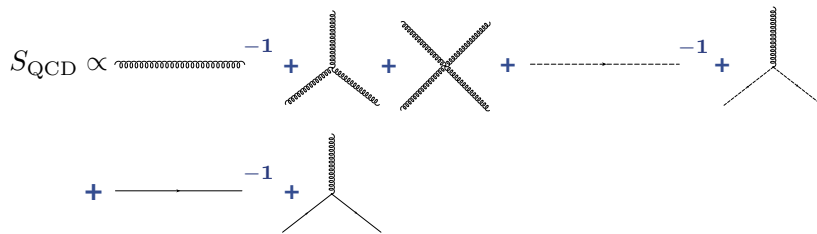


FIG. 1: Diagrammatical form of the QCD action.

II. STRONG CHIRAL SYMMETRY BREAKING

In the previous sections we discussed the ultraviolet renormalisation of QCD and its relation to the scale dependence of physics. This scale dependence is apparent in the momentum dependence of the strong running coupling $\alpha_s(p^2) = g^2(p^2)/(4\pi)$ defined in (??). Here p is the relevant momentum/energy scale of a given process. Let us briefly rehash the main properties of the running coupling: Its momentum dependence is captured by the β -function as leads to a running coupling which decreases with the momentum scale, i.e. ,

$$\beta_g = \frac{1}{2} p \partial_p \alpha_s = -b_0 \alpha^2 + O(\alpha_s^3) \quad \text{with} \quad b_0 = \frac{\alpha_s^2}{12\pi} (11 N_c + 2 N_f) . \quad (\text{II.1})$$

Integrating the β -function (II.1) at one loop leads to the running coup

$$\alpha_s(p) = \frac{\alpha_s(\mu)}{1 + \beta_0 \alpha_s(\mu) \log \frac{p^2}{\mu^2}} + O(\alpha_s^2), \quad (\text{II.2})$$

with some reference (momentum) scale μ^2 . The running coupling in (II.2) tends to zero logarithmically for $p \rightarrow \infty$. This property is called asymptotic freedom (Nobel prize 2004) and guarantees the existence of the perturbative expansion of QCD. Its validity for large energies and momenta is by now impressively proven in various scattering experiments, see e.g. [3]. These experiments can also be used to define a running coupling (which is not unique beyond two loop, see e.g. [4]) and the related plot of $\alpha_s(p^2)$ in Fig. 2 has been taken from [3].

In turn, in the infrared regime of QCD at low momentum scales, perturbation theory is not applicable any more. The coupling grows and the failure of perturbation theory is finally signaled by the so-called Landau pole with $\alpha_s(\Lambda_{\text{QCD}}) = \infty$. We emphasise that a large or diverging coupling does *not* imply confinement, the theory could still be QED-like showing a Coulomb-potential with a large coupling. The latter would not lead to the absence of coloured

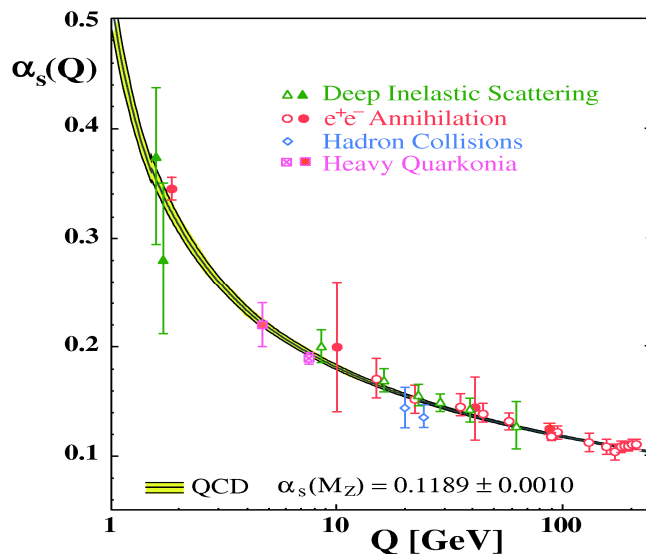


FIG. 2: Experimental tests of the running coupling, figure taken from [3].

asymptotic states but rather to so-called color charge superselection sectors as in QED. There, we have asymptotic charged states and no physics process can change the charge. For more details on this see e.g. [5].

A. Spontaneous symmetry breaking and the Goldstone theorem

In the Standard Model we have two phenomena involving spontaneous symmetry breaking. The first is the spontaneous symmetry breaking in the Higgs sector (Englert-Brout-Higgs-Guralnik-Hagen-Kibble) which provides (current) masses for the quarks and leptons as well as for the W, Z vector bosons, the gauge bosons of the weak interactions. The corresponding Goldstone boson manifest itself as the third polarisation of the massive vector bosons (Higgs-Kibble dinner).

The second phenomena is strong chiral symmetry breaking in the quark sector with a mass scale of ≈ 300 MeV. This mechanism, loosely speaking, lifts the current quark masses to constituent quark masses. For the up and down quarks the current quark mass is negligible, see Table I. The corresponding Goldstone bosons, the pions $\vec{\pi}$, are composite (quark-anti-quark) states and do not appear in the QCD action.

In the following we discuss similarities of and differences between these two phenomena. Before we come to the Standard Model, let us recall some basic facts about spontaneous symmetry breaking. Further details can be found in the literature. As a basic, but important, example we consider a simple scalar field theory with N real scalars and action

$$S[\phi] = \frac{1}{2} \int_x (\partial_\mu \phi^a)^2 + \int_x V(\rho), \quad \text{with} \quad a = 1, \dots, N, \quad \text{and} \quad \rho = \frac{1}{2} \phi^a \phi^a, \quad (\text{II.3})$$

and the ϕ^4 -potential

$$V(\rho) = -\mu^2(\phi^a \phi^a) + \lambda(\phi^a \phi^a)^2. \quad (\text{II.4})$$

In the following considerations we shall not need the specific form (II.4) but only its symmetries. Still, the simple potential (II.4) serves as a good showcase. The action (II.3) with the potential (II.4) has $O(N)$ -symmetry. Moreover, the potential (II.4) has a manifold of non-trivial minima, each of which breaks $O(N)$ -symmetry. This leads us to the vacuum manifold

$$V'(\rho_0) = 0, \quad \text{with} \quad \rho_0 = \frac{\mu^2}{4\lambda}, \quad (\text{II.5})$$

where the prime stands for the derivative w.r.t. ρ . In Fig. 3 the potential is depicted for the $O(2)$ -case with $N = 2$.

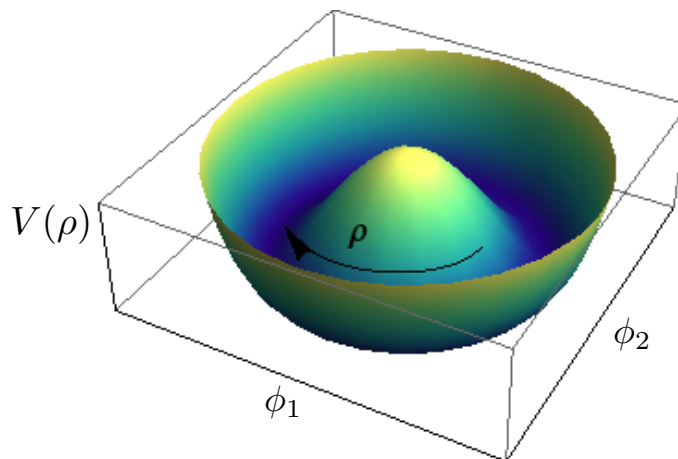


FIG. 3: Illustration of the Mexican hat potential for $N = 2$. The radial massive mode ρ is indicated by the arrow. The angular mode is the Goldstone mode.

Without loss of generality we pick a specific point on the vacuum manifold (II.5), to wit

$$\phi_0 = \begin{pmatrix} 0 \\ \vdots \\ 0 \\ \sqrt{2\rho_0} \end{pmatrix}. \quad (\text{II.6})$$

The vacuum vector ϕ_0 in (II.6) is invariant under the subgroup (little group) $O(N-1)$ with the generators t^a , $a = N, N+1, \dots, N(N-1)/2$ of $O(N)$ that acts trivially on the N th component field ϕ^N . This subgroup rotates the first $N-1$ component fields into each other. It leaves us with $N-1$ generators t^a , $a = 1, \dots, N-1$ (of the quotient $O(N)/O(N-1)$) of the $N(N-1)/2$ generators of the group $O(N)$. In turn, a rotation of the vacuum vector within this quotient generates the full vacuum manifold. Applied to a vector $\phi^a = \delta^{Na} \sqrt{2\rho}$ with length it generates all fields,

$$\phi = e^{\frac{\theta^a}{\sqrt{2\rho_0}} t^a} \begin{pmatrix} 0 \\ \vdots \\ 0 \\ \sigma \end{pmatrix}, \quad (\text{II.7})$$

where the denominator $1/\sqrt{2\rho_0}$ is chosen for convenience. Commonly, the N th component field ϕ^N is expanded about the minimum $\sigma_0 = \sqrt{2\rho_0}$.

In the present lecture we choose a slightly different approach and stick to the Cartesian fields ϕ which we split into the radial mode σ and the rest, $\vec{\pi}$, i.e.

$$\phi = \begin{pmatrix} \vec{\pi} \\ \sigma \end{pmatrix}, \quad \text{with} \quad \phi_0 = \begin{pmatrix} 0 \\ \sigma \end{pmatrix}. \quad (\text{II.8})$$

Note that in an expansion about the minimum ϕ_0 in the fields $\vec{\theta}$ and $\vec{\pi}$ agree in leading order. Using the representation (II.8) in the kinetic term in the action (II.3) we are led to

$$S_{\text{kinetic}}[\phi] = \frac{1}{2} \int_x [(\partial_\mu \sigma)^2 + (\partial_\mu \vec{\pi})^2]. \quad (\text{II.9})$$

The mass term of the model is given by the quadratic term of the potential in an expansion about the minimum. It reads generally

$$\frac{1}{2} \int_x m^{2ab}(\phi_0) \phi^a \phi^b, \quad \text{with} \quad m^{2ab}(\phi_0) = \partial_{\phi^a} \partial_{\phi^b} V(\rho_0) = \delta^{ab} V'(\rho_0) + \phi_0^a \phi_0^b V''(\rho_0). \quad (\text{II.10})$$

Using the expansion point (II.6) leads to the mass matrix

$$m^{2ab}(\phi_0) = \delta^{ab} V'(\rho_0) + 2 \delta^{Na} \delta^{Nb} \rho_0 V''(\rho_0) = 8 \delta^{Na} \delta^{Nb} \rho_0 \lambda. \quad (\text{II.11})$$

Eq.(II.11) entails that in the symmetry-broken phase of the model we have $N-1$ massless fields, the Goldstone fields. Note that we have not used the specific form (II.4) of the potential for this derivation.

The occurrence of the massless modes in (II.11) is a specific case/manifestation of the Goldstone theorem. It entails in general that in the case of a spontaneous symmetry breaking of a continuous symmetry massless modes, the Goldstone modes, occur. Their number is related to the number of generators in the Quotient G/H , where G is the symmetry group and H is the subgroup (little group) which leaves the vacuum invariant.

B. Spontaneous symmetry breaking, quantum fluctuations and masses*

The classical analysis done in chapter II A suffices to uncover the occurrence of massless modes in spontaneous symmetry breaking. However, it does not unravel the mechanism. The stability of the chosen vacuum, e.g. (II.6), necessitates, that an infinitesimal rotation on the vacuum manifold costs an infinite amount of energy. This does only happen (for continuous symmetries) in dimensions $d > 2$. In $d \leq 2$ no spontaneous symmetry breaking of a continuous symmetry occurs, which is covered by the Mermin-Wagner theorem (Mermin-Wagner-Hohenberg-Coleman). In $d = 2$ dimensions theories with discrete symmetry can exhibit spontaneous symmetry breaking, e.g. the Ising model.

Hence, the full analysis has to be done on the quantum level. A convenient way to address these questions is the quantum analogue of the classical action, the (quantum) effective action. Formally it is defined as the Legendre transform of the Schwinger functional, $W[J] = \log Z[J]$. In the present case this is

$$\Gamma[\phi] = \sup_J \left\{ \int_x J(x)\phi(x) - \log Z[J] \right\}, \quad \text{where} \quad Z[J] = \int D\varphi e^{-S[\varphi] + \int_x J\varphi}. \quad (\text{II.12})$$

In the following we simply assume that (II.12) has a maximum and is differentiable w.r.t. J . Then the definition in (II.12) leads to

$$\phi = \frac{1}{Z[J]} \frac{\delta Z[J]}{\delta J} = \langle \varphi \rangle, \quad \text{and} \quad J = \frac{\delta \Gamma}{\delta \phi}. \quad (\text{II.13})$$

The effective action also has a closed path integral representation in terms of a functional integro-differential equation, which we also quote for later use. For the derivation we substitute the current in (II.12) with (II.13) and use that $Z = \exp\{-\Gamma + \int_x J\phi\}$. This leads us to

$$e^{-\Gamma[\phi]} = \int D\varphi' e^{-S[\phi+\varphi'] + \int_x \frac{\delta \Gamma}{\delta \phi} \varphi'}, \quad \text{with} \quad \langle \varphi' \rangle_c = 0, \quad (\text{II.14})$$

where we also shifted the integration variable $\varphi = \varphi' + \phi$. Eq.(II.14) leads us immediately to the quantum equations of motion in general backgrounds ϕ , the Dyson-Schwinger equations. We simply take the ϕ -derivatives on both sides and arrive at

$$\frac{\delta \Gamma}{\delta \phi} = \left\langle \frac{\delta S}{\delta \varphi} \right\rangle, \quad (\text{II.15})$$

the quantum equations of motion (EoM) in a given background $\phi = \langle \varphi \rangle$ triggered by the current J . Evaluated on the EoM with $J = 0$,

$$\left. \frac{\delta \Gamma}{\delta \phi} \right|_{\phi=\phi_{\text{EoM}}} = 0, \quad (\text{II.16})$$

The effective action $\Gamma[\phi_{\text{EoM}}] = -\log Z[0]$ it is the free energy of the theory and implies $J[\phi_{\text{EoM}}] = 0$. It is also a generating functional and generates the one-particle-irreducible (1PI) diagrams of the theory. As all diagrams can be constructed from 1PI diagrams, it contains the full information about the correlation functions of the theory. In the present context, the interesting feature is its relation to the free energy. It allows us to define the effective potential

$$V_{\text{eff}}[\phi_c] = \Gamma[\phi_c] / \text{vol}_4, \quad (\text{II.17})$$

with constant fields ϕ_c and the four-volume $\text{vol}_4 = \int d^4x$. If the effective potential shows the vacuum structure discussed above in the classical case, the theory exhibits spontaneous symmetry breaking. The Mermin-Wagner theorem simply entails that in lower dimensions the long range nature of the quantum fluctuations washes out the non-trivial vacua.

The rôle of the effective action as the quantum analogue of the classical action is also very apparent in its relation to the propagator of the theory,

$$\langle \phi(p)\phi(-p) \rangle_c = \left. \frac{\delta^2 \log Z[J]}{\delta J(p)\delta J(-P)} \right|_{J=0} = \frac{1}{Z[0]} \left. \frac{\delta^2 Z}{\delta J(p)\delta J(-P)} \right|_{J=0} - \langle \phi(p) \rangle \langle \phi(-p) \rangle, \quad \text{with} \quad \langle \phi \rangle = \frac{1}{Z[0]} \frac{\delta Z}{\delta J}, \quad (\text{II.18})$$

where the subscript c stands for connected. Now we use the relation of $\log Z$ to the effective action defined in (II.12). We have

$$\delta(p-q) = \frac{\delta J(q)}{\delta J(p)} = \int_l \frac{\delta \phi(l)}{\delta J(p)} \cdot \frac{\delta J(q)}{\delta \phi(l)} = \int_l \frac{\delta^2 \log Z}{\delta J(l)\delta J(p)} \cdot \frac{\delta^2 \Gamma[\phi]}{\delta \phi(l)\delta(q)} \Rightarrow \langle \phi(p)\phi(q) \rangle_c = \frac{1}{\Gamma^{(2)}}(p, q), \quad (\text{II.19})$$

with the vertices

$$\frac{\delta^n \Gamma}{\delta \phi(p_1) \cdots \phi(p_n)} = \Gamma^{(n)}(p_1, \dots, p_n), \quad \text{with} \quad \langle \varphi(p_1) \cdots \varphi(p_n) \rangle_{1\text{PI}} = \Gamma^{(n)}(p_1, \dots, p_n). \quad (\text{II.20})$$

The proof of the latter identity of the n th φ -derivatives with the 1PI n -point correlation functions we leave to the reader. Instead let us now come back to our simple example for spontaneous symmetry breaking. Let us assume for the moment that the full effective action resembles the classical action in (II.3). Then the ϕ^4 -potential in (II.4) is the full quantum effective potential of the theory for $\rho \geq \rho_0$ (why is this not possible for smaller ρ ?). The full propagator of the theory is now given by

$$\langle \varphi(p) \varphi(-p) \rangle_c = \frac{1}{\Gamma^{(2)}[\phi_{\text{EOM}}]}(p, -p) = \frac{1}{p^2} (\delta^{ab} - \delta^{aN} \delta^{bN}) + \frac{1}{p^2 + 8\rho_0 \lambda} \delta^{ab}, \quad (\text{II.21})$$

which describes the massless propagation of the $N - 1$ Goldstone modes, and that of one massive one, the radial field σ , with mass $m_\sigma^2 = 8\rho_0 \lambda$. This links the curvature of the effective potential to the masses of the propagating modes in the theory. Note however, that this is a Euclidean concept and finally we are interested in the pole masses of the physical excitations. They are defined via the respective (inverse) screening lengths in the spatial and temporal directions. The latter are defined by

$$\lim_{\|\vec{x}-\vec{y}\| \rightarrow \infty} \langle \phi(x) \phi(y) \rangle \sim e^{-\|\vec{x}-\vec{y}\|/\xi_{\text{spat}}}, \quad \text{and} \quad \lim_{|x_0-y_0| \rightarrow \infty} \langle \phi(x) \phi(y) \rangle \sim e^{-|x_0-y_0|/\xi_{\text{temp}}}. \quad (\text{II.22})$$

The screening lengths $\xi_{\text{spat/temp}}$ are inversely related to the pole mass $m_{\text{pol}} = 1/\xi_{\text{temp}}$ and screening mass $m_{\text{screen}} = 1/\xi_{\text{spat}}$ respectively. In the present example with the classical dispersion p^2 these masses are identical and also agree with the curvature masses m_{curv} derived from the effective potential. This is easily seen from (II.21). The screening lengths and masses are derived from the Fourier transform of the propagator in momentum space and we have e.g. for the radial mode φ^N at $\vec{p} = 0$

$$\lim_{|x_0-y_0| \rightarrow \infty} \int \frac{dp_0}{(2\pi)} \langle \varphi^N(p_0, 0) \varphi^N(-p_0, 0) \rangle_c e^{ip_0(x_0-y_0)} \sim e^{-|x_0-y_0|8\rho_0 \lambda}, \quad (\text{II.23})$$

and hence $m_{\text{pol}} = 1/\xi_{\text{temp}} = m_{\text{curv}}$. Here $\vec{p} = 0$ has only be chosen for convenience. A similar computation can be made for the spatial screening length which agrees with the temporal one. In summary this leaves us with the definition of the pole mass as the smallest value for

$$\Gamma^{(2)}(p_0 = m_{\text{pol}}, \vec{p} = 0) = 0, \quad (\text{II.24})$$

related to the pole (or cut) that is closest to the Euclidean frequency axis. A similar definition holds for the screening mass.

In principle this allows for the extraction of the pole and screening masses from the Euclidean propagators. In practice this quickly runs in an accuracy problem if the propagator is only known numerically. Moreover, this problem is tightly related to reconstruction problems of analyticity properties from numerical data which is an ill-posed problem without any further knowledge.

As a last remark we add that the above identity between screening lengths, and pole, screening and curvature masses fails in the full quantum theory:

- the coincidence of curvature and screening/pole masses hinges on the classical dispersion proportional to p^2 , any non-trivial momentum dependence of the propagator leads to a violation.
- The coincidence of screening and pole mass hinges on the dispersion only being a function of p^2 . While this is true in the vacuum (at vanishing temperature $T = 0$ and density/chemical potential $n/\mu = 0$), finite temperature and density singles out a rest frame and the dispersion depends on \vec{p}^2 and p_0^2 separately.

Having said this, in the following we shall first use simple approximations to the full low energy effective action of QCD for extracting the physics of chiral symmetry breaking and confinement, as well as the mechanisms behind these phenomena.

C. Little reminder on the Higgs mechanism

Now we are in the position to discuss the Higgs mechanism in the Standard Model. Again we refer to the literature for the details. The Higgs mechanism serves as an example, at which we can discuss similarities and differences for strong chiral symmetry breaking. Moreover, it is the combination of both mechanisms of mass generation that leads to the observed world. The action of the Standard Model is given by

$$S_{\text{SM}}[\Phi] = \frac{1}{4} \int_x F_{\mu\nu}^a F_{\mu\nu}^a + \frac{1}{4} \int_x W_{\mu\nu}^a W_{\mu\nu}^a + \frac{1}{4} \int_x B_{\mu\nu} B_{\mu\nu} + (D\phi)^\dagger D\phi + V_H(\phi) + \int_x \bar{\psi} \cdot (i\not{D} + i m_\psi(\phi) + i\mu\gamma_0) \cdot \psi, \quad (\text{II.25})$$

where we have introduced the electroweak gauge bosons W, B and the Higgs, a complex scalar $SU(2)$ -doublet ϕ ,

$$\phi = \begin{pmatrix} \phi_1 \\ \phi_2 \end{pmatrix}, \quad (\text{II.26})$$

with complex components ϕ_1, ϕ_2 . The Higgs potential V_H is a ϕ^4 -potential as (II.4) with

$$V_H(\phi) = -\mu^2 \phi^\dagger \phi + \lambda (\phi^\dagger \phi)^2. \quad (\text{II.27})$$

with non-trivial vacuum manifold

$$\rho_0 = \frac{\mu^2}{4\lambda} \quad \text{with} \quad \rho = \frac{1}{2} \phi^\dagger \phi. \quad (\text{II.28})$$

In the spirit of the discussion at the end of chapter II A we should interpret V_H as an approximation of the full effective potential of the theory. The Higgs field couples to the electroweak gauge group with the covariant derivative

$$D_\mu \phi = (\partial_\mu - ig_W W_\mu - ig_H B_\mu) \phi, \quad (\text{II.29})$$

The mass term in (II.25) is linear in the Higgs field and vanishes for $\phi = 0$. The left-handed fermions ψ_L in the Standard Model, leptons and quarks, couple to the weak isospin (fundamental representation) with weak isospin $\pm 1/2$, while the right-handed fermions ψ_R do not couple (trivial representation) with weak isospin 0, that is for example

$$W_\mu \psi_R = 0. \quad (\text{II.30})$$

The related covariant derivative of the fermions reads

$$D_\mu \psi = (\partial_\mu - ig A_\mu - ig_W W_\mu - ig_H B_\mu) \psi. \quad (\text{II.31})$$

The mass term $m(\phi)$ is linear in the Higgs field ϕ and hence constitutes a Yukawa interaction. It relates to the Cabibbo-Kobayashi-Maskawa-Matrix (CKM), and is not discussed in further details here. What is important in the present context, is, that a non-vanishing expectation value of the Higgs field, $\langle \phi \rangle = (0, \rho_0/\sqrt{2})$ provides mass terms for the weak gauge fields, the W, Z as well as for the (left-handed) quarks and leptons:

As in our $O(N)$ -example in the previous section we expect spontaneous symmetry breaking in the scalar Higgs sector. The current masses of the leptons and quarks are then generated by the disappearance of the mass term for $\phi_0 \neq 0$. Since the structure of the full term is quite convoluted, we illustrate this at a simple example with one Dirac fermion ψ and a real scalar field σ . Then the Yukawa term reads in a mean field approximation

$$h\bar{\psi}\sigma\psi \xrightarrow{\text{mean field}} h\sigma_0 \bar{\psi}\psi, \quad (\text{II.32})$$

with mass $m = h\sigma_0$ which is proportional to the vacuum expectation value of the scalar field (vacuum expectation value of the Higgs) and the Yukawa coupling h .

For the masses of the gauge field we cut a long story short and simply note that in a mean field analysis as that done above for the fermion

$$(W_\mu \phi)^\dagger (W_\mu \phi) \xrightarrow{\text{mean field}} (W_\mu \phi_0)^\dagger (W_\mu \phi_0), \quad (\text{II.33})$$

leads to mass terms for the gauge fields. Since the vacuum field ϕ_0 has vanishing upper component ϕ_1 it is a

combination of the generator $t^3 = \sigma_3/2$ of the weak $SU(2)$ and the generator $\mathbb{1}$ of the hypercharge $U(1)$ which remains massless: the photon. This also determines the subgroup which leaves the vacuum invariant. The superficial analysis here also reveals that the quotient involves three generators and hence we have three Goldstone bosons. In summary we hence start with three gauge bosons with two physical polarisations each together with three Goldstone bosons, which adds up to nine field degrees of freedom (dof). A convenient reparameterisation (including an appropriate gauge fixing, e.g. the unitary gauge) of the Standard Model leads us to three massive vector bosons with three polarisations each, that is again nine dofs.

D. Low energy effective theories of QCD

The Higgs mechanism in the electroweak sector of the Standard Model leads to (current) quark masses for the up and down quark of a couple of MeVs, $(m_{u/d})_{\text{cur}} \approx 2\text{-}5$ MeV, see Table I. However, the masses of the nucleons, the protons and neutrons, is about 1 GeV (proton (uud) ≈ 938 MeV, neutron (udd) ≈ 940 MeV), that is two orders of magnitude bigger. In other words, the three constituent quarks in the nucleons must have an effective mass of about $(m_{u/d})_{\text{con}} \approx 300\text{-}400$ MeV, the constituent quark masses. We already infer from this that there should be a further mechanism to generate this mass scale.

In low energy QCD with its mass scale $\Lambda_{\text{QCD}} \approx 200 - 300$ MeV the electroweak sector of the Standard Model decouples as do the heavier quarks. We are left with two light (up and down) and one heavy quark (charm), Table I. Within fully quantitative computations of the QCD dynamics at low energies the strange quark with its current mass of about 1.2 GeV is also added. Still, its dynamics is very much suppressed at momentum scales of Λ_{QCD} . For the present structural analysis we first resort to two flavour QCD ($N_f = 2$) with the Euclidean action

$$S_{\text{QCD}}[\Phi] = \frac{1}{4} \int_x F_{\mu\nu}^a F_{\mu\nu}^a + \int_x \bar{\psi} \cdot (\not{D} + m_\psi + i\mu\gamma_0) \cdot \psi, \quad (\text{II.34})$$

where ψ is a Dirac spinor with two flavours and Φ is the two-flavour super field, see (I.35). The physics of the matter sector at low energies and temperatures, and not too large densities is well-described by quark-hadron models, the most prominent of which is the Nambu-Jona-Lasinio model. From the perturbative point of view these models are seeded in the four-fermi coupling already being generated from the propagators and couplings depicted in Fig. 1 at tree level. The related tree level diagram is depicted in Fig. 4. Its s -channel has the structure

$$g^2 (\bar{\psi} \gamma_\mu t^a \psi)(p) \Pi_{\mu\nu}(p) \frac{1}{p^2} (\bar{\psi} \gamma_\mu t^a \psi)(p), \quad (\text{II.35})$$

describing the scattering of quarks. In (II.35) the t^a are generators of the color gauge group and the fermions are summed over the two flavours. Accordingly, (II.35) generates a four-fermi interaction with a non-trivial momentum structure in the effective action of QCD.

The full momentum- and tensor structure is complicated even for the present simplified $N_f = 2$ case. As in the four-fermi theory (Fermi theory) for weak interactions we resort to an approximation with point-like interactions (no momentum dependence). Then (II.35) can be rewritten in terms of an effective *local* (point-like) four-fermi interaction. Such a rewriting in terms of local four-fermi interactions holds for energies that are sufficiently low and do not resolve the large momentum structure of the scattering in (II.35). Moreover, the coupling is dimensionful and has the canonical momentum dimension -2 (related to the $1/p^2$ term in (II.35)). In the Fermi theory of weak interactions this is the electroweak scale. In the present case it has to be related to the QCD mass gap proportional to Λ_{QCD} .

We postpone the detailed analysis of this scale, and first concentrate on the tensor structure of (II.35). This is constrained by the symmetries of the theory, for a full discussion of the symmetry pattern we refer to the literature, e.g. [6, 7] and literature therein. Since the current masses of the light quarks are nearly vanishing we first work in the chiral limit. Then, any interaction that is generated by the dynamics of QCD carries chiral symmetry: the related four-fermi interaction is chirally invariant, that is the invariance under the chiral transformations

$$\psi \rightarrow e^{i\frac{1\pm\gamma_5}{2}\alpha}\psi \quad \rightarrow \quad \bar{\psi} \rightarrow \bar{\psi} e^{i\frac{1\mp\gamma_5}{2}\alpha} \quad \text{with} \quad \gamma_5 = \gamma_0\gamma_1\gamma_2\gamma_3, \quad \text{and} \quad \{\gamma_5, \gamma_\mu\} = 0, \quad (\text{II.36})$$

which holds separately for each vector current $\bar{\psi}\gamma_\mu t^a\psi$. Furthermore, in the chiral limit QCD is invariant under flavour rotations $SU(N_f)$. For example, for $N_f = 2$ with up (u) and down (d) quarks and the flavour isospin group

with $SU(2)$, the transformation reads

$$\psi = \begin{pmatrix} u \\ d \end{pmatrix} \rightarrow V \begin{pmatrix} u \\ d \end{pmatrix}, \quad \text{with} \quad V = e^{i\theta^a \tau^a} \in SU(2), \quad (\text{II.37})$$

with $a = 1, 2, 3$. For the 2+1 flavour case also considered here the respective symmetry is $SU(3)_F$. Chiral symmetry entails that the flavour rotations are a symmetry for the left- and right-handed quarks separately and the combined symmetry is $SU(2)_L \times SU(2)_R$ with symmetry transformations $V_{L/R} = e^{i\frac{1 \pm \gamma_5}{2} \theta^a t^a}$. Including also the chiral $U(1)$ rotations leads us to the full symmetry group

$$G_{\text{sym}} = SU(N_c) \times SU(N_f)_V \times SU(N_f)_A \times U(1)_V \times U(1)_A, \quad (\text{II.38})$$

where we have also taken into account the gauge group $SU(N_c)$. If we approximate (II.35) by a point-like four-fermi interaction, one has to expand the tensor $\gamma_\mu \otimes \gamma_\nu$ multiplied by gauge group and flavour tensors. Then, the most general symmetric Ansatz is a combination of the tensor structures

$$\begin{aligned} (V - A) &= (\bar{\psi} \gamma^\mu \psi)^2 + (\bar{\psi} \gamma^\mu \gamma^5 \psi)^2 \\ (V + A) &= (\bar{\psi} \gamma^\mu \psi)^2 - (\bar{\psi} \gamma^\mu \gamma^5 \psi)^2 \\ (S - P) &= (\bar{\psi}^f \psi^g)^2 - (\bar{\psi}^f \gamma^5 \psi^g)^2 \\ (V - A)^{\text{adj}} &= (\bar{\psi} \gamma^\mu t^a \psi)^2 + (\bar{\psi} \gamma^\mu \gamma^5 t^a \psi)^2, \end{aligned} \quad (\text{II.39})$$

where f, g are flavour indices and $(\bar{\psi}^f \psi^g)^2 \equiv \bar{\psi}^f \psi^g \bar{\psi}^g \psi^f$. While each separate term in the tensors in (II.39) is invariant under gauge transformation, and under the flavour vector transformations, axial rotations in $SU(N_f)_A \times U(1)_A$ rotate the terms on the right hand side in (II.39) into each other. For a related full analysis we refer to the literature. However, below we shall exemplify these computations at the relevant example of the scalar–pseudo-scalar channel

The chiral invariants (II.39) can be rewritten using the Fierz transformations which relates different four-fermi terms on the basis of the Grassmann natures of the fermions. These transformations are explained and detailed in the literature, see e.g. [6, 7]. Here we just concentrate on the scalar–pseudo-scalar channels in physical two-flavour QCD with $N_c = 3$ and $N_f = 2$. These channels are related to the scalar σ -meson and the pseudo-scalar pions $\vec{\pi}$. The $(S - P)$ -channel is given by

$$(S - P) = \frac{1}{2} [(\bar{\psi} \psi)^2 + (\bar{\psi} \vec{\tau} \psi)^2 - (\bar{\psi} \gamma^5 \psi)^2 - (\bar{\psi} \gamma^5 \vec{\tau} \psi)^2], \quad (\text{II.40})$$

where $\vec{\tau} = (\sigma_1, \sigma_2, \sigma_3)$ with Pauli matrices

$$\sigma_1 = \begin{pmatrix} 0 & 1 \\ 1 & 0 \end{pmatrix}, \quad \sigma_2 = \begin{pmatrix} 0 & -i \\ i & 0 \end{pmatrix}, \quad \sigma_3 = \begin{pmatrix} 1 & 0 \\ 0 & -1 \end{pmatrix}, \quad (\text{II.41})$$

The representation (II.40) simplifies the identification of the scalar mode $\bar{\psi} \psi$ related to the scalar σ -meson, and the pseudo-scalar modes $i\bar{\psi} \gamma_5 \vec{\tau} \psi$ related to the pseudo-scalar (axial-scalar) pions $\vec{\pi}$.

We shall use the representation (II.40) in the following investigations of the chiral properties of low energy QCD. Hence we discuss its symmetry properties in more detail, and show explicitly its invariance under G_{sym} . To begin with, the invariance of $(S - P)$ under gauge and flavour $U_V(1)$ transformation is apparent. The flavour $SU(2)_V$ transformations $\psi \rightarrow e^{i\theta^a \tau^a} \psi$ trivially leaves $\bar{\psi} \psi$ and $\bar{\psi} \gamma_5 \psi$ invariant. For the vector and pseudo-vector bilinears we concentrate on infinitesimal transformations $e^{i\theta^a \tau^a} = 1 + i\theta^a \tau^a + O(\theta^2)$. Then the second term in (II.40) transforms as

$$(\bar{\psi} \vec{\tau} \psi)^2 \rightarrow (\bar{\psi} \vec{\tau} \psi)^2 + 2i\theta^a (\bar{\psi} \vec{\tau} \psi) (\bar{\psi} [\vec{\tau}, \tau^a] \psi) = (\bar{\psi} \vec{\tau} \psi)^2 - 2\theta^a \epsilon^{bac} (\bar{\psi} \tau^b \psi) (\bar{\psi} \tau^c \psi) = (\bar{\psi} \vec{\tau} \psi)^2. \quad (\text{II.42})$$

The invariance of the last term in (II.40) under $SU(2)_V$ transformations follows analogously. Finally, axial transformations related the first two terms to the last two terms. We exemplify this property with the axial $U_A(1)$ rotations $\psi \rightarrow e^{i\gamma_5 \alpha} \psi$, where we consider infinitesimal transformations with $e^{i\gamma_5 \alpha} = \mathbb{1} + i\gamma_5 \alpha + O(\alpha^2)$. Concentrating on the scalar and pseudo-scalar terms we have

$$(\bar{\psi} \psi)^2 - (\bar{\psi} \gamma^5 \psi)^2 \rightarrow (\bar{\psi} \psi)^2 - (\bar{\psi} \gamma^5 \psi)^2 + 4i\alpha \left[(\bar{\psi} \psi) (\bar{\psi} \gamma_5 \psi) - (\bar{\psi} \gamma^5 \psi) (\bar{\psi} \psi) \right] = (\bar{\psi} \psi)^2 - (\bar{\psi} \gamma^5 \psi)^2, \quad (\text{II.43})$$

The invariance for the full expression in (II.40) follows analogously. It is left to study $SU(2)_A$ transformations. Now

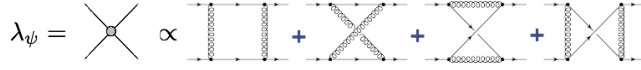


FIG. 4: One loop diagrams for the four-fermi coupling λ_ψ in QCD.

we show that (II.40) also carries the $SU(2)_A$ -invariance. To that end we consider infinitesimal $SU(2)_A$ transformations $e^{i\gamma_5\theta^a\tau^a} = 1 + i\gamma_5\theta^a\tau^a + O(\theta^2)$ of the combination $(\bar{\psi}\psi)^2 - (\bar{\psi}\gamma^5\vec{\tau}\psi)^2$, and use the Lie algebra identity

$$\tau^a\tau^b = \delta^{ab} + i\epsilon^{abc}\tau^c, \quad \rightarrow \quad \{\tau^a, \tau^b\} = 2\delta^{ab}. \quad (\text{II.44})$$

Then we are led to

$$(\bar{\psi}\psi)^2 - (\bar{\psi}\gamma^5\vec{\tau}\psi)^2 \longrightarrow (\bar{\psi}\psi)^2 - (\bar{\psi}\gamma^5\vec{\tau}\psi)^2 + 2i\theta^a \left[(\bar{\psi}\psi)(\bar{\psi}\gamma_5\tau^a\psi) - (\bar{\psi}\gamma^5\vec{\tau}^b\psi)(\bar{\psi}\{\tau^a, \tau^b\}\psi) \right] = (\bar{\psi}\psi)^2 - (\bar{\psi}\gamma^5\psi)^2. \quad (\text{II.45})$$

The invariance of the combination $(\bar{\psi}\gamma_5\psi)^2 - (\bar{\psi}\vec{\tau}\psi)^2$ is shown along the same lines. Consequently (II.40) is invariant under $SU(2)_A$ transformation and hence under the full symmetry group G_{sym} .

In QCD, we have experimental evidence for the breaking of the axial $U_A(1)$ -symmetry, i.e. the pseudo-scalar η' -meson (in $N_f = 2$ the η) is anomalously heavy. This mass-difference can be nicely explained by the anomalous breaking of axial $U_A(1)$ symmetry. Consequently, giving up axial $U_A(1)$ -symmetry we have to consider more four-fermi interactions as in (II.39) (altogether 10 invariants for $N_f = 2$), in particular

$$\frac{1}{2} \left[(\bar{\psi}\psi)^2 - (\bar{\psi}\vec{\tau}\psi)^2 + (\bar{\psi}\gamma^5\psi)^2 - (\bar{\psi}\gamma^5\vec{\tau}\psi)^2 \right]. \quad (\text{II.46})$$

It is the relative minus signs in the scalar and pseudo-scalar terms in comparison to (II.40) that leads to the breaking of $U_A(1)$ -symmetry. This is easily seen by re-doing the infinitesimal analysis (II.43) in (II.46). It also follows easily that the other symmetries still hold, in particular the $SU(2)_V \times SU_A(2)_A$ invariance follows as (II.46) contains the same $SU(2)_V \times SU_A(2)_A$ -invariant combinations of four-quark terms as (II.40). Hence we conclude that the combination (II.46) only breaks $U_A(1)$ -symmetry, and adding up the two channels (II.40) and (II.46) leads to the $U_A(1)$ -breaking combination

$$\frac{1}{2} \left[(\bar{\psi}\psi)^2 - (\bar{\psi}\gamma^5\vec{\tau}\psi)^2 \right]. \quad (\text{II.47})$$

Eq.(II.47) is invariant under the remaining symmetries $SU(N_c) \times SU(N_f)_V \times SU(N_f)_A \times U(1)_V$. This concludes our brief discussion of the global symmetries of QCD in the chiral limit.

In summary the following picture emerges: assume we perform a chain of scattering experiments of QCD/Standard Model starting at the electroweak scale ≈ 90 Gev towards the strong QCD scale Λ_{QCD} . At each scale we can describe the quantum equations of motion and scattering experiments by a suitably chosen effective action $\Gamma[\phi]$. On the level of the path integral for QCD, (I.33), this is described by the Wilsonian idea of integrating out momentum modes above some momentum scale μ ,

$$Z_\mu[J] = \int [d\Phi]_{p^2 \geq \mu^2} e^{-S_{\text{QCD}}[\Phi] + \int_x J \cdot \Phi} \quad \Rightarrow \quad \text{Effective Action } \Gamma_\mu[\Phi], \quad (\text{II.48})$$

where the path integral measure only contains an integration over fields Φ_μ that are non-vanishing for $p^2 \geq \mu^2$: $\Phi_\mu(p^2 < \mu^2) \equiv 0$. After Legendre transformation this leads us to an effective action $\Gamma_\mu[\Phi]$ that only contains the quantum effects of scales larger than the running (RG) scale μ and serves as a classical action for the quantum effects with momentum scales $p^2 < \mu^2$. This effective action also carries the symmetries of the fundamental QCD action, as long as these symmetries are not (anomalously broken by quantum effects).

We know already from the perturbative renormalisation programme that this amounts to adjusting the (running) coupling in the (classical) action with the sliding (experimental) momentum scale. In such a Wilsonian setting this is very apparent. The running of the coupling comes from the loop diagrams that are evaluated at the momentum scale μ . On top of this momentum adjustment of the fundamental parameters of the theory one also creates additional terms in the -effective- action. The one of importance for us is the four-fermi terms argued for above. It is created at one-loop with the box diagrams depicted in depicted in Fig. 4. This leads us finally to the following four-fermi

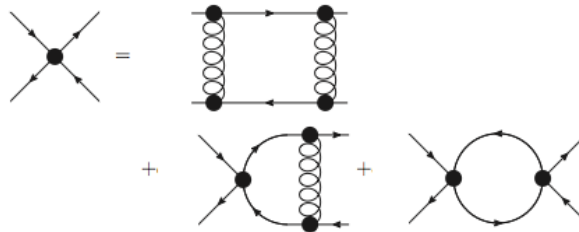


FIG. 5: One loop diagrams for the four-fermi coupling λ_ψ from the action (II.51).

interaction in the effective action,

$$\Gamma_{4\text{-fermi}}[\phi]|_{1\text{-loop}} = -\frac{\lambda_\psi}{4} \int [(\bar{\psi}\psi)^2 - (\bar{\psi}\gamma^5\vec{\tau}\psi)^2] + \dots \quad \text{with} \quad \lambda_\psi \propto \alpha_s^2, \quad (\text{II.49})$$

where it is understood that the coupling λ_ψ carries the running momentum or RG scale μ introduced above. Together with the kinetic term of the quarks this is the classical action of the Nambu–Jona-Lasinio type model. Eq.(II.49) holds for massless quarks and two flavours, $N_f = 2$. The two terms in (II.49) carry the same quantum number as the scalar and axial-scalar excitations in low energy QCD, the sigma-meson σ and pion $\vec{\pi}$ respectively. The one loop diagrams generating the four-fermi coupling λ_ψ are depicted in Fig. 4. In line with the picture outlined above the four-fermi coupling λ_ψ at a given momentum scale $p = \mu$ should be computed with the loop momenta q in the box diagrams in Fig. 4 being bigger than μ . Then the related diagram is peaked at this scale and we conclude by dimensional analysis that

$$\lambda_\psi(\mu) \simeq \alpha_s^2(\mu) \frac{1}{\mu^2}. \quad (\text{II.50})$$

Note that this coupling feeds back into the loop expansion of other correlations functions such as the quark propagator and quark-gluon vertices. However, in comparison to other (one-loop) diagrams it is suppressed by additional orders of the strong coupling α_s . In turn, in the low momentum regime where α_s grows strong it gives potentially relevant contributions. Indeed, taking as a starting point for a loop analysis the sum of the QCD action (II.34) and the four-fermi term (II.49)

$$\Gamma[\phi] \simeq S_{\text{QCD}}[\phi] + \Gamma_{4\text{-fermi}}[\phi], \quad (\text{II.51})$$

we get also self-interaction terms of the four-fermi coupling proportional to λ_ψ^2 as well as terms proportional to $\alpha_s \lambda_\psi$. This is depicted in Fig. 5.

The glue sector of QCD is expected to have a mass gap already present in the purely gluonic theory, related to the confinement property of Yang-Mills theory. Then this has to manifest itself in a decoupling of the gluonic contribution to the four-fermi coupling in Fig. 5. In the Landau gauge this mechanism is easily visible due to the mass gap in the gluon propagators, see Fig. 6 for lattice results and results from non-perturbative diagrammatic methods.

Note that the gluon propagator is gauge dependent, and the careful statement is that the Landau gauge facilitates the access to the related physics. One should not confuse this with a massive gluon, as the gluon is no physical particle and shows positivity violation. Moreover, the gluonic sector is certainly relevant for the confining physics and hence the decoupling discussed above only takes place in the matter sector for the specific question under investigation, the mechanism of strong chiral symmetry breaking.

E. Strong chiral symmetry breaking and quark-hadron effective theories

Assuming for the moment the gluonic decoupling we are left with a purely fermionic theory. The four-fermi term (II.49) is the interaction part of the Nambu–Jona-Lasinio model, one of the best-studied model for low energy QCD, see e.g. [6, 7, 9]. It is non-renormalisable as can be seen from the momentum dimension of the four-fermi coupling which is -2 . As shown above, in QCD it is generated by fluctuations with $\lambda_\psi(p) \propto \alpha_s(p)$ and tends to zero in the UV, that is for large momenta $p \rightarrow \infty$. Its momentum dependence is best extracted from the dimensionless coupling

$$\hat{\lambda}_\psi = \lambda_\psi(\mu)\mu^2, \quad (\text{II.52})$$

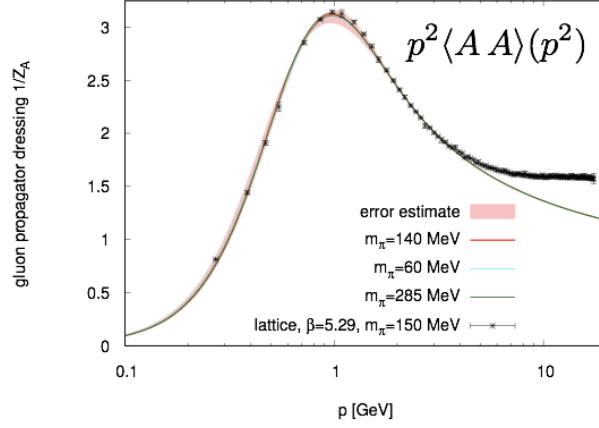


FIG. 6: Gluon propagator for $N_f = 2$ from the lattice and from non-perturbative diagrammatic methods, taken from [8].

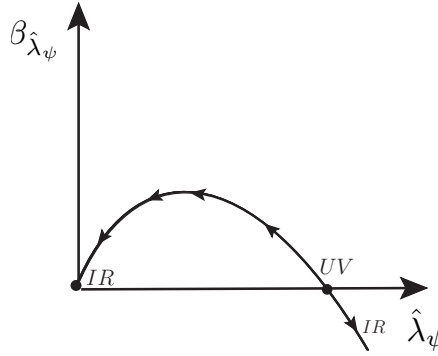


FIG. 7: Fixed point structure of λ_ψ for the four-fermi coupling in the NJL model.

where we have introduced the renormalisation group scale μ , here being identical with the momentum scale of the scattering process described, $\mu^2 = p^2$. The β -function of the dimensionless four-fermi coupling in (II.52) is given by

$$\beta_{\hat{\lambda}_\psi} = \mu \partial_\mu \hat{\lambda}_\psi = 2\hat{\lambda}_\psi - c\hat{\lambda}^2 \quad \text{with} \quad c > 0, \quad (\text{II.53})$$

and is depicted in Fig. 7. The first term on the right hand side of (II.53) encodes the trivial dimensional running of $\hat{\lambda} = \mu^2 \lambda$. The second term on the right hand side originates in the last diagram in Fig. 5, the pure four-fermi term. In the absence of other mass scales this loop has to be proportional to μ^2 leading to a factor two in the β -function in comparison to the loop itself. The key feature relevant for the description of chiral symmetry breaking is the sign of the diagram. It is negative, $-c\hat{\lambda}^2$, with a positive constant c leading to (II.53).

From the perspective of a one-loop investigation based on the classical fermionic action in (II.51) the coupling in the loop term on the right hand side of (II.53) is the classical one in this action. As we have done for the β -function of the strong coupling, e.g. (??), we can elevate this coupling to the full running coupling in terms of a one-loop RG-improvement. This accounts for a one-loop resummation of diagrams. In the present context the physics behind such an improvement is very apparent: As already indicated, the NJL-type action was derived within a successive integrating out of momentum modes, and constitutes an effective action for the UV physics with $p^2 \geq \mu^2$. Accordingly, its couplings depend on this RG-scale. In summary we end up with (II.53) with μ -dependent couplings on the right hand side. Note that this is only a one-loop RG improvement as we have discarded the μ -dependence of the couplings in the diagram when taking the μ -derivative. The related terms are proportional to $-c/2 \hat{\lambda} \mu \partial_\mu \hat{\lambda}_\psi$ and can be shuffled to the left hand side. This accounts for a further resummation leading to (II.53) with a global factor $1/(1 + c/2 \hat{\lambda})$ on the right hand side. In the following qualitative analysis it is dropped and we strictly resort to the one-loop improvement.

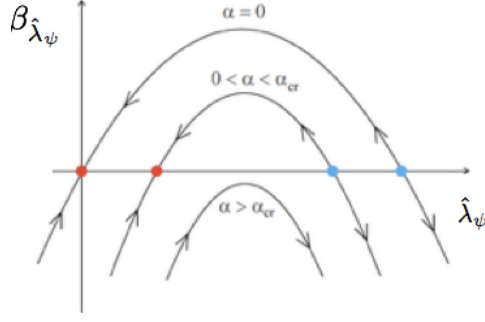


FIG. 8: Fixed point structure of λ_ψ of the full β -function

The β -function of (II.53) is depicted in Fig. 7. It divides the positive $\hat{\lambda}_\psi$ -axis into two physically distinct regimes,

$$I_1 = [0, \hat{\lambda}_{UV}) \quad \text{and} \quad I_2 = (\hat{\lambda}_{UV}, \infty) \quad \text{with} \quad \beta_{\hat{\lambda}_\psi}(\hat{\lambda}_{UV}) = 0 \quad \text{with} \quad \hat{\lambda}_{UV} = \frac{2}{c}. \quad (\text{II.54})$$

The zeroes of the β -function are fixed points of the renormalisation group flows, and $\hat{\lambda}_{UV} \neq 0$ is a non-trivial fixed point FP of the β -function while $\hat{\lambda}_{\text{GauB}} = 0$ is the trivial Gaußian fixed point (related to the free Gaußian theory). Now we initiate the RG-flow at an initial ultraviolet scale μ_{in} with some value of the dimensionless four-fermi coupling

$$\hat{\lambda}(\mu_{\text{in}}) = \hat{\lambda}_{\text{in}}. \quad (\text{II.55})$$

If $\hat{\lambda}_{\text{in}} < \hat{\lambda}_{UV}$ and we lower the running momentum scale, the RG-flow lowers the four-fermi coupling towards 0. Accordingly $\hat{\lambda}_\psi(\mu \rightarrow 0) = 0$. Since the regime of small couplings is governed by the linear term $2\hat{\lambda}_\psi$ in the β -function in (II.53) this entails $\lambda_\psi(\mu \rightarrow 0) = \lambda_0$. Here λ_0 is some finite value which is adjusted by the input $\hat{\lambda}_{\text{in}}$ at the initial scale μ_{in} .

In turn, if $\hat{\lambda}_{\text{in}} > \hat{\lambda}_{UV}$, the RG-flow toward smaller μ drives $\hat{\lambda}_\psi$ towards ∞ . Then the linear term can be neglected as it is sub-leading and the RG-flow reads

$$\mu \partial_\mu \hat{\lambda} = -c \hat{\lambda}_\psi^2, \quad \longrightarrow \quad \hat{\lambda}(\mu) = \frac{\hat{\lambda}(\mu_0)}{1 + \hat{\lambda}(\mu_0) c \log \mu / \mu_0}, \quad (\text{II.56})$$

where μ_0 is some reference scale at which the approximation in the RG-flow in (II.56) is already valid. We conclude from (II.56) diverges at

$$\mu = \mu_0 \exp \left\{ -\frac{1}{c \hat{\lambda}(\mu_0)} \right\}, \quad (\text{II.57})$$

which signals a resonance in the four-fermi scalar-pseudo-scalar channel.

At this scale chiral symmetry breaking occurs. To make this more apparent we resort to a further rewriting of our low energy effective theory in terms of the scalar, σ , and pseudo-scalar, $\vec{\pi}$, degrees of freedom. This is suggestive already for the reason that the divergence in (II.56) entails that these resonance are relevant degrees of freedom for lower momentum scales. For the rewriting of the theory we use the Hubbard-Stratonovich transformation, see e.g. [6, 7, 9]. With this transformation we a four-fermi interaction using a scalar auxiliary field. Concentrating on the scalar part of the four-fermi interaction in (II.49) we write at some momentum scale μ ,

$$-\frac{\lambda_\psi}{4} (\bar{\psi}\psi)^2 = \left[\frac{h}{2} (\bar{\psi}\psi) \sigma + \frac{m_\varphi^2}{2} \sigma^2 \right]_{\text{EoM}(\sigma)}, \quad \text{with} \quad \lambda_\psi = \frac{h^2}{m_\varphi^2}. \quad (\text{II.58})$$

Accordingly we can extend the effective action $\Gamma[\phi]$ given in (II.51) by the right hand side of (II.58) while dropping the four-fermi term. For the sake of simplicity we concentrate on the σ -meson first and reduce the four-fermi term to

its scalar part. Then

$$\Gamma[\phi] \rightarrow \Gamma[\phi, \sigma] = \Gamma[\phi]|_{\lambda_\psi \rightarrow 0} + \left[\frac{h}{2} (\bar{\psi}\psi)\sigma + \frac{m^2}{2} \sigma^2 \right]_{h^2/m^2=\lambda_\psi}, \quad (\text{II.59})$$

This new effective action agrees with the original one on the equation of motion of σ and hence carries the same physics. As a side remark, note that the 1PI correlation functions of quarks and gluon derived from $\Gamma[\phi, \sigma]$ at fixed σ do not agree with the quark and gluon correlation functions derived from $\Gamma[\phi] = \Gamma[\phi, \sigma_{\text{EoM}}(\phi)]$, the implicit dependences also contribute.

A similar derivation can be done for the pion part of the four-fermi interaction, and hence the whole four-fermi interaction can be bosonised. The mesonic equations of motion can be summarised in

$$\sigma_{\text{EoM}} = \frac{h}{2m_\varphi^2} \bar{\psi}\psi, \quad \vec{\pi}_{\text{EoM}} = \frac{h}{2m_\varphi^2} \bar{\psi} i\gamma_5 \vec{\tau}\psi. \quad (\text{II.60})$$

On the level of the generating functional of QCD, (II.58) and its extension to pions can be implemented by a Gaußian path integral with

$$\exp \left\{ \frac{\lambda_\psi}{4} \int [(\bar{\psi}\psi)^2 - (\bar{\psi}\gamma_5 \vec{\tau}\psi)^2] \right\} = \int d\sigma d\vec{\pi} \exp \left\{ - \int_x \left(\frac{1}{2} m^2 (\sigma^2 + \vec{\pi}^2) + \frac{h}{2} \bar{\psi} [\sigma + i\gamma_5 \vec{\tau}\vec{\pi}] \psi \right) \right\}_{h^2/m^2=\lambda_\psi}. \quad (\text{II.61})$$

We also remark that as shift in the σ -field,

$$\sigma \rightarrow -\frac{2}{h} m_\psi + \sigma, \quad (\text{II.62})$$

eliminates the quark mass term at the expense of the linear term in σ that can be interpreted as a source term. Inserting this identity in the path integral for the low energy dofs including the currents for the fundamental fields, the quarks and gluons (and ghosts) as well as current for the mesonic dofs we have the full generating functional in this setting. Performing the Legendre transformation we are immediately led to (II.59). Kinetic terms as well as a potential for σ are generated by further quantum effects. In summary this leads us finally to a low energy effective theory with a classical action $S_{\text{eff}} = \Gamma_{\text{UV}}$, where Γ_{UV} is the full quantum effective action including quantum fluctuations above a given cutoff scale Λ . This also entails that S_{eff} carries a Λ -dependence. S_{eff} is given by

$$S_{\text{eff}}[\psi, \bar{\psi}, \phi] \propto \int_x \bar{\psi} \cdot (\not{D} + m_\psi) \cdot \psi + \int_x [(\partial_\mu \sigma)^2 + (\partial_\mu \vec{\pi})^2] + \int_x \frac{h}{2} \bar{\psi} [\sigma + i\gamma_5 \vec{\tau}\vec{\pi}] \psi + \int_x V_{\text{UV}}(\rho) \quad (\text{II.63})$$

with $\phi = (\sigma, \vec{\pi})$ and

$$V_{\text{UV}}(\rho) = m_\varphi^2 \rho + \frac{\lambda}{2} \rho^2, \quad \text{with} \quad \rho = \frac{1}{2} (\sigma^2 + \vec{\pi}^2). \quad (\text{II.64})$$

As indicated above, the quark mass term can be eliminated at the expense of a linear term in σ by the shift of σ in (II.62). On the level of the quadratic quark-meson interaction (II.61) this triggers a linear term $c_\sigma \sigma$ and the full potential reads

$$V_{\text{UV}}(\rho) = m_\varphi^2 \rho + \frac{\lambda_\varphi}{2} \rho^2 - c_\sigma \sigma, \quad \text{with} \quad c_\sigma = \frac{2}{h} m_\varphi^2 m_\psi. \quad (\text{II.65})$$

This concludes the derivation of the low energy effective theory with the action (II.63) from QCD by *integrating-out* QCD quantum fluctuations above the validity scale of the low energy effective theory. From the gluonic decoupling scale $\Lambda_{\text{dec}} \lesssim 1$ GeV one concludes that (II.63) should be seen as a classical action for quantum fluctuations with momenta $p^2 \lesssim 1$ GeV, see Fig. 6. A more detailed analysis reveals that the initial scale for low energy effective theories has to be taken far lower for quantitative computations. Nonetheless, for qualitative considerations it is sufficient, and, as a matter of fact, low energy effective theories even work well quantitatively at surprisingly large moment scale about 1 GeV.

In (II.63) we have introduced a self-interaction of the mesonic fields proportional to ρ^2 as well as an explicit breaking term linear in σ related to the quark mass term. The question arises, is this the most general ϕ^4 -term one can generate from QCD? As mentioned before, the symmetries of this low energy effective field theory (EFT) are determined by those of the action of QCD. In the chiral limit the full symmetry group is (II.38). The axial $U_A(1)$ symmetry is

anomalously broken, hence our restriction to the $U_A(1)$ -breaking combination (II.47). In its bosonised quark-meson mode version the symmetry transformations with G_{sym} also involve transformations of the mesonic fields. Their transformation properties can be most easily accessed in the matrix notation for the field. To that end we introduce

$$\hat{\phi} = \mathbb{1}\sigma + i\gamma_5\vec{\tau}\vec{\pi} \quad \text{with} \quad \hat{\phi}_{\text{EoM}} = \frac{h}{2m_\phi^2} (\mathbb{1}\bar{\psi}\psi - \gamma_5\vec{\tau}\bar{\psi}\gamma_5\vec{\tau}\psi), \quad (\text{II.66})$$

where we have used (II.60) in the second equation. Now we can read-off the symmetry transformations under $V \in SU(N_c) \times SU(N_f)_V \times SU(N_f)_A \times U(1)_V$ from (II.66) by evoking the symmetry transformations of the quarks. One easily sees that axial $U(1)_A$ -rotations do not close on σ and $\vec{\pi}$. For example, σ_{EoM} transforms into $\bar{\psi}\gamma_5\psi$. Furthermore, ϕ is invariant under vector $U_V(1)$ transformations. Similarly, σ is invariant under transformations with $e^{i\theta^a\tau^a} \in SU(2)_V$, while π is rotated, $\vec{\pi} \rightarrow V\vec{\pi}$ with $V = e^{\theta^a t^a} \in O(3)$ with $(t^a)^{bc} = \epsilon^{abc}$. This follows from

$$\bar{\psi}\gamma_5\vec{\tau}\psi \rightarrow \bar{\psi}\gamma_5\vec{\tau}\psi + i\theta^a\bar{\psi}\gamma_5[\vec{\tau}, \tau^a]\psi = \bar{\psi}\gamma_5\vec{\tau}\psi - \theta^a\epsilon^{bac}\bar{\psi}\gamma_5\tau^c\psi. \quad (\text{II.67})$$

Finally, transformations with $e^{i\gamma_5\theta^a\tau^a} \in SU(2)_A$ rotate $(\sigma, \vec{\pi})$ into each other. This is read-off from the infinitesimal transformations of $\hat{\phi}_{\text{EoM}}$ leading to

$$\sigma \rightarrow \sigma + 2\theta^a\pi^a, \quad \pi^b \rightarrow \pi^b - \theta^b\sigma. \quad (\text{II.68})$$

Combining all the manifestations of the symmetry group we are led to an $O(4)$ invariance of our low energy effective field theory, sloppily written as

$$\psi \rightarrow V\psi \quad \text{with} \quad V \in G_{\text{sym}}/U_A(1), \quad \phi \rightarrow e^{\theta^a t^a}\phi, \quad \text{with} \quad \phi = \begin{pmatrix} \vec{\pi} \\ \sigma \end{pmatrix} \quad \text{and} \quad e^{\theta^a t^a} \in O(4). \quad (\text{II.69})$$

In conclusion chiral symmetry breaking is in one-to-one correspondence to the breaking of the $O(4)$ -symmetry. Moreover, the formulation with effective mesonic σ and pion degrees of freedom now allows us to discuss strong chiral symmetry breaking in complete analogy to the Higgs mechanism that served as an introductory example. Let us first consider the fully symmetric case with $c_\sigma = 0$. The mesonic sector of (II.63) simply is an $O(4)$ -model, and the QCD four-fermi coupling are related to the Yukawa coupling and the mesonic mass parameters via the relation (II.58) in the Hubbard-Stratonovich transformation. Accordingly, a diverging λ_ψ implies a vanishing m_ϕ if the Yukawa coupling is fixed. Hence, at the singularity of λ_ψ the mesonic mass parameter m_ϕ^2 changes sign. For $m_\phi^2 < 0$ we are in the phase of -spontaneously- broken $O(4)$ -symmetry. We choose the σ direction as our radial mode, and its expectation value is given by

$$\sigma_0 = \sqrt{\frac{-m_\phi^2}{\lambda_\phi}}, \quad (\text{II.70})$$

in the chiral limit. This leads to an effective quark mass term with

$$m_\psi = \frac{h}{2}\sigma_0 = \frac{h}{2}\sqrt{\frac{-m_\phi^2}{\lambda_\phi}}, \quad (\text{II.71})$$

which in QCD is of the order of 300 MeV.

In summary we have derivated low energy EFTs in QCD by successively integrating out momentum shells of quantum fluctuations in QCD. The first class of low energy EFTs we encountered are the *Nambu-Jona-Lasigno type four-quark models* (in short in a slight abuse of notation NJL-model), baptised after a seminal work of Nambu and Jona-Lasigno from 1961 introducing a four-fermi model for Nucleons. The NJL-model is not renormalisable and requires a ultraviolet cutoff scale Λ_{UV} that cannot be removed.

In a second step we have bosonised the resonant scalar-pseudo-scalar channels of the four-quark interaction leading us to a Yukawa-type model, the *Quark-Meson Model* (QM-model). This model is renormalisable and its UV cutoff Λ_{UV} seemingly can be removed to infinity. However, we emphasise that the two models are equivalent on the level of the respective path integrals via the Hubbard-Stratonovich transformation. In other words, if one considers all quantum fluctuations in both models the physics results are the same, as must be the necessity of a ultraviolet cutoff scale Λ_{UV} . In the QM model this necessity is encoded in a UV-instability of the model. In other words, its renormalisability is of no help if it comes to the existence of the model at large scales.

Finally, despite being low energy EFTs, these models have a complicated dynamics reflecting the strongly-correlated

nature of low energy QCD. Hence, typically one resorts to approximations within these models. In the reminder of this chapter we shall discuss different approximations to the Quark-Meson model ranging from a mean-field treatment to a full non-perturbative renormalisation group study.

F. Low energy quantum fluctuations

In the last chapter we have derived the action of the QM-model by integrating out quantum fluctuations above a momentum scale $\Lambda \approx 1$ GeV. We have argued that below this scale the gluonic degrees of freedom become less important and decouple from the theory below the mass gap of QCD. Practically, this can be seen from the results for gluonic correlation functions such as the gluon propagator displayed in Fig. 6. This entails that the action (II.63) serves as a classical action for the quantum fluctuations with momenta $p^2 \leq \Lambda^2$. More explicitly we use the definition (II.48) with $\mu = \Lambda$ and arrive at the path integral

$$Z \approx \int [d\phi d\psi d\bar{\psi}]_{p^2 \leq \Lambda^2} e^{-S_{\text{eff},\Lambda}[\psi_<, \bar{\psi}_<, \phi_<]} \quad \text{with} \quad Z_\Lambda \simeq e^{-S_{\text{eff},\Lambda}}, \quad (\text{II.72})$$

where we have dropped the source terms. The fields $\psi_<, \bar{\psi}_<, \phi_<$ only carry low momentum modes with momenta $p^2 < \Lambda^2$. Then the full quark field $\psi = \psi_< + \psi_>$ is a sum of $\psi_< = \psi_{p^2 \geq \mu^2}$ and $\psi_> = \psi_{p^2 \geq \mu^2}$. Note also that the path integral of the large momentum modes in (II.48) is performed in the presence of fields that also carry low momentum contributions,

$$Z_\Lambda[\psi_<, \bar{\psi}_<, \phi_<] = \int [d\Phi]_{p^2 \geq \mu^2} e^{-S[\phi, \Phi]}. \quad (\text{II.73})$$

where S is the QCD action with a bosonised scalar–pseudo-scalar channel. Eq.(II.72) is approximate as we do not integrate out the low momentum gluons. Therefore low energy quantum effects with momentum scales $p^2 \leq \Lambda$ are encoded in loop diagrams with the classical action $S_{\text{eff},\Lambda} \simeq \Gamma_\Lambda$ defined in (II.63). Here, Γ_Λ is the effective action that originates in the integrating-out of QCD fluctuations with momenta $p^2 \geq \Lambda^2$. Henceforth we drop the subscripts $<, >$ for the sake of readability.

As we have seen at the end of the last chapter, the coupling parameters in the mesonic potential play a crucial rôle for chiral symmetry breaking. Here we compute the one-loop correction to the 'classical' potential V in (II.65) as well as studying its the renormalisation group or flow equation.

1. Quark quantum fluctuations

First we note that the quark path integral in (II.72) with the action $S_{\text{eff},\Lambda}$ in (II.63) is Gaussian, and hence the one-loop computation is exact. This leads to the following representation of (II.72),

$$Z \approx \int \int [d\phi]_{p^2 \leq \Lambda^2} e^{-S_{\phi, \text{eff}, \Lambda}[\phi]}, \quad (\text{II.74})$$

with

$$S_{\phi, \text{eff}, \Lambda}[\phi] = \int_x [(\partial_\mu \sigma)^2 + (\partial_\mu \vec{\pi})^2] + \int_x V_{\text{UV}}(\rho) - \ln \left[\frac{1}{\mathcal{N}} \int [d\psi d\bar{\psi}]_{p^2 \leq \Lambda^2} e^{-\int_x \bar{\psi} \cdot (\not{D} + m_\psi) \cdot \psi + \int_x \frac{h}{2} \bar{\psi} [\sigma + i\gamma_5 \vec{\tau} \vec{\pi}] \psi} \right], \quad (\text{II.75})$$

where $1/\mathcal{N}$ is an appropriate, field-independent normalisation specified later. The quark path integral can be rewritten as follows,

$$\frac{1}{\mathcal{N}} \int [d\psi d\bar{\psi}]_{p^2 \leq \Lambda^2} e^{-\int_x \bar{\psi} \cdot (\not{D} + \frac{h}{2} [\sigma + i\gamma_5 \vec{\tau} \vec{\pi}]) \cdot \psi} = \frac{1}{\mathcal{N}} \det_\Lambda \left(\not{D} + \frac{h}{2} [\sigma + i\gamma_5 \vec{\tau} \vec{\pi}] \right), \quad (\text{II.76})$$

where \det_Λ is the determinant from momentum modes with $p^2 \leq \Lambda^2$. Expanded in powers of the field, the logarithm of (II.76) adds to the kinetic term in (II.75) as well as to the potential V . It also leads to terms with higher order derivatives or derivative couplings such as $Z(\rho)(\partial_\mu \phi)^2$, $(\phi \Delta \phi)^2$. As we work at low energies we drop these terms in the spirit of an expansion in p^2/m_{gap}^2 where m_{gap}^2 is the lowest mass scale in QCD. Evidently the pion plays a special role as it has a very small mass in comparison to the QCD mass scale Λ_{QCD} . The mass scales m_{had} of all other hadronic

low energy degrees of freedom in QCD satisfy $m_{\text{had}} \gtrsim \Lambda_{\text{QCD}}$. Accordingly the pion carries the quantum fluctuations in QCD for scales below Λ_{QCD} . These scale considerations are also behind the impressively successful framework of chiral perturbation theory. In summary at leading order the low energy effective action $S_{\phi,\text{eff}}$ only changes to $V_{\text{UV}} \rightarrow V_{\phi,\text{eff}}$,

$$V_{\phi,\text{eff}}(\rho) = V_{\text{UV}}(\rho) + \Delta V_q(\rho), \quad (\text{II.77})$$

with

$$\Delta V_q(\rho) = -\text{Tr}_\Lambda \ln \left(\not{D} + \frac{h}{2} [\sigma + i\gamma_5 \vec{\tau} \vec{\pi}] \right) + \ln \mathcal{N}, \quad V_{\text{UV}}(\rho) = m_\varphi^2 \rho + \frac{\lambda_\varphi}{2} \rho^2. \quad (\text{II.78})$$

In (II.78) we have used that for a given operator \mathcal{O} we have $\ln \det_\Lambda \mathcal{O} = \text{Tr}_\Lambda \ln \mathcal{O}$, where the trace sums over momenta with $p^2 \leq \Lambda^2$, as well as Dirac and internal indices, and the 'classical' potential V defined in (II.64). For the present considerations and scales the gluonic fluctuations and background are irrelevant. Thus we have dropped the gluonic fluctuations and we also put the gauge field to zero, $A_\mu = 0$. At finite temperature and density we also will consider constant temporal backgrounds $A_0 \neq 0$ which is related to so-called *statistical confinement*. Finally we introduce a convenient choice for the normalisation $\ln \mathcal{N}$: the quark determinant at vanishing background,

$$\ln \mathcal{N} = \text{Tr}_\Lambda \ln \not{\partial}. \quad (\text{II.79})$$

Due to the symmetry analysis performed above the fermionic determinant can only depend on the $O(4)$ -invariant combination $\rho = 1/2(\sigma^2 + \vec{\pi}^2)$, and we can simplify the computation by using $\vec{\pi} \equiv 0$. In momentum space we have

$$\begin{aligned} V_{\phi,\text{eff}}(\sigma^2/2) &= V_{\text{UV}}(\sigma^2/2) - N_f N_c \int \frac{d\Omega_4}{(2\pi)^4} \int_0^\Lambda dp p^3 \text{tr}_{\text{Dirac}} \ln \frac{i\not{p} + \frac{h}{2}\sigma}{i\not{p}} \\ &= V_{\text{UV}}(\sigma^2/2) - \frac{6}{\pi^2} \int_0^\Lambda dp p^3 \ln \frac{p^2 + \frac{h^2}{4}\sigma^2}{p^2}, \end{aligned} \quad (\text{II.80})$$

where $\int d\Omega_4 = 2\pi^2$ is the four-dimensional angular integration. The prefactor $N_f N_c = 6$ in the middle part in (II.80) comes from the trace over flavour and colour space. The Dirac trace gives a factor 4, while the momentum symmetrisation with $p \rightarrow -p$ provides a factor 1/2. The denominators in (II.80) come from the normalisation (II.79). Note also that up to these prefactors (II.80) is nothing but the Coleman-Weinberg potential of a φ^4 -theory with interaction $\lambda/4! \varphi^2$ where we substitute $\lambda \varphi^2 \rightarrow h^2 \rho$. We have an important relative minus sign due to the fermion loop and a symmetry factor $4N_f N_c = 24$ due to the number of degrees of freedom. We simply could take over this well-known result, for a detailed discussion see e.g. chapter 1.4 in the QFTII lecture.

For its importance we recall the computation here, and also discuss some particularities due to the embedding in QCD in the present low energy EFT context. The momentum integral in (II.80) is easily performed. We also restore the full mesonic field content, $\sigma^2/2 \rightarrow \rho$, and arrive at

$$V_{\phi,\text{eff}}(\rho) = V_{\text{UV}}(\rho) - \frac{3}{8\pi^2} \left[2\Lambda^2 h^2 \rho + h^4 \rho^2 \left[\ln \frac{h^2 \rho}{2\Lambda^2} - \ln \left(1 + \frac{h^2 \rho}{2\Lambda^2} \right) \right] + 4\Lambda^4 \ln \left(1 + \frac{h^2 \rho}{2\Lambda^2} \right) \right]. \quad (\text{II.81})$$

Up to the symmetry factor -24 this is precisely the result of the Coleman-Weinberg computation performed originally in the context of the Higgs mechanism. We note that (II.81) seemingly depends on the momentum cutoff scale Λ . However, the potential $V_{\text{UV}}(\rho)$ is the result of integrating-out quantum fluctuations up to the momentum scale Λ and hence also is Λ -dependent. Indeed, the full generating functional Z of QCD in (II.72) cannot be Λ -dependent, to wit

$$\Lambda \frac{\partial Z}{\partial \Lambda} = 0. \quad (\text{II.82})$$

Eq.(II.82) is the (cutoff) RG-equation for the generating functional of QCD. In the present context it is only approximately valid as we did not include the quantum fluctuations of gluons below the cutoff scale Λ . Accordingly, (II.82) only holds in our present EFT setting if the cutoff scale Λ is small enough. This will be apparent in the final, renormalised result, and we shall resume the discussion of the sufficient smallness of the cutoff scale there.

For the time being let us also drop the integration of the mesonic fluctuations. In this approximation $V_{\phi,\text{eff}}(\rho)$ is the full effective potential of our low energy EFT. Using (II.82) for the full effective potential (II.80) or (II.81), $\Lambda \partial_\Lambda V_{\text{eff}} = 0$, leads us to scaling relations for the couplings in the potential V . As Λ only appears in the integration

limit in (II.80), the integrand simply is the Λ -derivative and we obtain

$$\begin{aligned}\Lambda\partial_\Lambda V_{\text{UV}} &= \frac{6}{\pi^2}\Lambda^4 \ln\left(1 + \frac{h^2\rho}{2\Lambda^2}\right) \\ &= \frac{3}{\pi^2}\left(\Lambda^2 h^2\rho - \frac{h^4}{4}\rho^2\right) + O(\rho^3/\Lambda^2),\end{aligned}\tag{II.83}$$

and

$$\Lambda\partial_\Lambda V_{\text{UV}} = \Lambda\frac{\partial m_\varphi^2}{\partial\Lambda}\rho + \frac{1}{2}\Lambda\frac{\partial\lambda_\varphi}{\partial\Lambda}\rho^2.\tag{II.84}$$

The RG equation (II.84) signifies that the present quark-meson model is indeed renormalisable: the divergences can be absorbed in the couplings of the classical action. For the sake of completeness we also remark that In a full analysis two further logarithmic singularities occur, the wave function renormalisations of quarks and mesons which also can be absorbed by wave functions in the classical action with e.g. $\partial_\mu\phi^2 \rightarrow Z_{\phi,\Lambda}\partial_\mu\phi^2$. The scale derivatives of m_φ^2 and λ_φ define the β -functions of meson mass and self-coupling respectively,

$$\beta_{m_\varphi^2} = \Lambda\frac{\partial(m_\varphi^2/\Lambda^2)}{\partial\Lambda}, \quad \beta_{\lambda_\varphi} = \Lambda\frac{\partial\lambda_\varphi}{\partial\Lambda},\tag{II.85}$$

in analogy to the β -function of the strong coupling in (II.1) and the four-fermi coupling in (II.53) discussed before. Now we use $\Lambda\partial_\Lambda\Lambda^2 = 2\Lambda^2$ and $\Lambda\partial_\Lambda\ln\Lambda^2/\Lambda_{\text{QCD}}^2 = 2$ for integrating the RG-equation (II.83). For the logarithmic term we have to introduce a reference scale which we choose to be the dynamical scale of QCD, Λ_{QCD}^2 . Practically this scale is identified with the UV cutoff scale of the low energy EFT which is proportional to Λ_{QCD}^2 , and is typically of the order of 1 GeV. In summary this leads us to

$$m_\varphi^2 = m_{\varphi,r}^2 + \frac{3}{2\pi^2}\Lambda^2 h^2, \quad \lambda_\varphi = \lambda_{\varphi,r} - \frac{3}{4\pi^2}h^4 \ln\frac{\Lambda^2}{\Lambda_{\text{QCD}}^2},\tag{II.86}$$

with the renormalised couplings $m_{\varphi,r}^2, \lambda_{\varphi,r}$. In the present approximation without the mesonic quantum fluctuations they directly carry the physics. The Λ -independent constant part in the subtraction is chosen such that the ρ^2 -term in the effective potential has the coupling $\lambda_{\varphi,r}$. It is evident from (II.86) that a variation of the reference scale in the logarithmic term can be absorbed in an according variation of $\lambda_{\varphi,r}$,

$$\Lambda_{\text{QCD}}\frac{\partial\lambda_\varphi}{\partial\Lambda_{\text{QCD}}} = 0 \quad \longrightarrow \quad \Lambda_{\text{QCD}}\frac{\partial\lambda_{\varphi,r}}{\partial\Lambda_{\text{QCD}}} = \beta_{\lambda_\varphi},\tag{II.87}$$

where we have assumed the absence of other scales. This relation is again governed by the β -function β_{λ_φ} , and reflects the invariance observables do not depend on this choice. Inserting these results back into (II.81) leads us to the final, Λ -independent effective potential

$$V_{\phi,\text{eff}}(\rho) = m_{\varphi,r}^2\rho + \frac{\lambda_{\varphi,r}}{2}\rho^2 - \frac{3}{8\pi^2}h^4\rho^2\left[\ln\frac{h^2\rho}{2\Lambda_{\text{QCD}}^2} - \frac{1}{2}\right].\tag{II.88}$$

As already discussed in the beginning of the derivation, (II.88) is the Coleman-Weinberg result in disguise. Multiplying with the symmetry factor $-4N_f N_c = -24$ gives precisely the same logarithmic term in the ρ^2 contribution. The missing constant term simply originates in the different renormalisation procedure: with the present one all corrections to the relevant couplings including the constant parts are absorbed, that is $m_\varphi^2 \rightarrow m_{\varphi,r}^2$ and $\lambda_\varphi \rightarrow \lambda_{\varphi,r}$. As these couplings have to be fixed by appropriate infrared observables this is a convenient choice. In summary we have the following practical and consistent RG procedure:

- (0) Regularisation: Sharp momentum cutoff with $p^2 \leq \Lambda^2$ in all loops.
- (1) Renormalisation: Remove all divergent terms in the loop contributions. For the logarithmic term substitute $\ln\Lambda^2 \rightarrow \ln\Lambda_{\text{QCD}}^2$.
- (2) Renormalisation scheme: we demand $\partial_\rho V_{\phi,\text{eff}} = \partial_\rho V_{\phi,\text{UV}} + O(\rho^2) + \ln\rho$ -terms. This is arranged by the $-1/2$ in the bracket in (II.88). It enforces that the ρ -dependent pion mass function $m_\pi(\rho) = \partial_\rho V_{\phi,\text{eff}}(\rho)$ simply is $m_{\varphi,r}^2$ in

the symmetric regime, that is for vanishing ρ . Moreover, the linear term in ρ of m_π^2 is given by the UV coupling $\lambda_{\phi,r}$. This cannot be expressed within a Taylor expansion at $\rho = 0$ due to the logarithmic term.

- (3) Physics: The relevant parameters $h, m_{\varphi,r}, \lambda_{\varphi,r}$ and the explicit symmetry breaking scale c are fixed by the pion decay constant f_π , the physical pion and σ pole masses, $m_{\pi,\text{pol}}, m_{\sigma,\text{pol}}$ and the constituent quark mass $m_{q,\text{const}}$.

Depending on the values of $m_{\varphi,r}^2, \lambda_{\varphi,r}$, the effective potential in (II.88) has non-trivial minima or describes the symmetric phase. The effect of the fermionic quantum fluctuations is most easily accessed via the scale-running of the parameters in the 'classical' potential $V(\rho)$. Concentrating on the scale-dependence of the mass parameter m_φ^2 in (II.86) we conclude that lowering the cutoff scale Λ lowers the effective mass m_φ^2 . This entails that the fermionic quantum fluctuations indeed lower the mass parameter. Put differently, the quark fluctuations trigger chiral symmetry breaking.

Moreover, deep in the symmetric phase, that is for large Λ , the mesonic quantum fluctuations are suppressed in comparison to the quark fluctuations. In the vicinity of the symmetry breaking scale Λ_χ the mesonic fluctuations are getting massless, $m_\varphi \rightarrow 0$ and the mesonic fluctuations kick in. In turn, the effective quark mass grows in the chirally broken regime with $m_\psi = h/2\sigma_0$, and eventually the quark fluctuations are switched off for Λ below the constituent quark mass. ...

2. Mesonic quantum fluctuations

The remaining mesonic fluctuations can be treated at one loop similarly to the fermionic computation done above. The result is a Coleman-Weinberg type potential without the relative minus sign. Accordingly, the mesonic fluctuations work against chiral symmetry breaking. Due to the different scales and coupling sizes this is a marginal effect even in the chiral limit. In the physical scale with explicit chiral symmetry breaking and a pion mass of about 140 MeV the mesonic quantum fluctuations also decouple for scales Λ below the pion mass.

It is left to integrate-out the quantum fluctuations of the mesonic degrees of freedom in (II.74). Again concentrating on the low energy effective potential in the spirit of the lowest order of a derivative expansion we have

$$V_{\text{eff}}(\rho) = V_{\phi,\text{eff}}(\rho) + \Delta V_\phi(\rho) + c_\sigma \sigma \quad \text{with} \quad \Delta V_\phi(\rho) = \frac{1}{2} \text{Tr}_\Lambda \ln [-\partial_\mu^2 + m_\phi^2(\rho)], \quad (\text{II.89})$$

where ΔV_ϕ is the one loop approximation to the mesonic path integral (II.74) with the 'classical' potential $V_{\phi,\text{eff}}(\rho)$, and Tr_Λ sums over all momenta $p^2 \leq \Lambda^2$. In (II.89) we have re-introduced the linear term in σ that triggers the explicit symmetry breaking. In the present case ΔV_ϕ boils down to

$$\Delta V_\phi(\rho) = \frac{1}{4\pi^2} \int_0^\Lambda dp p^3 \left[3 \ln(p^2 + m_\pi^2(\rho)) + \ln(p^2 + m_\sigma^2(\rho)) \right]. \quad (\text{II.90})$$

For (II.90) we have used that we can evaluate the expressions for vanishing $\vec{\pi} = 0$ as done in the quark case. Then the mass matrix is diagonal, see (II.11), and reads for a given potential V

$$m_\pi^2(\rho) = \partial_\rho V(\rho), \quad m_\sigma^2(\rho) = \left(\partial_\rho + 2\rho \partial_\rho^2 \right) V(\rho). \quad (\text{II.91})$$

Accordingly, the factor three in front of the first term on the right hand side in (II.90) accounts for the $N_f^2 - 1 = 3$ pions. In the present case we have $V_{\phi,\text{eff}}(\rho)$ and the mass functions read

$$\begin{aligned} m_\pi^2(\rho) &= m_{\varphi,r}^2 + \left(\lambda_{\varphi,r} - \frac{3}{4\pi^2} h^4 \ln \frac{h^2 \rho}{2\Lambda_{\text{QCD}}^2} \right) \rho, \\ m_\sigma^2(\rho) &= m_{\varphi,r}^2 + 3 \left(\lambda_{\varphi,r} - \frac{1}{2\pi^2} - \frac{3}{4\pi^2} h^4 \ln \frac{h^2 \rho}{2\Lambda_{\text{QCD}}^2} \right) \rho \end{aligned} \quad (\text{II.92})$$

The integration in (II.91) is the same as in the quark case and we arrive at

$$\begin{aligned} \Delta V_\phi(\rho) = & \frac{3}{16\pi^2} \left[\Lambda^2 m_\pi^2 + m_\pi^4 \left[\ln \frac{m_\pi^2}{\Lambda^2} - \ln \left(1 + \frac{m_\pi^2}{\Lambda^2} \right) \right] + \Lambda^4 \ln \left(1 + \frac{m_\pi^2}{\Lambda^2} \right) \right] \\ & + \frac{1}{16\pi^2} \left[\Lambda^2 m_\sigma^2 + m_\sigma^4 \left[\ln \frac{m_\sigma^2}{\Lambda^2} - \ln \left(1 + \frac{m_\sigma^2}{\Lambda^2} \right) \right] + \Lambda^4 \ln \left(1 + \frac{m_\sigma^2}{\Lambda^2} \right) \right], \end{aligned} \quad (\text{II.93})$$

where m_π^2, m_σ^2 are the ρ -dependent masses defined in (II.91). Seemingly (II.93) introduces divergent terms that are neither proportional to ρ^0, ρ, ρ^2 due to ΔV_q in (II.91). However, (II.93) goes beyond one-loop (ΔV_q is already one-loop) and these terms are to be expected and can be removed within a consistent renormalisation procedure. Here, our simple renormalisation procedure discussed below (II.88) pays off. Then after renormalisation (II.93) turns into

$$\Delta V_\phi(\rho) = \frac{3}{16\pi^2} m_\pi^4 \left[\ln \frac{m_\pi^2}{\Lambda_{\text{QCD}}^2} - \frac{1}{2} \right] + \frac{1}{16\pi^2} m_\sigma^4 \left[\ln \frac{m_\sigma^2}{\Lambda_{\text{QCD}}^2} - \frac{1}{2} \right], \quad (\text{II.94})$$

where $m_\pi(\rho), m_\sigma(\rho)$ are derived from (II.91). As described in the discussion of the renormalisation scheme described below (II.88), the factor $-1/2$ in the brackets arrange for

$$m_{\text{eff},\pi}^2(\rho) = \partial_\rho V_{\text{eff}}(\rho) = m_{\varphi,r}^2 + \lambda_{\varphi,r,\rho} - \frac{3}{8\pi^2} \rho \ln \frac{h^2 \rho}{2\Lambda_{\text{QCD}}^2} + \frac{3}{8\pi^2} m_\pi^2 (\partial_\rho m_\pi^2) \ln \frac{m_\pi^2}{\Lambda_{\text{QCD}}^2}. \quad (\text{II.95})$$

From (II.94) we can proceed in several ways:

- (0) We drop ΔV_ϕ completely. As in (2) the missing quantum fluctuations are partially absorbed in the couplings $m_\varphi, \lambda_\varphi$. This approximation is also called 'extended mean field' in the literature. It is very close to the mean field approximation with $V_{\text{eff}}(\rho) = V(\rho)$, where we also drop ΔV_q .
- (1) As ΔV_q already is a one loop expression we drop it in the computation of (II.94). This leads us to a consistent one-loop computation. This amounts to dropping some quantum contributions in comparison to (1). However, as in (1) we have to fix the parameters $h, m_\varphi, \lambda_\varphi$ in the effective potential with the low energy observables. This implicitly absorbs (part of the) dropped contributions in these couplings. Differences between (1) and (2) only occur due to missing contributions in (2) in the couplings $\lambda_{\varphi,n}$ of the ρ^n -terms in V_{eff} with $n \geq 3$.
- (2) For the evaluation of (II.89) with $V + \Delta V_q$ in (II.88) and ΔV_ϕ in (II.94) we have to take into account that already the effective potential $V + \Delta V_q$ may not be convex. In non-convex regimes its second derivatives are not positive definite: $m_\pi < 0$ for $\rho < \rho_\pi$, where ρ_π is the solution of the reduced EoM: $V'_{\text{cl}}(\rho_\pi) + \Delta V'_q(\rho_\pi) = 0$. The σ mass also gets negative for even smaller ρ .

A simple resolution of this artefact of the approximation is to continue the result from larger $\rho \geq \rho_\pi$. The more consistent way is to resolve the related renormalisation group (RG) equation for the effective potential. The RG approach is able to deal consistently with the regimes with negative curvature which are indeed flattened out by quantum fluctuations. This effect cannot be seen in perturbation theory.

In any case the result of this computation is an effective potential $V_{\text{eff}}(\rho)$ which depends on the couplings $h, m_\varphi, \lambda_\varphi$. We either compute these couplings from QCD or we fix them with low energy observables such as the meson mass, the pion decay constant and the constituent quark mass. Here we use the latter way which is described in details below.

- (3) We solve the full renormalisation group equation, (II.82), for the effective potential, that governs its scale-dependence, see (II.96) below. Integrating the RG equation provides an iterative and fully consistent inclusion of the fluctuation effects. The RG is described in the chapter IIF 3 below, where it is also detailed how it boils down to the procedures (0)-(2) described above.

In the following we will consider all of these approximations, in particular at finite temperature and density. This allows us to evaluate the importance of the quantum (and later thermal) fluctuations as well as the stability of the results.

3. RG equation for the effective potential*

The present considerations are but one step away from a consistent treatment of the low energy effective theory with functional renormalisation group methods. For that purpose let us reconsider the RG equation for the ultraviolet potential V_{UV} derived from (II.82). Below (II.82) we have discussed the renormalisation group scaling that originates in the quark quantum fluctuations. In the general case the RG-scaling of the potential comes from both quark and meson fluctuations. This leads us to

$$\Lambda \partial_\Lambda V_{\text{UV}} = -\Lambda \partial_\Lambda (\Delta V_q + \Delta V_\phi) . \quad (\text{II.96})$$

(II.96) entails how the UV effective potential V_{UV} at a large cutoff scale Λ changes with lowering or increasing the cutoff scale. In the discussion so far we have concentrated on the UV relevant terms that scale with positive powers of the cutoff Λ . Then we ensured the cutoff independence of the full effective potential $V_{\text{eff}} = V_{\text{UV}} + \Delta V_q + \Delta V_\phi$ by an appropriate renormalisation procedure. The low energy quark and meson fluctuation are encoded in the terms $\Delta V_q + \Delta V_\phi$. Such a treatment assumes an asymptotically large cutoff scale.

Here we take a different point of view: iteratively lowering to cutoff scale Λ from large values (w.r.t. the non-perturbative infrared physics) leads to shifting more and more infrared fluctuations from $\Delta V_q + \Delta V_\phi$ to V_{UV} . Indeed, at $\Lambda = 0$ we have

$$V_{\text{eff}} = V_{\Lambda=0} , \quad \text{with} \quad V_\Lambda = V_{\text{UV},\Lambda} , \quad (\text{II.97})$$

the former 'UV' effective potential is the full quantum effective potential. Evidently, if the cutoff scale is not asymptotically large, also the UV-irrelevant terms cannot be neglected in (II.96). Note also that its right hand side has to be seen as a function of V_Λ , the one-loop computations done before indeed used V_Λ as a classical potential. Hence, it is only left to bring (II.96) in a form that only depends on V_Λ on both sides.

To that end we consider an infinitesimal RG step with $\Lambda^2 \rightarrow \Lambda^2(1 - \epsilon)$. This is governed by the path integral

$$Z \approx \int_{\Lambda^2(1-\epsilon)}^{\Lambda^2} [d\phi d\psi d\bar{\psi}] e^{-S_{\text{eff},\Lambda}[\psi, \bar{\psi}, \phi]} \quad \text{with} \quad e^{-S_{\text{eff},\Lambda}} \simeq Z_\Lambda . \quad (\text{II.98})$$

Now we exploit that each loop in a loop expansion of (II.98) is proportional to ϵ as it only takes into account momenta with $\Lambda^2(1 - \epsilon) \leq p^2 \leq \Lambda^2$. Hence, for $\epsilon \rightarrow 0$ the one-loop contribution is leading, and the ϵ -derivative can be converted in the Λ -derivative of the momentum integration boundary of the one-loop expressions for ΔV_q and ΔV_ϕ , (II.78) and (II.89) respectively. This leads us to

$$\Lambda \partial_\Lambda V_\Lambda = -\frac{1}{4\pi^2} \Lambda^4 \left[3 \ln \left(1 + \frac{m_\pi^2(\rho)}{\Lambda^2} \right) + \ln \left(1 + \frac{m_\sigma^2(\rho)}{\Lambda^2} \right) \right] + \frac{6}{\pi^2} \Lambda^4 \ln \left(1 + \frac{h^2}{2} \frac{\rho}{\Lambda^2} \right) , \quad (\text{II.99})$$

where

$$m_{\pi/\sigma}^2(\rho) = \Gamma_{\Lambda,\pi\pi/\sigma\sigma}^{(2)}(\rho, p=0) = V_{\Lambda,\pi\pi/\sigma\sigma}^{(2)}(\rho) , \quad \frac{h^2}{2} \rho = \Gamma_{\Lambda,\psi\bar{\psi}}^{(2)}(\rho, p=0) , \quad \text{with} \quad \Gamma_\Lambda^{(2)} = \Gamma_{\text{UV},\Lambda} , \quad (\text{II.100})$$

are the second derivatives of the scale-dependent 'UV' effective action Γ_Λ . We emphasise that the implicit Λ -dependence in $\Gamma^{(2)}$ is not hit by the ϵ -derivative.

The approximations (0)-(2) now follow from respective approximations of (II.99): For (0) we drop the meson fluctuations, for (1) we do not feed back the RG-running of V_{UV} on the right hand side of (II.99), for (2) we integrate out the quarks first. This is done with introducing separate cutoffs for quarks, Λ_q and mesons, Λ_ϕ and take the limit $\Lambda_q/\Lambda_\phi \rightarrow 0$.

Eq.(II.99) is the Wegner-Houghton equation [10] for the effective potential of the current Quark-Meson Model. For the sake of completeness we also quote the full Wegner-Houghton equation for the effective action: as the derivation of (II.99) simply follows from the RG-invariance of the generating functional Z , it also applies to the full effective action. Hence we conclude

$$\Lambda \partial_\Lambda \Gamma_\Lambda[\psi, \bar{\psi}, \phi] = -\frac{1}{2} \text{Tr}_{p^2=\Lambda^2} \ln \frac{\Gamma_{\phi\phi}^{(2)}}{\Lambda^2} + \text{Tr}_{p^2=\Lambda^2} \ln \frac{\Gamma_{\psi\bar{\psi}}^{(2)}}{\Lambda^2} , \quad (\text{II.101})$$

where the trace $\text{Tr}_{p^2=\Lambda^2} = \text{Tr} \delta(\sqrt{p^2} - \Lambda)$ only sums over the momentum shell with $p^2 = \Lambda^2$. Eq.(III.34) is, together with the Callan-Symanzik equation [11, 12], the first of many functional renormalisation group equations for the

effective action. These continuum RG equations are based on continuum version [13, 14] of the Kadanoff block spinning procedure on the lattice, [15], for the first seminal work on the RG see [16, 17]. In particular the pioneering work [16] already emphasises and details the full power of the renormalisation group, and is still very much underappreciated by the community.

4. EFT couplings

It is left to fix the couplings parameters in our low energy effective theory with the classical action S_{eff} defined (II.63). After integrating out the quarks and mesons we are led to the full low energy effective action Γ_{lowE} with

$$\Gamma_{\text{lowE}}[\psi, \bar{\psi}, \phi] = \int_x \bar{\psi} \cdot (\not{D} + m_\psi) \cdot \psi + \int_x [(\partial_\mu \sigma)^2 + \partial_\mu \vec{\pi}^2] + \int_x \frac{h}{2} \bar{\psi} [\sigma + i\gamma_5 \vec{\tau} \vec{\pi}] \psi + \int_x V_{\text{eff}}(\rho), \quad (\text{II.102})$$

with the effective potential $V_{\text{eff}} = V_{\phi, \text{eff}} + \Delta V_\phi + c\sigma$ defined in (II.89) with $V_{\phi, \text{eff}} = V_{\text{UV}} + \Delta V_q$. In the best approximation discussed here, $V_{\phi, \text{eff}}$ is given by (II.88) and ΔV_ϕ by (II.94). We have the fermion mass m_ψ or mesonic shift parameter c , the Yukawa coupling h , the mesonic mass parameter m_ϕ^2 and the mesonic self-coupling λ_ϕ . The fermion mass can be traded for the shift parameter c as argued before. The value of the latter determines the expectation value of the σ -field which is, in the present approximation, simply is the pion decay constant,

$$\sigma_0 = \langle \sigma \rangle = f_\pi, \quad f_\pi \approx 93 \text{ MeV}. \quad (\text{II.103})$$

The latter value related to the physical f_π 's (f_π^\pm, f_π^0) measured in the experiment. Consequently c could be dropped, we simply evaluate the theory on this expectation value. Accordingly, h is determined by the constituent quark mass,

$$m_{\psi, \text{con}} = \frac{1}{2} h \langle \sigma \rangle = \frac{1}{2} h f_\pi \quad \longrightarrow \quad h \approx 6.45 \quad \text{with} \quad m_{\psi, \text{con}} \approx 300 \text{ MeV}. \quad (\text{II.104})$$

Note that the constituent quark masses of the quarks depend on the model and approximation used, typical values for up and down quark masses are $m_{\psi, \text{con}} \approx 340 \text{ MeV}$ in full QCD. A reduced value in (II.104) for two flavour QCD is common place in the $N_f = 2$ quark-meson model. The related observable is the chiral condensate,

$$\langle \bar{\psi}(x) \psi(x) \rangle = - \int \frac{d^4 p}{(2\pi)^4} \text{tr} \langle \psi(p) \bar{\psi}(-p) \rangle, \quad (\text{II.105})$$

where the trace sums over Dirac and flavour indices.

Finally we have to fix λ_ϕ and m_ϕ with the Yukawa coupling and σ -expectation value σ_0 deduced above, see also Table II. Note also, that a potential further input is the value of the pion decay constant in the chiral limit,

$$f_{\pi, \chi} = f_\pi(m_\pi = 0) \approx 88 \text{ MeV}, \quad (\text{II.106})$$

which can be determined with chiral perturbation theory, functional continuum methods or from chiral extrapolations of lattice results at different finite pion masses. This leaves us with a triple of 'observables' ($m_\pi, m_\sigma, f_{\pi, \chi}$), see Table II, and a triple of EFT couplings ($m_\phi, \lambda_\phi, c_\sigma$). Note that the inclusion of $f_{\pi, \chi}$ as an 'observable' relates to the correct chiral dynamics reflected in the curvature and four-meson interaction in the chiral limit. The pion and sigma masses are related to those found in the Particle Data Booklet (2016), [18] of the Particle Data Group (PDG). Here, the pion mass is taken between that of the charged pions π^\pm with $m_{\pi^\pm} \approx 139.57 \text{ MeV}$ and the neutral pion π^0 with $m_{\pi^0} \approx 134.98 \text{ MeV}$, and the mass of the sigma meson is taken to be that of the $f_0(500)$, see [19], that is $m_\sigma \approx 450 \text{ MeV}$, despite the f_0 certainly not being a simple $q\bar{q}$ state. The unclear nature of the value of m_σ is one of the biggest uncertainties for low energy EFTs. Typically, its values range from 400–550 MeV, see PDG, [18].

Seemingly, this leaves us with as many unknowns as physics input. However, c can be determined from the pion mass and the pion decay constant with $m_\pi^2 = \partial_\rho V_{\text{eff}}(\rho_0)$ and $\rho_0 = \sigma_0^2/2 = f_\pi^2/2$. This follows from the EoM for σ ,

$$\partial_\sigma V_{\text{eff}}(\rho_0) = \sigma_0 m_\pi^2 = c_\sigma \quad \longrightarrow \quad c_\sigma = f_\pi m_\pi^2 \approx 1.77 * 10^6 \text{ MeV}^3. \quad (\text{II.107})$$

We conclude that in the current approximation to the UV effective action, the pion decay constant in the chiral limit, $f_{\pi, \chi}$, is a prediction.

Here we present a crude (mean-field) estimate of its value based on the assumption of being close to the chiral limit.

Observables	Value [MeV]	EFT couplings	Value
f_π	93	$\sigma_0 = f_\pi$	93 MeV
m_{con}	300	$h = \frac{2m_{\text{con}}}{f_\pi}$	6.45
m_π	138	m_ϕ	$m_\phi(m_\pi, m_\sigma)$
m_σ	450	λ_ϕ	$\lambda_\phi(m_\pi, m_\sigma)$
$f_{\pi,\chi}$	88	$c_\sigma = f_\pi m_\pi^2$	$1.77 * 10^6 \text{MeV}^3$

TABLE II: Low energy observables and related EFT couplings as used for the $N_f = 2$ computations. While the σ -expectation value σ_0 and the Yukawa coupling are directly related to pion decay constant and constituent quark masses in the present approximations, the other EFT couplings depend on the approximations (0)–(3) described below (II.95).

It is based on the expansion of the full effective potential about the unperturbed minimum in the broken phase,

$$V_{\text{eff}} = \sum_{n=2}^{\infty} \frac{\lambda_n}{n!} (\rho - \kappa)^n + c_\sigma \sigma, \quad \text{with} \quad \kappa = \frac{f_{\pi,\chi}^2}{2}, \quad \lambda_2 = \lambda_{\phi,\text{eff}}. \quad (\text{II.108})$$

Close to the chiral limit the difference $(f_\pi - f_{\pi,\chi})/f_\pi \ll 1$ is small. In the vicinity of the unperturbed minimum κ the full effective potential can be written as

$$V_{\text{eff}} = \frac{\lambda_{\phi,\text{eff}}}{2} (\rho - \kappa)^2 + c_\sigma \sigma + O\left((\rho - \kappa)^2\right). \quad (\text{II.109})$$

Dropping the higher terms leads us to

$$m_\pi^2 = \lambda_{\phi,\text{eff}} \frac{f_\pi^2 - f_{\pi,\chi}^2}{2}, \quad m_\sigma^2 = \lambda_{\phi,\text{eff}} \frac{3f_\pi^2 - f_{\pi,\chi}^2}{2}. \quad (\text{II.110})$$

In this leading order, the mesonic self-coupling drops out of the relation for $f_{\pi,\chi}$ and we arrive at the estimate

$$f_{\pi,\chi} = f_\pi \sqrt{\frac{1 - 3\frac{m_\pi^2}{m_\sigma^2}}{1 - \frac{m_\pi^2}{m_\sigma^2}}} \approx 83 \text{ MeV}, \quad \text{and} \quad \lambda_{\phi,\text{eff}} = \frac{m_\sigma^2 - m_\pi^2}{f_\pi^2} \approx 21.2. \quad (\text{II.111})$$

This is a very good agreement with the theoretical prediction of $f_{\pi,\chi} \approx 88 \text{ MeV}$, in particular given the crude nature of the present estimate. Beyond the current mean field level it improves further Still, the current EFT makes a prediction for either $f_{\pi,\chi}$ or m_σ , and the question arises which of them should be taken as a physics input: we first note that $f_{\pi,\chi} \approx 88 \text{ MeV}$ is under far better theoretical control than the mass of the σ -meson. Apart from the difficulties of

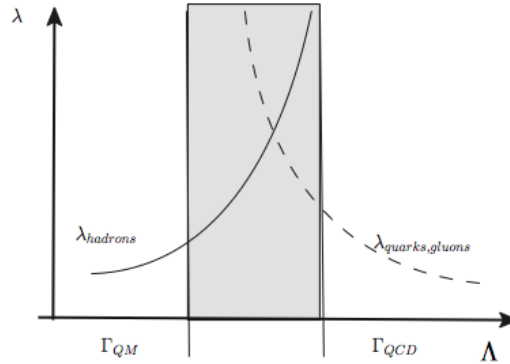


FIG. 9: Scale dependence of the effective four-fermi coupling. The shaded area is the regime where the effective field theory is triggered.

identifying directly the σ -mesons in the EFT's at hand with a resonance in the particle spectrum, it has a large width. Hence it cannot be assumed that the curvature mass $m_{\sigma,\text{curv}}$ we use here is in good agreement with the pole mass $m_{\sigma,\text{pol}}$, see the discussion at the end of chapter II B. This is in stark contradistinction to the pion masses where the (non-trivial) identification $m_{\pi,\text{curv}} \approx m_{\pi,\text{pol}}$ holds true on the percent level. This suggests to adjust m_σ such that $f_{\pi,\chi} \approx 88$ MeV. In the mean field discussion done here this leads to $m_\sigma^2 \approx 600 - 650$ MeV. Note that with a future better determination of the curvature mass $m_{\sigma,\text{curv}}$ a semi-quantitative EFT might require higher order mesonic UV-couplings such as $\lambda_{3,\text{UV}} \neq 0$ in (II.109). This is related to the fact that the physical UV cutoff $\Lambda_{\text{UV}} \approx 1$ GeV, at which the low energy EFT is initiated, is less than one order of magnitude larger than the physical scales.

This discussion completes our EFT picture of chiral symmetry breaking in QCD. In essence it also extends to the $N_f = 2 + 1$ flavour case and beyond, then, however, a consistent determination of the low energy couplings including the correct chiral dynamics, e.g. $f_{\pi,\chi}$ is far more intricate.

III. CHIRAL PHASE TRANSITION

In the last chapter we have learned that chiral symmetry breaking is triggered by the quark fluctuations, while the mesonic low energy fluctuations work against symmetry breaking. The symmetry breaking scale Λ_χ is of the order of 300-400 MeV.

The vacuum physics is used to fix the parameters of the low energy effective theory such as the mesonic mass function, the Yukawa coupling, and the expectation value of the radial mode, $\langle\sigma\rangle$. The related observables are the pion and sigma pole masses, the constituent quark mass as well as the pion decay constant.

In heavy ion collisions or the early universe the temperature is/has been high of the order of hundreds of MeV. In Kelvin this translates into $100\text{ MeV} \approx 1.16 * 10^{12}$ Kelvin. It is expected that a high temperatures the system undergoes a phase transition to the chirally symmetric phase. As a rough estimate the phase transition temperature T_c is expected to be of the order of the chiral symmetry breaking scale Λ_χ which itself has been argued to be of the order of Λ_{QCD} , the only intrinsic scale in QCD.

A. Mesons at finite temperature

For a more quantitative investigation we need a thermal formulation of QCD or at least of the low energy effective theory we have derived in the previous chapter. Here we give a brief introduction to the -Euclidean- path integral at finite temperature, where we follow the introduction of the path integral in chapter 1, QFT II. We start with the partition function of a scalar theory at finite temperature

$$Z_T = \text{Tr} e^{-\beta\hat{H}} = \sum_n e^{-\beta E_n} \quad \text{with} \quad \beta = \frac{1}{T} \quad \text{and} \quad \hat{H}|n\rangle = E_n|n\rangle, \quad (\text{III.1})$$

with the Hamiltonian operator of a scalar theory

$$\hat{H}[\hat{\phi}, \hat{\pi}] = \int d^3x \left[\frac{1}{2}\hat{\pi}^2 + \frac{1}{2}(\vec{\nabla}\hat{\phi})^2 + V(\hat{\phi}) \right]. \quad (\text{III.2})$$

with field operator $\hat{\phi}$ and field momentum operator $\hat{\pi}$. In (III.1) we dropped the source term for the sake of brevity. Eq.(III.1) is the standard statistical partition function at finite temperature well known from quantum mechanics. Now we rewrite this partition function in terms of a basis in field and canonical momentum space. First we note that the trace in (III.1) can be rewritten in terms of field eigenstates with

$$\text{Tr} e^{-\beta\hat{H}} = \int d\phi \langle\phi| e^{-\beta\hat{H}} |\phi\rangle \quad \text{with} \quad \hat{\phi}(\vec{x})|\phi\rangle = \phi(\vec{x})|\phi\rangle, \quad (\text{III.3})$$

with the eigenvalues $\phi(\vec{x})$. Moreover, the statistical operator $e^{-\beta\hat{H}}$ can be interpreted as the evolution operator $U(0, i\beta)$ in an imaginary time from the initial state $|\phi(t_i)\rangle$ at $t_i = 0$ to the final state $|\phi(t_f)\rangle$ at $t_f = i\beta$ with

$$U(0, i\beta) = e^{i\hat{H}(t_f - t_i)} \quad \text{and} \quad |\phi(t_f)\rangle = |\phi(t_i)\rangle. \quad (\text{III.4})$$

The identification of initial and final state is the trace condition in (III.3). Now we simply repeat all the steps for the derivation of the path integral of a scalar theory. Also adding a source term we arrive at

$$Z_T[J] = \int_{\phi(\beta, \vec{x}) = \phi(0, \vec{x})} d\phi e^{-S_T[\phi] + \int_0^\beta d^4x J(t, \vec{x})\phi(\vec{x})}, \quad (\text{III.5})$$

with the periodic fields $\phi(t + \beta, \vec{x}) = \phi(t, \vec{x})$ and the finite temperature action $S_T[\phi]$ with

$$S_T[\phi] = \int_0^\beta d^4x \left[\frac{1}{2}(\partial_\mu\phi)^2 + V(\phi) \right], \quad \text{where} \quad \int_0^\beta d^4x = \int_0^\beta dt \int d^3x. \quad (\text{III.6})$$

Accordingly, the path integral of a finite temperature field theory is related to a Euclidean path integral with a finite time extent in imaginary time $t \in [0, \beta]$. Note that this time does *not* describe the time evolution of the system but simply the statistical nature of the thermal partition function. The real time correlation function are obtained by a Wick rotation, for more details see finite temperature quantum field theory books such as Le Bellac or Kapusta. The

correlation functions are periodic in imaginary time,

$$\langle \phi(x_1) \cdots \phi(t_i + \beta, \vec{x}) \cdots \phi(x_n) \rangle = \langle \phi(x_1) \cdots \phi(t_i, \vec{x}) \cdots \phi(x_n) \rangle. \quad (\text{III.7})$$

Finally we want to repeat the computation of the effective potential in the last chapter section IIF at finite temperature. This is done in momentum frequency space and we would like to illustrate the differences at finite temperature at the important example of the propagator

$$G_\phi(x - y) = \langle \phi(x)\phi(y) \rangle - \langle \phi(x) \rangle \langle \phi(y) \rangle. \quad (\text{III.8})$$

The propagator in spatial momentum and frequency space is given by

$$G_\phi(\omega_n, \vec{p}) = \int_0^\beta d^4x e^{i(\omega_n t + \vec{p}\vec{x})} G_\phi(t, \vec{x}), \quad \text{where} \quad \omega_n = 2\pi T n, \quad \text{with} \quad n \in \mathbb{Z}. \quad (\text{III.9})$$

The discrete frequencies ω_n are called Matsubara frequencies and originate in the finite imaginary time extent. The frequency Fourier transformation back gives

$$G_\phi(t, \vec{p}) = \sum_{n \in \mathbb{Z}} e^{-i\omega_n t} G_\phi(\omega_n, \vec{p}), \quad (\text{III.10})$$

which has the necessary periodicity in imaginary time, $G(t + \beta, \vec{p}) = G(t, \vec{p})$, of a correlation function, see (III.7). In frequency and spatial momentum space the classical propagator looks the same as in the vacuum. We have

$$G_\phi(\omega_n, \vec{p}) = \frac{1}{\omega_n^2 + \vec{p}^2 + m^2} \quad \text{with} \quad m^2(\phi) = \partial_\phi^2 V(\phi). \quad (\text{III.11})$$

While the Fourier transformation w.r.t. spatial momentum is also the same as at $T = 0$, that w.r.t. frequency changes. Here we discuss the Fourier transformation for $t = 0$ for the mixed representation $G_\phi(t, \vec{p})$,

$$G_\phi(t = 0, \vec{p}) = T \sum_{n \in \mathbb{Z}} \frac{1}{\omega_n^2 + \vec{p}^2 + m^2} = \frac{1}{2\epsilon_p^\phi} \coth \beta \epsilon_p^\phi = \frac{1}{2\epsilon_p^\phi} [1 + 2n_B(\epsilon_p^\phi)], \quad (\text{III.12})$$

with the dispersion ϵ_p^ϕ and the thermal distribution function $n_B(\omega)$ given by

$$\epsilon_p^\phi(m) = \sqrt{\vec{p}^2 + m^2}, \quad n_B(\omega) = \frac{1}{e^{\beta|\omega|} - 1} \quad (\text{III.13})$$

The latter is the standard Bose-Einstein distribution and clearly shows the thermal nature of the Matsubara path integral.

As a warm-up of the computation for the effective potential in the quark-meson theory at finite temperature we compute that of the scalar theory used here as an example. Its thermal part is related to the thermal pressure of the theory with potential. To that end we remind ourselves that the scalar free energy density Ω_ϕ and the pressure of the theory are given by

$$Z_T[0] = e^{-\beta \mathcal{V} \Omega_\phi}, \quad p_\phi = -\frac{\partial \mathcal{V} \Omega_\phi}{\partial \mathcal{V}} \quad \text{with} \quad \mathcal{V} = \int d^3x. \quad (\text{III.14})$$

The one-loop contribution to the free energy density and pressure are hence given by

$$\Omega_\phi \simeq \frac{1}{2\mathcal{V}} T \text{Tr} \ln(-\partial_\mu^2 + m^2) = \frac{1}{2} T \sum_{n \in \mathbb{Z}} \int \frac{d^3p}{(2\pi)^3} \ln(\omega_n^2 + \vec{p}^2 + m^2), \quad p_\phi \simeq -\frac{1}{2} T \sum_{n \in \mathbb{Z}} \int \frac{d^3p}{(2\pi)^3} \ln(\omega_n^2 + \vec{p}^2 + m^2), \quad (\text{III.15})$$

where we dropped the normalisations in Ω_ϕ and p_ϕ . We also remind the reader that $m^2 = m^2(\phi)$ as introduced in (III.11). Note also that the pressure is nothing but (minus) the effective potential at finite temperature. At vanishing temperature we encountered singularities in the computation of the effective potential proportional to Λ^4, λ^2 and $\ln \Lambda$ that had to be absorbed in the bare couplings. The highest singularity proportional to Λ^4 we disregarded as the absolute value of the potential energy which cannot be measured. The expressions in (III.15) are also infinite,

showing the standard divergence of zero point functions at vanishing temperature. Similarly, we could introduce a spatial momentum cutoff Λ with $p^2 \leq \Lambda^2$ and proceed as in the last chapter. In the following we shall not make this cutoff explicit for the following reason: it is one of the cornerstones, and can be proven in thermal field theory all singularities are temperature-independent. This statement can be understood heuristically as the ultraviolet singularities are short-distance singularities. At short-distance singularities the finite extent in time-direction cannot be accessed. For detailed discussions we refer to the literature, here this fact will simply come out.

For the computation we take the mass (squared) derivative of the pressure, $\partial_{m_\phi^2} p$. This removes the logarithm from the expression and leaves us with integrals and sums that can be computed by complex analysis. The mass-derivative of the pressure is related to the momentum integral of the propagator in the mixed representation $G(0, \vec{p})$ computed in (III.12),

$$\partial_{m^2} p_\phi \simeq -\frac{1}{2} \int \frac{d^3 p}{(2\pi)^3} G_\phi(0, \vec{p}) = -\frac{1}{4} \int \frac{d^3 p}{(2\pi)^3} \frac{1}{\epsilon_p^\phi} [1 + 2n_B(\epsilon_p^\phi)]. \quad (\text{III.16})$$

Eq.(III.16) entails that the mass-derivative of the pressure, and hence the pressure, only carries a temperature-independent singularity proportional to $1/\epsilon_p^\phi$. The term proportional to n_B vanishes in the zero temperature limit. Upon integration over m^2 the pressure is given by

$$p_\phi \simeq - \int \frac{d^3 p}{(2\pi)^3} \left[\frac{1}{2} \epsilon_p^\phi + T \ln \left(1 - e^{-\beta \epsilon_p^\phi} \right) \right]. \quad (\text{III.17})$$

The singular, temperature-independent piece pressure in (III.17) proportional to ϵ_p^ϕ is nothing but the effective potential at vanishing temperature which we have computed for a fermionic theory in the last chapter. Its renormalisation can be performed analogously. Here we are only interested in the thermal pressure, and we subtract the pressure at vanishing temperature,

$$\begin{aligned} p_{\phi, \text{thermal}} &= p_\phi(T) - p_\phi(T=0) \\ &= -T \int \frac{d^3 p}{(2\pi)^3} \ln \left(1 - e^{-\beta \epsilon_p^\phi} \right) = -\frac{T}{2\pi^2} \int_0^\infty dp p^2 \ln \left(1 - e^{-\beta \epsilon_p^\phi} \right). \end{aligned} \quad (\text{III.18})$$

Eq.(III.18) is manifestly finite as for large momenta $p^2 \gg m_\phi^2, T^2$ the exponential in the logarithm decays with $\exp(-p/T)$, the typical thermal decay. It is also positive as the argument in the logarithm is always smaller than one and hence the logarithm is strictly negative. With the minus sign in front of the integral this leads to a positive expression, as expected for a thermal pressure. For a given temperature (III.18) takes its maximal value for $m_\phi^2 = 0$ and decays monotonously with increasing m_ϕ^2 as the thermal part of the mass-derivative is negative, see (III.16). For $m_\phi^2 \rightarrow \infty$ the thermal pressure vanishes. Accordingly the pressure is positive for all m_ϕ^2 . For large masses $m_\phi \gg T$ the pressure decays exponentially with $\exp(-m_\phi/T)$ (up to polynomial prefactors). For vanishing masses the momentum integration can be performed easily and we arrive at

$$p_{\phi, \text{thermal}}|_{m^2=0} = \frac{\pi^2 T^4}{90}. \quad (\text{III.19})$$

The explicit result for vanishing mass is the Stefan-Boltzmann pressure of a free gas. It is the tree-level thermal pressure. Note also that (III.18) is the result for the thermal part of the (one-loop) effective potential of a bosonic theory, see (III.18).

Now we have collected all results for discussing the mesonic fluctuations in our $N_f = 2$ low energy effective theory. The mesonic contribution to the pressure and hence to minus the free energy density/effective potential are simply given by summing up (III.18) for the sigma and the three pions leading to

$$\left[\Omega_{\phi, T}(\phi) - \Omega_{\phi, T=0}(\phi) \right]_{\text{mes. flucs.}} \simeq \frac{T}{2\pi^2} \int_0^\infty dp p^2 \ln \left(1 - e^{-\beta \epsilon_p^\phi(m_\sigma)} \right) + 3 \frac{T}{2\pi^2} \int_0^\infty dp p^2 \ln \left(1 - e^{-\beta \epsilon_p^\phi(m_\pi)} \right), \quad (\text{III.20})$$

The concentration on the thermal part of the fluctuations allows us to simply add (III.20) to the low energy effective action at vanishing temperature regardless of how we have treated the mesonic fluctuations there. Note also in this context that (III.20) is finite as it should be: in thermal field theory all UV divergences can be treated already in the $T = 0$ case and the subtractions can be chosen to be temperature-independent.

In (III.20) this comes about as it only summarises the thermal fluctuations and momentum fluctuations with

$p \gg T$ are suppressed. Accordingly in the context of our low energy EFT setup (III.20) is only valid for $T/\Lambda \ll 1$. For larger temperatures already the Matsubara sum that takes account of high frequencies is at odds with the fact that $p_0^2 + \vec{p}^2 \leq \Lambda^2$.

B. Quarks at finite temperature

In summary we are but one step away from our goal of accessing the thermal chiral phase transition in QCD in the quark-meson EFT. For that task we need to translate the results above to the -free- quark path integral. The computation of the last chapter in the vacuum carries over here, we only have to discuss the fermionic Matsubara frequencies. For that end we redo the derivation of the thermal path integral for fermions again by starting from partition function Z_T as defined in the scalar case in (III.1). Everything goes as in the scalar case except one subtlety concerning the trace. Again more details can be found in the QFT II lecture notes, chapter 2. As in the case of the bosonic field we need coherent states that allow us to define $\hat{\psi}|\psi\rangle = \psi|\psi\rangle$. For the sake of the argument we restrict ourselves to one creation and annihilation operator a, a^\dagger and Grassmann variable c . A coherent state is given by

$$|c\rangle = (1 - c a^\dagger)|0\rangle = e^{-c a^\dagger}|0\rangle \quad \text{with} \quad a|c\rangle = c a a^\dagger|0\rangle = c|0\rangle = c(1 - c a^\dagger)|0\rangle = c|c\rangle, \quad (\text{III.21})$$

where the latter property proves the coherence property of the state. The dual state $\langle c| = |c\rangle^\dagger$ has the property

$$\langle c|a^\dagger = -\langle c|c^*. \quad (\text{III.22})$$

In consequence, instead of periodicity of the fields in time in the scalar case coming from the trace in (III.1) we have anti-periodicity,

$$\psi(t + \beta, \vec{x}) = -\psi(t, \vec{x}), \quad (\text{III.23})$$

that reflects the Grassmannian nature of the fermionic field. The fermionic path integral Z_q with the Dirac action at finite temperature then reads

$$Z_{q,T}[J] = \int_{\psi(\beta, \vec{x}) = -\psi(0, \vec{x})} d\bar{\psi} d\psi e^{-S_{D,T}[\phi] + \int_0^\beta d^4x \bar{J}_\psi(t, \vec{x})\psi(\vec{x}) - \bar{\psi} J_\psi}, \quad S_{D,T}[\psi] = \int_0^\beta d^4x \bar{\psi} \cdot (\not{D} + m_\psi + i\gamma_0\mu) \cdot \psi. \quad (\text{III.24})$$

As in the scalar case we can reveal the thermal nature of correlation functions derived from the generating functional (III.24) by looking at the Dirac propagator of the quarks in the mixed representation at vanishing time, $G_q(t, \vec{p})$. To that end we first notice that the Fourier transformation of the anti-periodic fermionic fields is reflected in a shift of the Matsubara modes by πT . We have

$$\psi(x) = T \sum_{n \in \mathbb{Z}} \int \frac{d^3p}{(2\pi)^3} e^{-i(\omega_{n,f}t + \vec{p}\vec{x})} \psi(p_0, \vec{p}), \quad \omega_{n,f} = 2\pi \left(n + \frac{1}{2} \right), \quad (\text{III.25})$$

where the additional factor $e^{i\pi T t}$ leads to the minus sign in the periodicity relation (III.23) with $e^{i\pi T(t+\beta)} = e^{i\pi} e^{i\pi T t} = -e^{i\pi T t}$. Now we perform the computation for the frequency sum of the quark propagator G_q with N_f flavours and N_c colors,

$$\frac{1}{m_\psi} \frac{1}{4N_f N_c} \text{tr} G_q(t=0, \vec{p}) = T \sum_{n \in \mathbb{Z}} \frac{1}{\omega_{n,f}^2 + \vec{p}^2 + m_\psi^2} = \frac{1}{2\epsilon_p^\psi} \tanh \beta \epsilon_p^\psi = \frac{1}{2\epsilon_p^\psi} [1 + 2n(\epsilon_p^\psi)], \quad (\text{III.26})$$

where the trace tr in (III.26) sums over flavour, color and Dirac space. The dispersion ϵ_p and the thermal distribution function $n(\omega)$ are given by

$$\epsilon_p^\psi(m_\psi) = \sqrt{\vec{p}^2 + m_\psi^2}, \quad n_F(\omega) = \frac{1}{e^{\beta\omega} + 1}. \quad (\text{III.27})$$

The latter is the expected Fermi-Dirac distribution. The difference to the Bose-Einstein statistics in the scalar case originates in the anti-periodicity of the fermions related to their Grassmannian nature. The free energy and pressure can be derived analogously to the scalar case. The one-loop contribution to the quark free energy density Ω_q and the

pressure are hence given by

$$\begin{aligned}\Omega_q &\simeq -\frac{T}{2\mathcal{V}} \text{Tr} \ln(-\partial_\mu^2 + m^2) = -2N_c N_f T \sum_{n \in \mathbb{Z}} \int \frac{d^3 p}{(2\pi)^3} \ln(\omega_{n,f}^2 + \vec{p}^2 + m^2), \\ p_q &\simeq 2N_c N_f T \sum_{n \in \mathbb{Z}} \int \frac{d^3 p}{(2\pi)^3} \ln(\omega_{n,f}^2 + \vec{p}^2 + m^2) = 12T \sum_{n \in \mathbb{Z}} \int \frac{d^3 p}{(2\pi)^3} \ln(\omega_{n,f}^2 + \vec{p}^2 + m^2),\end{aligned}\quad (\text{III.28})$$

where as in the scalar case we dropped the normalisations in Ω_q and p_q . For the pressure we have also inserted the $N_f = 2, N_c = 3$ case discussed here.

For a first simple computation we also use $\mu = 0$, a vanishing quark chemical potential. The prefactor -2 in comparison to the prefactor $1/2$ in the scalar case comes from the relative minus sign and factor 2 of the fermionic loop, the symmetrisation of the frequency and spatial momentum trace and the Dirac trace: $-1 * 1/2 * 4 = -2$ instead of $1/2$ in the scalar case. The factor $N_c N_f$ counts the degrees of freedom. For the computation of the thermal pressure we proceed similar to the scalar case with a m_ψ^2 -derivative which maps the pressure to (III.26). We also remove the divergent vacuum contribution which is the effective potential at vanishing temperature, see (II.88). The grand potential and thermal quark pressure in the $N_f = 2$ case is then given by

$$\Omega_{q,T}(\psi, \bar{\psi}, \phi) - \Omega_{q,T=0}(\psi, \bar{\psi}, \phi) = -\frac{12}{\pi^2} T \int_0^\infty dp p^2 \ln\left(1 + e^{-\beta \epsilon_p^\psi}\right) = -p_{q,\text{thermal}}, \quad (\text{III.29})$$

where

$$m_\psi^2(\phi) = \frac{1}{2} h^2 \rho. \quad (\text{III.30})$$

This has to be compared with (III.20) for the mesons. Both expressions for the pressure are strictly positive which is due to

$$\mp \ln\left(1 \mp e^{-\beta \epsilon_p^{\phi/\psi}}\right) \geq 0, \quad (\text{III.31})$$

with the minus signs in the bosonic case and the plus sign in the fermionic one. The global \mp in (III.31) reflects the relative sign of fermionic and bosonic loops while the \mp reflects the Bose-Einstein vs Fermi-Dirac quantum statistics.

The sum of (III.20) and (III.38),

$$\Omega_T(\psi, \bar{\psi}, \phi) - \Omega_{T=0}(\psi, \bar{\psi}, \phi) = \Omega_{\phi,T} + \Omega_{q,T} - \Omega_{\phi,T=0} + \Omega_{q,T=0} \quad (\text{III.32})$$

encodes all thermal fluctuations on one loop. As in the vacuum case for $T = 0$ we have several possibilities of how to integrate out the thermal fluctuations, e.g. either in parallel or successively. Even though being relevant for the quantitative results, it is irrelevant for the access of the mechanism of chiral symmetry restoration at large temperatures: At large temperatures the quark exhibits a Matsubara gapping as the lowest lying Matsubara mode is πT in comparison to the vanishing one in the mesonic case. For higher temperatures more and more of the infrared quark fluctuations are gapped. However, the quark fluctuations triggers strong chiral symmetry breaking in the first place. Consequently at large enough temperatures chiral symmetry breaking is melted away.

C. RG for the effective potential at finite temperature*

For quantitative statements the RG equation as in chapter II F 3 or similar non-perturbative techniques such as Dyson-Schwinger equations or 2PI/nPI techniques (2-particle irreducible/n-particle irreducible) should be used. Here we just extend the Wegner-Houghton equation we have derived for the $T = 0$ case in chapter II F 3. There we have the frequency and spatial momentum integration with an $O(4)$ -dimensional momentum cutoff with $p^2 \geq \Lambda^2$ in the integrals.

At finite temperature the four-momentum is given by $(2\pi T)^2 n^2 + \vec{p}^2$ and the related θ -function is $\theta(2\pi T)^2 n^2 + \vec{p}^2 - \Lambda^2$. A four dimensional cutoff leads to discontinuous flows as it jumps if we sweep over one of the Matsubara modes. In (III.34) we would have to substitute

$$\text{Tr}\delta(\sqrt{p^2} - \Lambda) \rightarrow \text{Tr}\delta(\sqrt{(2\pi T)^2 n^2 + \vec{p}^2} - \Lambda), \quad (\text{III.33})$$

which makes the non-analyticity apparent. Even though the spatial momentum integration smoothens the non-analyticity, it is present and hampers in particular the simple computation of the thermodynamical properties such as the pressure, see [20]. This is not a conceptual problem as these jumps have to be absorbed in the Λ -dependence of the initial condition, it hampers explicit computations.

For that reason we choose a spatial momentum cutoff $p^2 > \Lambda^2$, leading us to the functional Wegner-Houghton equation

$$\Lambda \partial_\Lambda \Gamma_\Lambda[\psi, \bar{\psi}, \phi] = -\frac{1}{2} \text{Tr}_{\bar{p}^2=\Lambda^2} \ln \frac{\Gamma_{\phi\phi}^{(2)}}{\Lambda^2} + \text{Tr}_{\bar{p}^2=\Lambda^2} \ln \frac{\Gamma_{\psi\bar{\psi}}^{(2)}}{\Lambda^2}, \quad (\text{III.34})$$

where the trace

$$\text{Tr}_{\bar{p}^2=\Lambda^2} = T \sum_n \int \frac{d^3 p}{(2\pi)^3} \delta(\sqrt{p^2} - \Lambda), \quad (\text{III.35})$$

now only sums over the spatial momentum shell with $p^2 = \Lambda^2$, but over all Matsubara modes. In the line of the arguments in chapter IIF 3 this cutoff is now applied to all fluctuations and not only to the thermal ones.

Practically our computations so far allow us to read off the flow equation for the effective potential. For the meson part we start with (III.17) for a scalar mode, leading to

$$\Omega_{\phi,\Lambda} \simeq \frac{1}{2\pi^2} \int_\Lambda^{\Lambda_{UV}} dp p^2 \left[\frac{1}{2} \epsilon_p^\phi + T \ln \left(1 - e^{-\beta \epsilon_p^\phi} \right) \right] + \Omega_{\phi,\Lambda_{UV}}, \quad (\text{III.36})$$

including the vacuum part. Hence, we simply read-off (minus) the integrand as the Λ -derivative of Ω_ϕ . Applying this immediately to the mesonic part of our EFT we arrive at

$$\Lambda \partial_\Lambda \Omega_{\phi,\Lambda}(\phi) = -\frac{\Lambda^3}{2\pi^2} \left\{ \frac{1}{2} \left[\epsilon_\Lambda^\phi(m_\sigma) + \frac{3}{2} \epsilon_\Lambda^\phi(m_\pi) \right] + T \left[\ln \left(1 - e^{-\beta \epsilon_\Lambda^\phi(m_\sigma)} \right) + \ln \left(1 - e^{-\beta \epsilon_\Lambda^\phi(m_\pi)} \right) \right] \right\}, \quad (\text{III.37})$$

where the spatial momentum arguments in the dispersions ϵ_p^ϕ are now taken at the cutoff scale, $p = \lambda$. The first two terms on the right hand side is the $T = 0$ flow as the second term vanishes for $T = 0$. It is different from its counterpart in (II.99) as (III.37) only involves a spatial momentum cutoff, reflected in the cubic power of Λ .

The derivation of the quark part of the flow proceeds similarly. We start with the expression for Ω_q or $-p_q$ after integration of the Matsubara frequency, (III.38) and restore the $T = 0$ part,

$$\Omega_{q,\Lambda}(\psi, \bar{\psi}, \phi) = -\frac{12}{\pi^2} \int_\Lambda^{\Lambda_{UV}} dp p^2 \left[\epsilon_p^\psi + T \ln \left(1 + e^{-\beta \epsilon_p^\psi} \right) \right] + \Omega_{q,\Lambda_{UV}}(\psi, \bar{\psi}, \phi), \quad (\text{III.38})$$

leading us to the flow

$$\Lambda \partial_\Lambda \Omega_{q,\Lambda}(\psi, \bar{\psi}, \phi) = \frac{12\Lambda^3}{\pi^2} \left[\epsilon_\Lambda^\psi + T \ln \left(1 + e^{-\beta \epsilon_\Lambda^\psi} \right) \right]. \quad (\text{III.39})$$

As in the mesonic part, the first term on the right hand side is the $T = 0$ part of the flow. It also does not match its counterpart in (II.99) due to the different cutoffs.

In summary we are led to the full flow

$$\begin{aligned} \Lambda \partial_\Lambda \Omega_\Lambda(\psi, \bar{\psi}, \phi) = & -\frac{\Lambda^3}{2\pi^2} \left\{ \frac{1}{2} \left[\epsilon_\Lambda^\phi(m_\sigma) + \frac{3}{2} \epsilon_\Lambda^\phi(m_\pi) \right] - 12 \epsilon_\Lambda^\psi \right. \\ & \left. + T \left[\ln \left(1 - e^{-\beta \epsilon_\Lambda^\phi(m_\sigma)} \right) + \ln \left(1 - e^{-\beta \epsilon_\Lambda^\phi(m_\pi)} \right) - 24 T \ln \left(1 + e^{-\beta \epsilon_\Lambda^\psi} \right) \right] \right\}, \end{aligned} \quad (\text{III.40})$$

where the first line is the $T = 0$ part of the flow, while the second line is the thermal part. Note that both parts are dependent on derivatives of Ω via the mass-functions and hence feed into each other. One cannot simply solve the $T =$ -part first. For example, the thermal pressure is given by (minus) the Λ -integral of the second line on the solution of the full flow equation. If we take Λ -independent mass functions, the Λ -integral gives the one-loop expressions we have started with.

IV. CONFINEMENT

In chapter II we have discussed the emergence of strong chiral symmetry breaking in QCD which is ultimately related to the growth of the strong coupling $\alpha_s(p^2)$ towards the infrared, $p^2 \rightarrow 0$. This growth triggers a resonance at the chiral symmetry breaking (momentum) scale. It is also the simplicity of this mechanism or better its representation in terms of correlation functions that allowed us to derive a relatively simple low energy effective theory that incorporates strong chiral symmetry breaking in QCD.

In chapter III this set-up was used to explore strong chiral symmetry breaking at finite temperature. Thermal fluctuations decrease the strong coupling $\alpha_s(p^2)$ and finally melt-down chiral symmetry breaking. This is monitored in a simple way by the temperature-dependence of the chiral order parameter, the expectation value of the scalar sigma field, $\sigma_0 \propto \langle \bar{\psi}\psi \rangle$.

We hope for a similarly simple picture for the phenomenon of confinement in the formulation of QCD in terms of correlation functions. Indeed we shall see that while the mechanism and dynamics of confinement is rather intricate in comparison, we have simple signatures of confinement in terms of its order parameter, the potential of which can be derived from low order correlation functions of quarks and gluons. It also allows us to extend the low energy EFTs introduced and used in the last chapters to also incorporate confinement. This set-up then enables us to study the confinement-deconfinement phase transition at finite temperature as well as the full phase structure at finite temperature and density. Before we start, a word of caution is required: this fascinating area has been the subject of intense studies over the past decades and has many facets ranging from mathematical physics -and in particular topological considerations- to phenomenological applications and the relation of the confinement dynamics to hadronic properties of QCD. Here we only can scratch the surface and shall take a practical approach: the lecture aims at being self-contained for the computations discussed, other equally interesting subjects are mentioned but not detailed. A fully comprehensive study is way beyond the scope of the current lecture course.

To begin with we discuss the question of the symmetry behind confinement and the related order parameter. For having a clean setting we restrict ourselves to pure Yang-Mills theory with static quark sources. Then confinement is the phenomenon that a quark-anti-quark pair experiences a linear potential when pulled apart. The expectation value of such a state $\langle \mathcal{O}_{q\bar{q}}(\vec{x}, \vec{y}) \rangle$ with a static quark q at the position \vec{x} and a static anti-quark \bar{q} at the position \vec{y} is related to its free energy $F_{q\bar{q}}$,

$$\langle \mathcal{O}_{q\bar{q}}(\vec{x}, \vec{y}) \rangle \propto e^{-F_{q\bar{q}}(r)}, \quad r = \|\vec{x} - \vec{y}\|. \quad (\text{IV.1})$$

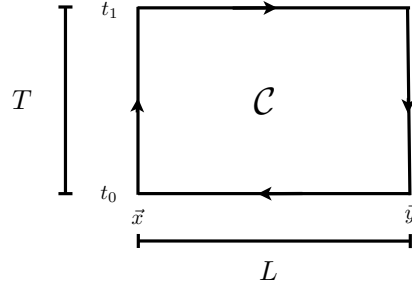
In (IV.1) we have used translation invariance present in an infinite volume, and hence the free energy only depends on the distance r between the quark and the anti-quark. For small distances the strong coupling $\alpha_s(p \propto 1/r \rightarrow \infty) \rightarrow 0$ gets small and perturbation theory is applicable. Therefore we expect a Coulomb-type potential with a $1/r$ dependence for $r \rightarrow \infty$. At large distances $r \rightarrow \infty$ the strong coupling grows large and perturbation theory is not applicable anymore. In this regime confinement predicts a linear dependence of the free energy/potential on r . This leads us to

$$\lim_{r\Lambda_{\text{QCD}} \rightarrow 0} F_{q\bar{q}}(r) \propto \frac{1}{r} \quad \text{and} \quad \lim_{r\Lambda_{\text{QCD}} \rightarrow \infty} F_{q\bar{q}}(r) \propto \sigma r, \quad (\text{IV.2})$$

where $\sigma \propto (420 \text{ MeV})^2$ in pure Yang-Mills theory is the string tension. As remarked before there are no scales in pure Yang-Mills theory except the dynamical scale Λ_{QCD} , so the explicit value above is up to our disposal, and we should rather determine a ratio of scales such as $\sqrt{\sigma}/\Lambda_{\text{QCD}}$. Typically the string tension is used to gauge other observables such as the critical temperature of the confinement-deconfinement phase transition at finite temperature. We will come back to this point later.

A. Order parameters for confinement

The computation of the expectation value in (IV.1) enables us at vanishing temperature to monitor the r -dependence of the free energy of a $q\bar{q}$ -pair. It also provides us with an order parameter for confinement: to that end we consider the limit $r \rightarrow \infty$. If confinement is present the free energy tends towards infinity in this limit and the expectation value $\langle \mathcal{O}_{q\bar{q}} \rangle$ vanishes. In turn, if we still had a Coulomb-type potential for large distances we get a finite value for $\langle \mathcal{O}_{q\bar{q}} \rangle$. This is what we expect for large temperature. As we have seen in the discussion of chiral symmetry breaking at finite temperature, increasing temperatures effectively increases the energy scale of the system. This heuristic

FIG. 10: e^+e^- pair.

argument is discussed in more details later. In summary we expect

$$\lim_{r \rightarrow \infty} \langle \mathcal{O}_{q\bar{q}} \rangle = \begin{cases} 0, & T < T_{\text{conf}} \\ > 0, & T > T_{\text{conf}} \end{cases}. \quad (\text{IV.3})$$

Accordingly, we have a clear signature for the confining phase as well as the deconfining phase. The above discussion also makes clear why we restricted ourselves first to pure Yang-Mills theory with static quarks: in the presence of dynamical quarks quark-anti-quark pairs can be created if the potential $V_{q\bar{q}}$ between quark and anti-quark is large enough. These additional q, \bar{q} can bind with the original pair into new $q\bar{q}$ pairs. This leads to a shielding of color force between the original pair and the effective potential levels at a finite value for $r \rightarrow \infty$.

It is left to determine the operator $\mathcal{O}_{q\bar{q}}$ as well as the underlying symmetry behind the confinement-deconfinement phase transition in pure Yang-Mills, as well as its breaking by dynamical quarks. To that end let us first consider an electron-positron pair, which is created at some initial time, pulled apart, kept at some distance L and then is annihilated, this describes a path \mathcal{C} in space-time, see Fig. 10. The related free energy is described by a path integral, where the current J_μ of the worldlines of the e^+e^- pair is coupled to the photon field A_μ with

$$\int_x J_\mu A_\mu = -i e \left(\int_{t_0}^{t_1} d\tau [A_0(t, \vec{x}) - A_0(t, \vec{y})] + \int_{\vec{x}}^{\vec{y}} d\vec{z} [\vec{A}(t_1, \vec{x}) - \vec{A}(t_0, \vec{y})] \right), \quad (\text{IV.4})$$

with the worldline current

$$J_\mu(x) = -i e \int_{\mathcal{C}} dz_\mu \delta(z - x). \quad (\text{IV.5})$$

The global sign in the current is pure convention and is related to that in the covariant derivative, in our case we have $D_\mu = \partial_\mu - i g A_\mu$, see (I.1).

In conclusion the source term (or operator of such a static electron-positron pair) is given by

$$\mathcal{W}_{\mathcal{C}}[A] = e^{\int_x J_\mu A_\mu} = \underbrace{e^{-i e \int_{\mathcal{C}} dz_\mu A_\mu(z)}}_{\text{Wegner-Wilson Loop}}. \quad (\text{IV.6})$$

The Wegner-Wilson loop in QED has a very simple interpretation which we shall discuss briefly. Consider a closed path \mathcal{C} that is the boundary of an area \mathcal{A} . Then the integral in the exponent can be rewritten with Stokes' theorem as

$$e \int_{\mathcal{C}=\partial\mathcal{A}} dz_\mu A_\mu(z) = e \frac{1}{2} \int_{\mathcal{A}} dx_\mu dy_\nu F_{\mu\nu}. \quad (\text{IV.7})$$

Accordingly, the phase in the Wegner-Wilson loop simply is the flux through the area \mathcal{A} with the boundary \mathcal{C} . This is an observable quantity and its gauge invariance is evident from the flux representation (IV.7). In the gauge field representation the gauge invariance of (IV.6) follows with the $U(1)$ gauge transformations $U = \exp i\omega \in U(1)$ of $A_\mu \rightarrow A_\mu + 1/e \partial_\mu \omega$ with,

$$\mathcal{W}_{\mathcal{C}}[A^U] = e^{-i e \int_{\mathcal{C}} dz_\mu A_\mu^U(z)} = e^{-i e \int_{\mathcal{C}} dz_\mu (A_\mu(z) + \frac{1}{e} \partial_\mu \omega)} = e^{-i e \int_{\mathcal{C}} dz_\mu A_\mu(z)}, \quad (\text{IV.8})$$

where we have used that $\int_{\mathcal{C}} dz_\mu \partial_\mu \omega = 0$. Note also that an open Wilson line related to a path from the position x to

the position y is a *parallel transporter* that transports gauge transformations from the position x to y ,

$$\mathcal{W}_{C_{x,y}}[A] = e^{-ie \int_{C_{x,y}} dz_\mu A_\mu(z)}, \quad \text{with} \quad \mathcal{W}_{C_{x,y}}[A^U] = U(x) \mathcal{W}_{C_{x,y}}[A] U^\dagger(y), \quad (\text{IV.9})$$

This allows to define gauge-invariant correlation functions of e.g. fermionic fields ψ such as

$$\langle \bar{\psi}(x) \mathcal{W}_{C_{x,y}}[A] \psi(y) \rangle. \quad (\text{IV.10})$$

In the case with dynamical electrons (IV.10) describes a e^+e^- pair.

The above definitions and relations extend straightforwardly to non-Abelian gauge groups. The only change comes from the fact that now the gauge field is matrix valued and the simple exponential of $ig \int dz_\mu A_\mu$ does not have the necessary transformation properties (IV.9) and the closed loop would fail to be gauge invariant. This situation is similar to that of defining the time-evolution operator in quantum mechanics and quantum field theory (S-matrix) on the basis of a Hamiltonian operator \hat{H} . There the resolution is to resort to time-ordering. In the present case we resort to path ordering which then transports the gauge transformation along the path. We define

$$U_{C_{x,y}} = \mathcal{P} e^{-ig \int_{C_{x,y}} dz_\mu A_\mu(z)}, \quad \text{with} \quad U_{C_{x,y}}[A^U] = U(x) U_{C_{x,y}} U^\dagger(y), \quad U(x) \in SU(N_c). \quad (\text{IV.11})$$

The loop $U_C \in SU(N_c)$ is a group element and the transformation property under gauge transformation of A_μ , (I.6), originates in the path ordering defined with

$$\mathcal{P} A_{\mu_1}(x(s_1)) \cdots A_{\mu_n}(x(s_n)) = A_{\mu_{\sigma(1)}}(x(s_{\sigma(1)})) \cdots A_{\mu_{\sigma(n)}}(x(s_{\sigma(n)})), \quad \text{with} \quad s_{\sigma(1)} \leq s_{\sigma(2)} \leq \cdots \leq s_{\sigma(n)}. \quad (\text{IV.12})$$

In (IV.12) $s \in [0, 1]$ is an isomorphic (invertible) parameterisation $x(s)$ of the given path $C_{x,y}$ with $x(0) = x$ and $x(1) = y$. For integrals this leads to the relations well-known from the time ordering, the simplest one being that for a product of two integrals,

$$\frac{1}{2} \mathcal{P} \left[\int_x^y dz_\mu A_\mu(z) \int_x^y dz'_\nu A_\nu(z') \right] = \int_x^y dz_\mu A_\mu(z) \int_z^y dz'_\nu A_\nu(z'). \quad (\text{IV.13})$$

Higher products follow similarly. Due to the path ordering derivatives of $U_{C_{x,y}}$ w.r.t. x or y pull down a gauge field to the left or to the right respectively.

$$\partial_\mu^x U_{C_{x,y}} = ig A_\mu(x) U_{C_{x,y}}, \quad \partial_\mu^y U_{C_{x,y}} = U_{C_{x,y}} (-i) g A_\mu(y). \quad (\text{IV.14})$$

With these properties the covariant derivative can be simply expressed as a parallel transport of the partial derivative, to wit

$$U_{C_{x,y}} \partial_\mu^x U_{C_{x,y}}^\dagger = \partial_\mu^x - ig A_\mu(x). \quad (\text{IV.15})$$

The property (IV.15) can be used to get a solution of the Dirac equation in terms of a phase factor \mathcal{W}_C and the solution of the free dirac equation ψ_0 . This is discussed in detail later for the static finite temperature case. In summary we conclude that the expectation value of a static quark–anti-quark pair $q\bar{q}$ is given by

$$W[L, T] = \frac{1}{Z} \int dA \mathcal{W}_C(A) e^{-S_{\text{YM}}[A]}, \quad \text{with} \quad \mathcal{W}_C[A] = \text{tr}_f U_C. \quad (\text{IV.16})$$

In the limit, where the time T tends towards infinity, the correlation function (??) is proportional to the exponential of the interaction energy $E(L)$ of this state (times T). All other contributions vanish exponentially fast with $(E_i - E(L))T > 0$, where E_i is the energy of the related state. We have

$$\lim_{T \rightarrow \infty} W[L, T] = F(L) E^{-E(L)T}, \quad (\text{IV.17})$$

which relates to the exponential of the free energy of a static quarkanti-quark state. The prefactor $F(L)$ relates to the overlap of the Wilson loop with the ground state. In the confining phase the Wegner-Wilson loop is given by $\mathcal{W}[T, L] \simeq e^{-F_{\bar{q}q}[T, L]}$ with $F_{\bar{q}q}[T, L]$ having a linear dependence on both L and T . The linear dependence in L we have discussed before. The linear dependence in T simply follows from the fact that in our Euclidean formulation the

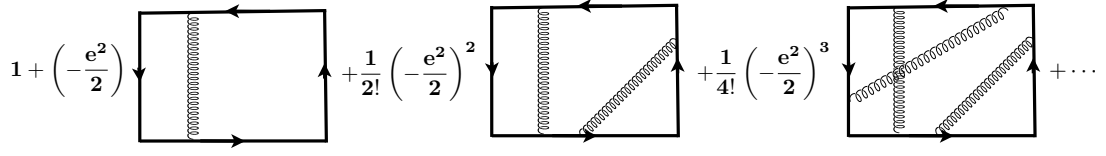


FIG. 11: Perturbative expansion of the Wilson loop expectation value for e^+e^- .

time direction is not different from the spatial ones. Hence we conclude

$$\lim_{LT \rightarrow \infty} W[T, L] \simeq e^{-\sigma LT}, \quad (\text{IV.18})$$

with the string tension σ . Eq.(IV.18) is the area law that signals confinement as does the linear potential. It is left to discuss the symmetry behind the confinement-deconfinement phase transition. This will be discussed in chapter IV B.

For its computation let us first discuss the far simpler case of an electron-positron pair e^+e^- . Then the static potential is the standard Coulomb potential. Indeed in the static limit there is no self-interaction of the photon and the expectation value of the Wilson loop is simply given by the sum of boxes with n photon exchanges from positions x_i to y_i where one integrates over x_i and y_i on the contour $\mathcal{C}[L, T]$. This is depicted in Fig. 11.

In other words we have

$$W[L, T] = e^{-\frac{e^2}{2} \int_{\mathcal{C}[L, T]} dx_\mu \int_{\mathcal{C}[L, T]} dy_\nu \langle A_\mu(x) A_\nu(y) \rangle_{\text{sub}}}, \quad (\text{IV.19})$$

where we have used that $\langle A_{\mu_1} \cdots A_{\mu_{n+1}} \rangle = 0$. The subscript $\langle \cdots \rangle_{\text{sub}}$ refers to the necessary subtraction of infinite selfenergies related to close loops with endpoints $x = y$. Moreover, all correlation functions decay in products of two-point functions (Wick-theorem), schematically we have $\langle A_1 \cdots A_{2n} \rangle = \langle A_1 A_2 \rangle \cdots \langle A_{2n-1} A_{2n} \rangle + \cdots$, and there are $(2n-1)(2n-3) \cdots$ combinations. Upon contour integration all combinations give the same contribution and overall we have the n th order term in the propagator

$$\frac{(2n-1)(2n-3) \cdots}{(2n)!} 2^n \left(-\frac{e^2}{2} \right)^n \left(\int_{\mathcal{C}} dx_\mu \int_{\mathcal{C}} dy_\nu \langle A_\mu(x) A_\nu(y) \rangle \right)^n = \frac{1}{n!} \left(-\frac{e^2}{2} \int_{\mathcal{C}} dx_\mu \int_{\mathcal{C}} dy_\nu \langle A_\mu(x) A_\nu(y) \rangle \right)^n, \quad (\text{IV.20})$$

for a general contour \mathcal{C} , leading to the Gaussian expression (IV.19). This leaves us with the task of computing

$$\begin{aligned} \int_{\mathcal{C}} dx_\mu \int_{\mathcal{C}} dy_\nu \langle A_\mu(x) A_\nu(y) \rangle &= \int_{\mathcal{C}} dx_\mu \int_{\mathcal{C}} dy_\nu \int \frac{d^4 p}{(2\pi)^4} \frac{1}{p^2} \left(\delta_{\mu\nu} - (1-\xi) \frac{p_\mu p_\nu}{p^2} \right) e^{ip(x-y)} \\ &= \int_{\mathcal{C}} dx_\mu \int_{\mathcal{C}} dy_\mu \int \frac{d^4 p}{(2\pi)^4} \frac{1}{p^2} e^{ip(x-y)} \\ &= \int_{\mathcal{C}} dx_\mu \int_{\mathcal{C}} dy_\mu \frac{1}{4\pi^2} \frac{1}{(x-y)^2}. \end{aligned} \quad (\text{IV.21})$$

To be explicit, we picked a covariant gauge in (IV.21). However, we have already proven that the *closed* Wilson line is gauge invariant which now is explicit as the ξ -dependent term drops out with the help of

$$\int_{\mathcal{C}} dx_\mu p_\mu e^{ipx} = -i \int_{\mathcal{C}} dx_\mu \partial_\mu^x e^{ipx} = 0, \quad (\text{IV.22})$$

which eliminates all longitudinal contributions for closed loops. Note that this is not valid for open Wilson lines.

Finally we are interested in the large T -limit in (IV.17) where we have

$$\begin{aligned}
V_{e^+e^-}(L) &= - \lim_{T \rightarrow \infty} \frac{1}{T} \log W[L, T] = \lim_{T \rightarrow \infty} \frac{1}{T} \frac{e^2}{2} \lim_{T \rightarrow \infty} \int_{C[L, T]} dx_\mu \int_{C[L, T]} dy_\mu \left(\frac{1}{4\pi^2} \frac{1}{(x-y)^2} \right)_{\text{sub}} \\
&= - \lim_{T \rightarrow \infty} \frac{1}{T} \frac{e^2}{2} \lim_{T \rightarrow \infty} \int_{t_0}^{t_1} dx_0 \int_{t_0}^{t_1} dy_0 \left(\frac{1}{4\pi^2} \frac{1}{(x_0 - y_0)^2 + L^2} \right) \\
&= - \lim_{T \rightarrow \infty} \frac{1}{T} \frac{e^2}{4\pi} \lim_{T \rightarrow \infty} \int_{t_0}^{t_1} dx_0 \int_{t_0 - x_0}^{t_1 - x_0} dy_0 \left(\frac{1}{\pi} \frac{1}{y_0^2 + L^2} \right) \\
&= - \lim_{T \rightarrow \infty} \frac{1}{T} 2 \frac{e^2}{4\pi} \int_0^T dx_0 \arctan \left(\frac{x_0}{L} \right) \\
&= - \frac{e^2}{4\pi} \frac{1}{L}. \tag{IV.23}
\end{aligned}$$

Eq.(IV.23) is the Coulomb potential as expected. The L -dependence we could have determined without any computation from dimensional arguments.

Adapting, within a bold step, the above analysis in QCD within a Gaussian approximation (no self-interaction of the gluons), we are led to the same result, up to a colour factor $\text{tr}_f t^a t^a = N_c C_F = (N_c^2 - 1)/2$, see (??). This is to be expected in perturbation theory, which is what the Gaussian approximation relies on.

In turn, relying on this approximation also in the non-perturbative confining sector of QCD or Yang-Mills theory, the static potential has the behaviour $V_{q\bar{q}} \sim L$, it is linear in the distance between quark and anti-quark. This requires a gluon propagator

$$\lim_{p \rightarrow 0} \langle A_\mu(p) A_\nu(-p) \rangle \propto \frac{1}{(p^2)^2}, \tag{IV.24}$$

which is the limit of what is allowed in a covariant local quantum field theory. Eq.(IV.24) suggests gluon dominance (over the ghost) in the infrared. Indeed, such propagators have been computed in the Landau gauge in the Mandelstam approximation (no ghosts). However, it turns out that in the Landau gauge the gluon propagators are not infrared enhanced as (IV.24) but infrared suppressed. Moreover, any n -loop contribution (even in full propagators and vertices) to the Wilson loop expectation value does not show the required linear behaviour, it only comes about by a full resummation of all diagrams. Nonetheless these considerations show that gauge fixing should be rather seen as offering the possibility to devise an appropriate parameterisation of the theory rather than a liability. For example, it can be shown that in Coulomb gauge the Gaussian approximation is working at least qualitatively.

B. Confinement-deconfinement phase transition at finite temperature

The dynamics of confinement and the confinement-deconfinement phase transition is the second cornerstone of the low energy QCD phenomenology we have to unravel. Here we aim at a treatment of this phenomenon within the continuum formulation of QCD similar to that of the chiral phase structure in chapter III. We mainly concentrate on the effective potential of the order parameter, the Polyakov loop. This observable is derived directly from the Wilson loop discussed before.

1. Polyakov loop

We consider a rectangular Wilson loop, Fig. 10, within the static situation also used in the previous chapters IV A, ???. At finite temperature T the time is limited to $t \in [0, \beta]$ with $\beta = 1/T$, see chapter III A. Moreover, the gauge fields are periodic in time up to gauge transformations, i.e.

$$A_\mu(t + \beta, \vec{x}) = \frac{i}{g} T(t, \vec{x}) (D_\mu T^\dagger(t, \vec{x})) , \quad c(t + \beta, \vec{x}) = T(t, \vec{x}) c(t, \vec{x}) T^\dagger(t, \vec{x}) , \quad \bar{c}(t + \beta, \vec{x}) = T(t, \vec{x}) \bar{c}(t, \vec{x}) T^\dagger(t, \vec{x}) \tag{IV.25}$$

with $T(t, \vec{x}) \in SU(N)$ are the *transition functions*. It follows from (IV.25) that under gauge transformations they transform as

$$T^U(t, \vec{x}) = U(t + \beta, \vec{x}) T(t, \vec{x}) U^\dagger(t, \vec{x}), \quad (\text{IV.26})$$

they parallel transport gauge transformations from t to $t + \beta$. The transformation property (IV.25) ensures the periodicity of gauge invariant quantities. It is indeed possible to restrict ourselves to strictly periodic fields, $t \equiv \mathbb{1}$, even though this limits the possible gauge choice. For the time being we restrict ourselves to the periodic case and discuss the general case at the end. The state we want to construct is the one, where we describe a static quark–anti-quark pair for all times. To that end we take a path that extends in time direction from $t = 0$ to β . Then the spatial paths at fixed time $t = 0$ and $t = \beta$ have to be identified (up to the orientation) due to the periodicity on the lattice, as well as the fact that we have restricted ourselves to periodic gauge fields. We conclude that the path $\mathcal{C}[L, \beta]$ splits into two loops winding around the time direction at the points \vec{x} and \vec{y} with $L = |\vec{x} - \vec{y}|$. The Wilson loop expectation value is then given by

$$\frac{1}{N_c^2} W[L, \beta] = \langle \mathcal{W}_{\mathcal{C}[L, \beta]}[A] \rangle = \langle L[A_0](\vec{x}) L^\dagger[A_0](\vec{y}) \rangle, \quad (\text{IV.27})$$

where $L[A_0]$ is the Polyakov loop variable with

$$L = \frac{1}{N_c} \text{tr}_f P(\beta, \vec{x}), \quad \text{with} \quad P(t, \vec{x}) = \mathcal{P} e^{-ig \int_0^t A_0(\tau, \vec{x}) d\tau}. \quad (\text{IV.28})$$

The normalisation of the Polyakov loop is such that it is unity for a vanishing gauge field, $L[0] = 1$. It lives in the fundamental representation as it is related to a creation operator of a quark. It is gauge invariant under periodic gauge transformations that keep the strict periodicity of the gauge field we have required. In general we have

$$L[A^U] = \frac{1}{N_c} \text{tr}_f [U^\dagger(\beta, \vec{x}) U(0, \vec{x})] P(\beta, \vec{x}), \quad (\text{IV.29})$$

where we have used the cyclicity of the trace. The combination $[U^\dagger(\beta, \vec{x}) U(0, \vec{x})]$ is unity for periodic gauge transformations, which is the case we have restricted ourselves to when deriving (IV.27) from the gauge invariant Wilson loop. In the general case the two spatial parts of the path at $t = 0, \beta$ only cancel up to the transition functions. Working through the derivation we get

$$L = \frac{1}{N_c} \text{tr}_f T(0, \vec{x}) P(\beta, \vec{x}), \quad (\text{IV.30})$$

which is also gauge invariant under non-periodic gauge transformations. Here we only consider $T \equiv \mathbb{1}$ but (IV.30) has to be used for example in the temporal axial gauge $A_0 \equiv 0$. Evidently, in this gauge (IV.28) simply is one. However, in order to achieve this gauge non-periodic gauge transformations (in time) have to be used. Then, the whole physics information of the Polyakov loop is stored in the transition function T instead of the gauge field. While this is not a convenient choice in continuum formulations it is a common choice on the lattice. There is obtained by taking trivial temporal link variables $U_0 = \mathbb{1}$ for all but the last link from $t = \beta - a$ to β .

We now come back to our main line of arguments, and restrict ourselves to the fully periodic case. The Wilson loop in (IV.27) is an order parameter for confinement. More precisely in the confining phase it tends towards zero for large distances, $L \rightarrow \infty$, due to the area law,

$$\lim_{L \rightarrow \infty} W[L, \beta] \simeq \lim_{L \rightarrow \infty} e^{-\sigma \beta L} = 0. \quad (\text{IV.31})$$

In turn, in the deconfined regime of the theory the quark–anti-quark potential $V_{q\bar{q}}$ is Coulomb-like, $V_{q\bar{q}} \propto 1/|\vec{x} - \vec{y}|$ and the Wilson loop follows a perimeter law, leading to

$$\lim_{L \rightarrow \infty} W[L, \beta] > 0. \quad (\text{IV.32})$$

In conclusion the Wilson loop expectation value or Polyakov loop two-point correlation function for $L \rightarrow \infty$ serves as an order parameter for confinement at finite temperature. Moreover, in this limit we can use the clustering

decomposition property of a *local* quantum field theory,

$$\lim_{|\vec{x}-\vec{y}|\rightarrow\infty} \langle A(\vec{x})B(\vec{y}) \rangle - \langle A(\vec{x}) \rangle \langle B(\vec{y}) \rangle = 0. \quad (\text{IV.33})$$

for local operators A and B . Hence we conclude that

$$\lim_{L\rightarrow\infty} W[L, \beta] = \langle L[A_0](\vec{x}) \rangle \langle L^\dagger[A_0](\vec{y}) \rangle, \quad (\text{IV.34})$$

it only depends on the temporal component of the gauge field. The Polyakov loop expectation value $\langle L[A_0] \rangle$ does not depend on the spacial variable due to translation invariance. Thus also the Polyakov loop expectation value itself serves as an order parameter for confinement,

$$\langle L[A_0] \rangle = \begin{cases} 0 & \text{confining regime} \\ \neq 0 & \text{deconfining regime} \end{cases} \quad (\text{IV.35})$$

So far we have argued on a heuristic level which led us to (IV.35) as an order parameter, without even discussing the symmetry behind the pattern in (IV.35): we are searching for a symmetry that is preserved by the Yang-Mills action but does not keep $\langle L[A_0] \rangle$ invariant. This is the center symmetry of the gauge group. The center elements are those elements that commute with all other elements in the gauge group. In $SU(N)$ these are the N th roots of unity in the groups. For the cases used here, the example group $SU(2)$ and the physical group $SU(3)$, the centers \mathcal{Z} are

$$\mathcal{Z}_{SU(2)} = \{\mathbb{1}, -\mathbb{1}\} \simeq \mathbb{Z}_2, \quad \mathcal{Z}_{SU(3)} = \{\mathbb{1}, \mathbb{1}e^{\frac{2\pi i}{3}}, \mathbb{1}e^{\frac{4\pi i}{3}}\} \simeq \mathbb{Z}_3. \quad (\text{IV.36})$$

where the identities $\mathbb{1}$ in $SU(2)$ and $SU(3)$ are $\mathbb{1}_{2\times 2}$ and $\mathbb{1}_{3\times 3}$ respectively. The non-trivial center elements in (IV.36) are related to combinations of generators in the algebra. This relation is not unique as the eigenvalues of the combination of algebra elements is only determined up to $2\pi n$ with $n \in \mathbb{Z}$. For example, one representation is

$$SU(2): \quad -\mathbb{1} = e^{\pi i \sigma_3}, \quad SU(3): \quad \mathbb{1}e^{\frac{2\pi i}{3}} = e^{2\pi i \frac{1}{\sqrt{3}} \lambda_8}, \quad \mathbb{1}e^{\frac{4\pi i}{3}} = e^{2\pi i \frac{2}{\sqrt{3}} \lambda_8}. \quad (\text{IV.37})$$

with the Pauli matrices in (II.41) and the Gell-Mann matrices

$$\begin{aligned} \lambda_1 &= \begin{pmatrix} 0 & 1 & 0 \\ 1 & 0 & 0 \\ 0 & 0 & 0 \end{pmatrix}, & \lambda_2 &= \begin{pmatrix} 0 & -i & 0 \\ i & 0 & 0 \\ 0 & 0 & 0 \end{pmatrix}, & \lambda_3 &= \begin{pmatrix} 1 & 0 & 0 \\ 0 & -1 & 0 \\ 0 & 0 & 0 \end{pmatrix}, & \lambda_4 &= \begin{pmatrix} 0 & 0 & 1 \\ 0 & 0 & 0 \\ 1 & 0 & 0 \end{pmatrix}, \\ \lambda_5 &= \begin{pmatrix} 0 & 0 & -i \\ 0 & 0 & 0 \\ i & 0 & 0 \end{pmatrix}, & \lambda_6 &= \begin{pmatrix} 0 & 0 & 0 \\ 0 & 0 & 1 \\ 0 & 1 & 0 \end{pmatrix}, & \lambda_7 &= \begin{pmatrix} 0 & 0 & 0 \\ 0 & 0 & -i \\ 0 & i & 0 \end{pmatrix}, & \lambda_8 &= \frac{1}{\sqrt{3}} \begin{pmatrix} 1 & 0 & 0 \\ 0 & 1 & 0 \\ 0 & 0 & -2 \end{pmatrix}, \end{aligned} \quad (\text{IV.38})$$

in the fundamental representation of $SU(3)$. The generators of the $SU(3)$ algebra are $t_{\text{fund}}^a = \lambda^a/2$. In the adjoint representation the generators of the algebra are given by the structure constants, see (I.4). The $SU(3)$ structure constants are given by

$$\begin{aligned} SU(2): \quad f^{abc} &= \epsilon^{abc}, \\ SU(3): \quad f^{123} &= 1, \quad f^{147} = f^{246} = f^{257} = f^{345} = \frac{1}{2}, \quad f^{156} = f^{367} = \frac{1}{2}, \quad f^{458} = f^{678} = \frac{1}{2}. \end{aligned} \quad (\text{IV.39})$$

Hence, in the adjoint representation these elements are all represented by $\mathbb{1}$,

$$Z_{\text{ad}} = \mathbb{1}_{\text{ad}}, \quad \text{for} \quad Z \in \mathcal{Z}. \quad (\text{IV.40})$$

In the adjoint representation every center element is mapped to the identity, $z = \mathbb{1}_{\text{ad}}, \forall z \in \mathcal{Z}$. Hence we have

$$\mathcal{Z}_{\text{ad}} = \{\mathbb{1}_{\text{ad}}\}. \quad (\text{IV.41})$$

As the gauge fields and the ghosts live in the adjoint representation, the gauge-fixed Yang-Mills action is trivially invariant under center transformations. In turn, the Polyakov loop $L[A_0]$ is the trace of the Polyakov line $P(\beta, \vec{x})$ in

the *fundamental* representation, see (IV.28). It transforms with

$$P(\beta, \vec{x}) \rightarrow z P(\beta, \vec{x}), \quad \text{with} \quad z \in \mathcal{Z}. \quad (\text{IV.42})$$

We conclude that in the center-symmetric phase of the theory the Polyakov loop expectation value (IV.35) has to vanish while in the center-broken phase it is finite. Having identified the symmetry we can invoke universality to predict the scaling of the order parameter in the vicinity of the phase transition:

For $SU(2)$ we are in the Ising universality class, the symmetry group being Z_2 . If $SU(2)$ -Yang-Mills exhibits a second order phase transition (and it does), it should have Ising scaling. This is indeed seen. For $SU(3)$ the symmetry group is Z_3 and we expect a first order phase transition which is also seen. Our explicit computations later will not incorporate the full fluctuation analysis so detecting Ising scaling is out of reach here. However, we are able to see the second and first order nature of the respective phase transitions. This closes our very rough symmetry discussion.

We also would like to get an intuitive understanding for the Polyakov loop expectation value. We have argued for the Wilson loop expectation value, that it is related to the expectation value of a static quark–anti-quark pair,

$$W[L, \beta] \simeq \langle \bar{q}(\vec{x}) \mathcal{P} e^{-i g \int_{\mathcal{C}_{\vec{x}, \vec{y}}} A_\mu dz_\mu} q(\vec{y}) \rangle, \quad (\text{IV.43})$$

where the path-ordered phase ensures gauge invariance. Using -naively- the clustering decomposition property (or short declustering) for $|\vec{x} - \vec{y}| \rightarrow \infty$, we can decompose the expectation value in (IV.43) in the product of the expectation value of a quark state and an anti-quark state. Naturally the latter have to vanish as the creation of a single quark or anti-quark requires an infinite energy. However, be aware of the fact that the quark and anti-quark states do not belong to the Hilbert space of QCD and hence we cannot apply declustering that easily.

Still, the Polyakov loop expectation value is related to the heuristic situation described above. To see this more clearly let us consider a static quark. This situation can be achieved by taking the infinite quark mass limit, $m_q \rightarrow \infty$. The Dirac equation

$$(\not{D} + m_\psi) \psi = 0, \quad (\text{IV.44})$$

then reduces to a space-independent equation as the quark cannot move, $\vec{\partial}_x \psi = 0$. Hence, the Dirac equation (IV.44) reads in the static limit

$$(\gamma_0 D_0 + m_\psi) \psi = 0. \quad (\text{IV.45})$$

A solution to this equation is given by

$$\psi(x) = P(t, \vec{x}) \psi_0(x), \quad \text{with} \quad (\gamma_0 \partial_0 + m_\psi) \psi_0 = 0. \quad (\text{IV.46})$$

where ψ_0 solves the free Dirac equation, and $P(t, \vec{x})$ is the untraced Polyakov loop (IV.28). For proving (IV.46) we use that $(D_0 P(t, \vec{x})) = 0$ following from (IV.14). Hence, in a -vague- sense we can identify the Polyakov loop expectation value with the interaction part of a static quark.

2. Polyakov loop potential

As in the case of chiral symmetry breaking we would like to compute the effective potential of the order parameter, $V_{\text{Pol}}[L]$. This turns out to be a formidable task both on the lattice and in the continuum. Note however, that the computation of the expectation value itself is simple on the lattice.

In the continuum we compute the effective potential of QCD, that is the effective action $\Gamma[\Phi]$ for constant fields. Before we embark on the explicit computation we first have to deal with the issue of gauge invariance in the gauge-fixed approach we are working in. To that end we upgrade our covariant gauge fixing to the *background gauge*: To that end we split our gauge field in a background \bar{A} and a fluctuation a , to wit

$$A_\mu = \bar{A}_\mu + a_\mu. \quad (\text{IV.47})$$

While the background \bar{A} is kept fixed, a carries all the quantum fluctuations. In the path integral the integration over A then turns into one over a . So far nothing has been changed. Now we modify our gauge fixing,

$$\partial_\mu A_\mu = 0 \rightarrow \bar{D}_\mu a = 0, \quad \text{with} \quad \bar{D}_\mu = D_\mu(\bar{A}). \quad (\text{IV.48})$$

For $\bar{A} = 0$ we regain the original covariant gauge fixing. For the background gauge fixing the gauge fixed classical action with ghost term reads

$$S_A[\bar{A}, a, c, \bar{c}] = S_A[A] + \frac{1}{2\xi} \int_x (\bar{D}_\mu^{ab} a_\mu^b)^2 + \bar{c}^a \bar{D}_\mu^{ad} D_\mu^{db} c^b. \quad (\text{IV.49})$$

In the presence of the background field and with the gauge fixing (IV.48) we have an additional -auxiliary- gauge symmetry: the gauge-fixed action is invariant under *background gauge transformations*

$$\bar{A}_\mu^U = \frac{i}{g} U (\bar{D}_\mu U^\dagger), \quad a^u = U a_\mu U^\dagger \quad \longrightarrow \quad A^U = \frac{i}{g} U (D_\mu U^\dagger). \quad (\text{IV.50})$$

Evidently this is true for the Yang-Mills action, it is left to show this for the gauge fixing and ghost term. The gauge fixing condition (IV.48) transforms as a tensor under (IV.50): $\bar{D}_\mu a \rightarrow U \bar{D}_\mu a U^\dagger$ and hence $\text{tr}(\bar{D}_\mu a)^2$ is invariant under (IV.50). The Faddeev-Popov operator \mathcal{M} in the background gauge is given by

$$\mathcal{M} = -\bar{D}_\mu D_\mu \rightarrow U \bar{D}_\mu D_\mu U^\dagger. \quad (\text{IV.51})$$

It also transforms as a tensor and hence the ghost term is gauge invariant under (IV.50). However, the background gauge transformations are an auxiliary symmetry. The physical gauge transformations are those of the fluctuation field at fixed background \bar{A} , the *quantum gauge transformations*

$$\bar{A}_\mu^U = \bar{A}_\mu, \quad a^u = U (D_\mu U^\dagger) \quad \longrightarrow \quad A^U = \frac{i}{g} U (D_\mu U^\dagger). \quad (\text{IV.52})$$

Again this can be understood by choosing the standard covariant gauge with a vanishing background. Then, (IV.52) is the only gauge transformation left, while (IV.50) leads to a non-vanishing background and hence changes the gauge fixing. The neat feature of the background field formalism is that it can be shown that both transformations are indeed related via *background independence* of the quantum equations of motion. Therefore background gauge invariance under the transformations (IV.50) carries physical gauge invariance, more details can be found in Appendix C

Still, the introduction of the background seems to complicate matters but it indeed facilitates computations and gives a more direct access to physics. Here we explore both properties. First we note that the introduction of \bar{A} leads to an effective action that depends on two fields,

$$\Gamma[A] \rightarrow \Gamma[\bar{A}, a]. \quad (\text{IV.53})$$

Switching of the mean value of the fluctuation field, $a = 0$ leads to a (background) gauge invariant action

$$\Gamma[A] = \Gamma[A, a = 0] \quad (\text{IV.54})$$

As mentioned before, this is the physical gauge invariance. Moreover, one can show that the background correlation functions are directly related to S -matrix elements. In summary the effective action $\Gamma[A]$ defined in (IV.54) carries the information about the Polyakov loop potential.

Now we proceed with the explicit computation of the effective potential at one loop. For the Polyakov loop potential the only mean field of interest is the temporal component of the gauge field, and the other fields are put to zero. We will perform this computation first on the one-loop level with the classical ghost and gluon propagators. Finally we will introduce the fully non-perturbative propagators to this one-loop computation. This re-sums infinitely many diagrams and carries the essential non-perturbative computation. The explicit results are in semi-quantitative agreement with the full results obtained with functional renormalisation group methods and also show a good agreement with the lattice results.

In summary the Polyakov loop potential for constant temporal gauge fields is given by

$$V_{\text{Pol}}(A_0) = \frac{1}{2} \text{Tr} \ln G_A^{-1}(A_0) - \text{Tr} G_c^{-1}(A_0) - \mathcal{N}, \quad (\text{IV.55})$$

where the color traces in (IV.55) are in the adjoint representation and CN is the normalisation of the potential which we leave open for now. For the one-loop computation we have $G^{-1} = S_A^{(2)}$ with S_A in (IV.49) and hence

$$G_A^{-1}(A_0) = -D_\rho^2 \delta^{\mu\nu} + \left(1 - \frac{1}{\xi}\right) D_\mu D_\nu, \quad G_c^{-1}(A_0) = -D_\rho^2. \quad (\text{IV.56})$$

In (IV.56) we have used that the spin one terms proportional to $F_{\mu\nu}$ drop out for a constant A_0 -background. In the re-summed non-perturbative approximation we use numerical results, e.g. the Yang-Mills analog of Figure 6 at finite temperature. For constant fields we can assume the fields to lay in the Cartan subalgebra, as we can always rotate the field into the Cartan subalgebra with constant gauge transformations. We expand the Cartan-valued field A_0 in the fundamental representation in the color eigenfunctions and eigenvalues of A_0 . In the present context it always occurs in combination with temperature and coupling in Matsubara sums with $2\pi Tn + gA_0 = 2\pi T(n + \beta g/(2\pi)A_0)$, and we define the dimensionless algebra-valued field

$$\hat{\varphi} = \frac{\beta g}{2\pi} A_0, \quad L(\hat{\varphi}) = L[A_0] = \text{tr} e^{-2\pi i \hat{\varphi}}. \quad (\text{IV.57})$$

The eigenvalue equation of the field $\hat{\varphi}$ in the fundamental representation is given by

$$\hat{\varphi}^f |\varphi_n^f\rangle = \nu_n^f |\varphi_n^f\rangle, \quad n \in 1, \dots, N_c, \quad (\text{IV.58})$$

where the superscript f indicates the fundamental representation. The eigenvalues for $SU(2)$ and $SU(3)$ are given by

$$SU(2) : \nu_n^f \in \left(\pm \frac{\varphi}{2} \right), \quad SU(3) : \nu_n^f \in \left(\pm \frac{\varphi_3 + \frac{1}{\sqrt{3}}\varphi_8}{2}, -\frac{1}{\sqrt{3}}\varphi_8 \right). \quad (\text{IV.59})$$

Using (IV.58) and (IV.59) in the Polyakov loop in $SU(2)$ we arrive at

$$\hat{\varphi} = \varphi_3 \frac{\sigma^3}{2} \xrightarrow{\varphi = \varphi_3} L(\varphi) = \cos \pi \varphi, \quad (\text{IV.60})$$

For $SU(3)$ we have

$$\hat{\varphi} = \frac{2\pi}{\beta g} \left(\varphi_3 \frac{\lambda^3}{2} + \varphi_8 \frac{\lambda^8}{2} \right) \longrightarrow L(\varphi_3, \varphi_8) = \frac{1}{3} \left(e^{\frac{2\pi i \varphi_8}{\sqrt{3}}} + 2 \cos(\pi \varphi_3) e^{-\frac{2\pi i \varphi_8}{\sqrt{3}}} \right), \quad (\text{IV.61})$$

with $\lambda^{3,8}$ given in (IV.38). As the Polyakov loop potential (for vanishing chemical potential) has minima at $\varphi_3 = 0$ we can work with the Polyakov loop variable at $\varphi_8 = 0$,

$$L(\varphi) = \frac{1}{3} (1 + 2 \cos \pi \varphi), \quad (\text{IV.62})$$

with $L(\varphi) = L(\varphi_3 = \varphi, 0)$. Then, confinement is signaled by the (mean) gauge field configurations

$$\varphi = \frac{1}{2} \quad \text{for } SU(2), \quad \text{and} \quad \varphi = \frac{2}{3} \quad \text{for } SU(3). \quad (\text{IV.63})$$

As a preparation for the full computation we go through the perturbative computation. This already reveals the main mechanism we need for the access of the confinement-deconfinement phase transition. This computation has been done independently in [21] and [22] in 1980 (published 81). The potential is often called the Weiss potential.

For the explicit computation we restrict ourselves to $SU(2)$. The result does not depend on the gauge fixing parameter ξ and we choose $\xi = 1$, Feynman gauge, in order to facilitate the computation. Then the Lorentz part of the trace in the gauge field loop can be performed immediately, leading to a factor four for the four polarisations of a vector field. We have

$$V_{\text{Pol}}(A_0) \simeq 4 * \frac{1}{2} \text{Tr} \ln(-D_\rho^2) - 2 * \frac{1}{2} \text{Tr} \ln(-D_\rho^2) = 2 \frac{1}{2} \text{Tr} \ln(-D_\rho^2), \quad (\text{IV.64})$$

where we have made explicit the multiplicities of gluon and ghost, and we dropped the normalisation. The gluon dominates and the final result is twice that of one polarisation, which accounts for the two physical polarisations of the gluon. This is an expected property as we compute a gauge invariant potential that should reflect the fact that we only have two physical polarisations, and the gauge fixing is only a means to finally compute gauge invariant quantities. Now we use that we can diagonalise the operator D_ρ^2 in the adjoint representation in the algebra. The color eigenfunctions and eigenvalues in the adjoint representation are given by

$$\frac{g\beta}{2\pi} A_0^{\text{ad}} |\varphi_n^{\text{ad}}\rangle = \nu_n^{\text{ad}} |\varphi_n^{\text{ad}}\rangle, \quad n \in 1, \dots, N_c^2 - 1, \quad (\text{IV.65})$$

and

$$SU(2) : \nu_n^{\text{ad}} \in (0, \pm\varphi), \quad SU(3) : \nu_n^{\text{ad}} \in \left(0, 0, \pm\varphi_3, \pm\frac{\varphi_3 \pm \sqrt{3}\varphi_8}{2}\right). \quad (\text{IV.66})$$

Note that the eigenvalues of T_{ad}^3 are ± 1 , while they are $\pm 1/2$ in the fundamental representation. The relative factor $1/2$ reflects the sensitivity to center transformations in the fundamental representation and the insensitivity in the adjoint representation. Performing the trace in (IV.64) in terms of the eigenfunctions $|\varphi_n\rangle$ and momentum modes, we arrive at

$$V_{\text{Pol}}(A_0) \simeq 2 \left[V_{\text{mode}}(\varphi) + V_{\text{mode}}(-\varphi) \right], \quad (\text{IV.67})$$

with V_{Pol} being $1/2 \text{Tr} \ln(-D^2)$, where the gauge field is substitute by one eigenmode,

$$\begin{aligned} V_{\text{mode}}(\varphi) &= \frac{T}{2} \sum_{n \in \mathbb{Z}} \int \frac{d^3 p}{(2\pi)^3} \left\{ \ln \frac{(2\pi T)^2 (n + \varphi)^2 + \vec{p}^2}{(2\pi T)^2 n^2 + \vec{p}^2} \right\} \\ &= \frac{T}{4\pi^2} \sum_{n \in \mathbb{Z}} \int_0^\infty dp p^2 \left\{ \ln \frac{(2\pi T)^2 (n + \varphi)^2 + p^2}{(2\pi T)^2 n^2 + p^2} \right\}, \end{aligned} \quad (\text{IV.68})$$

where the denominator in the logarithm in (IV.68) is a normalisation of the mode potential at vanishing φ : $V_{\text{mode}}(0) = 0$. The sum in (IV.68) can be performed analytically by taking first a derivative w.r.t. p^2 and then using contour integrals. It results in

$$V_{\text{mode}}(\varphi) = \frac{T}{4\pi^2} \int_0^\infty dp p^2 \left\{ \left[\sum_{\pm} \ln \sinh \frac{\beta p \pm 2\pi i \varphi}{2} \right] - 2 \ln \sinh \frac{\beta p}{2} \right\}. \quad (\text{IV.69})$$

Now we use that

$$\begin{aligned} \sum_{\pm} \ln \sinh \frac{\beta p \pm 2\pi i \varphi}{2} - 2 \ln \sinh \frac{\beta p}{2} &= \sum_{\pm} \ln(1 - e^{-\beta p \pm 2\pi i \varphi}) - 2 \ln(1 - e^{-\beta p}) \\ &= \sum_{\pm} \sum_{n=1}^{\infty} \frac{1}{n} e^{-\beta p n} (e^{\pm 2\pi i n \varphi} - 1). \end{aligned} \quad (\text{IV.70})$$

In (IV.70) we have pulled out a factor $\ln \exp(\beta p \pm 2\pi i \varphi)/2 = (\beta p \pm 2\pi i \varphi)/2$ from the $\ln \sinh$ -terms with φ , and $2 \ln \exp \beta p/2 = \beta p$ from the $\ln \sinh$ -term in the normalisation. These terms cancel each other and we are led to the right hand side of (IV.70). Then we have expanded the logarithms in a Taylor expansion in the exponentials. In summary this leads us to

$$\begin{aligned} V_{\text{mode}}(\varphi) &= \frac{T}{4\pi^2} \int_0^\infty dp p^2 \sum_{\pm} \sum_{n=1}^{\infty} \frac{1}{n} e^{-\beta p n} (e^{\pm 2\pi i n \varphi} - 1) \\ &= \frac{T^4}{\pi^2} \sum_{n=1}^{\infty} \frac{1}{n^4} (\cos 2\pi n \varphi - 1). \end{aligned} \quad (\text{IV.71})$$

The sum in (IV.71) is gain easily performed with methods of complex analysis and we arrive at

$$\beta^4 V_{\text{mode}}(\varphi) = \frac{\pi^2}{48} \left[4 \left(\tilde{\varphi} - \frac{1}{2} \right)^2 - 1 \right]^2, \quad \tilde{\varphi} = \varphi \bmod 1, \quad (\text{IV.72})$$

where we have divided out the trivial dimensional thermal factor T^4 . Inserting (IV.72) in (IV.67) for the Polyakov

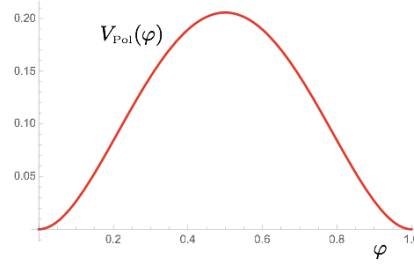


FIG. 12: One loop Polyakov loop potential for $SU(2)$.

loop potential we are led to

$$\beta^4 V_{\text{pol}}(A_0) = \frac{\pi^2}{12} \left[4 \left(\tilde{\varphi} - \frac{1}{2} \right)^2 - 1 \right]^2, \quad (\text{IV.73})$$

for $SU(2)$, while for $SU(3)$ the potential is given by

$$V_{\text{pol}}(A_0) = \sum_{n=1}^8 V_{\text{mode}}(\nu_n), \quad (\text{IV.74})$$

with the eigenvalues ν_n in (IV.66). We have plotted the $SU(2)$ potential in Figure 12 as it has a very simple form which carries already the relevant information. The potential has minima at $\varphi = 0, 1$ and a maximum at $\varphi = 1/2$. For the minima the Polyakov loop variable $L[A_0]$ takes the value ± 1 , the maximum is the center-symmetric value $L[A_0] = 0$. This structure is also present for all $SU(N)$ -theories and originates in the -necessary- center symmetry of the potential. The center transformation in $SU(2)$ is given by

$$\varphi \rightarrow 1 - \varphi, \quad (\text{IV.75})$$

which maps $L[\varphi = 0] = 1 \rightarrow L[\varphi = 1] = -1$ and vice versa, this comes via the multiplication of the Polyakov line $P(\vec{x})$ with the center element -1 . We conclude that in perturbation theory the potential has its minimum at the maximally center-breaking values, the theory is in the center-broken phase. At large temperatures perturbation theory is valid and quantum fluctuations are small: the fluctuating gauge field is close to $A_0 = 0$. This leads to

$$\lim_{T \rightarrow \infty} L[\langle A_0 \rangle] = 1. \quad (\text{IV.76})$$

In turn, for small temperatures the potential should exhibit a minimum at $\varphi = 1/2$. Interestingly, this is achieved within the one loop computation if the gluon contributions are switched off, and the ghost contribution is left.

Finally we come back to the normalisation of $V_{\text{pol}}(A_0)$ in (IV.55). We have normalised it such that $V_{\text{pol}}(A_0) = 0$. However, if we choose the normalisation as

$$\mathcal{N} = \left[\frac{1}{2} \text{Tr} \ln G_A^{-1}(0) - \text{Tr} G_c^{-1}(0) \right]_{T=0}, \quad (\text{IV.77})$$

the value of the effective potential simply is the thermal pressure of the theory. The difference between (IV.77) and that chosen in (IV.68) for the mode potential is given by

$$\Delta \mathcal{N} = 2(N_c^2 - 1) \left[\frac{T}{2} \sum_{n \in \mathbb{Z}} \int \frac{d^3 p}{(2\pi)^3} \ln [(2\pi T)^2 n^2 + \vec{p}^2] - \int \frac{d^4 p}{(2\pi)^4} \ln p^2 \right] = -p_{A,\text{SB}} \quad \text{with} \quad p_{A,\text{SB}} = \frac{\pi^4 T^4}{45} (N_c^2 - 1). \quad (\text{IV.78})$$

Eq.(IV.78) is nothing but (minus) the Stefan-Boltzmann pressure of a $SU(N_c)$ gauge theory, see (III.19) for the scalar case. It is the scalar pressure times the number of physical modes: two physical transversal polarisations times the

number of color modes, $(N_c^2 - 1)$, leading to $2(N_c^2 - 1)p_{\phi, \text{SB}}$. This leads us to our final result

$$\beta^4 V_{\text{pol}}(A_0) = \frac{\pi^2}{12} \left[4 \left(\tilde{\varphi} - \frac{1}{2} \right)^2 - 1 \right]^2 - \frac{\pi^4}{45} (N_c^2 - 1). \quad (\text{IV.79})$$

We proceed with a non-perturbative computation of the Polyakov loop potential which still keeps the analogy to the one loop computation above. Even though this is an approximation, both the numerical result as well as the conceptual structure are also present in the full computation. We again start with (IV.55). Now, instead of using the classical inverse propagators we utilise the fully non-perturbative ones. These propagators can only be computed with numerical non-perturbative approaches, either gauge fixed lattice simulations or with functional methods such as the functional renormalisation group (FRG) already used in the low energy EFT for chiral symmetry breaking or Dyson-Schwinger equations (DSEs). Instead of using the available numerical data we add another approximation in order to keep our approach semi-analytic.

From Fig. 6 we know that the gluon propagator exhibits a mass gap for low momenta. In turn, for large momenta it runs logarithmically. This behaviour is also present at finite temperature, see Fig. 14. There we plot the momentum dependence of the dressing of the chromo-magnetic gluon propagator for different temperatures. Both, results from functional methods and from gauge-fixed lattice simulations are shown. The dressing is defined as

$$\frac{1}{Z_A^M(\vec{p}^2)} = \frac{1}{2} \vec{p}^2 \langle A_i(0, \vec{p}) A_i(0, -\vec{p}) \rangle, \quad (\text{IV.80})$$

it is the dressing of the gluon propagator perpendicular to the heat bath. In Fig. 13 we plot the temperature-dependent mass (screening mass) of chromo-electric gluon propagator, the gluon propagator parallel to the heat bath,

$$\frac{1}{Z_A^E(\vec{p}^2)} = \vec{p}^2 \langle A_0(0, \vec{p}) A_0(0, -\vec{p}) \rangle. \quad (\text{IV.81})$$

Note that the simple relations (IV.80), (IV.81) are only valid for $p_0 = 0$. For $p_0 \neq 0$ one has to use the thermal projection operators, see e.g. [23]. At large temperatures we expect them to tend towards their perturbative values. This is indeed happening, however, we need higher order thermal perturbation theory. The one-loop Debye mass is given by

$$m_D^0 = \sqrt{\frac{N}{3}} g_T T + \mathcal{O}(g_T^2 T), \quad (\text{IV.82})$$

and is also displayed in Fig. 13. For the comparison, the temperature-dependent coupling is fully non-perturbative and has been also taken from [23] for internal consistency, for more details see there. In [24] higher order effects have been taken into account, leading to

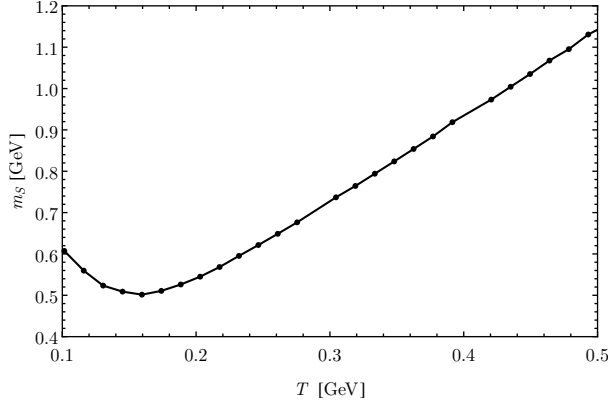
$$m_D = m_D^0 + \left(c_D + \frac{N}{4\pi} \ln \left(\frac{m_D^0}{g_T^2 T} \right) \right) g_T^2 T + \mathcal{O}(g_T^3 T). \quad (\text{IV.83})$$

Eq.(IV.83) already leads to a very good agreement with the full result above 600 MeV. At low temperatures, the mass settles at its $T = 0$ value, indicated by the $1/T$ behaviour of m_d/T in Fig. 13b, and the perturbative prescriptions fail even with the full non-perturbative coupling. The Debye mass itself for low temperatures is depicted in Fig. 13a, from which it is evident that a temperature-independent (or decaying) additional part $\Delta m_D(T = 0) \approx 380$ MeV to m_D^0 would lead to agreement up to ≈ 150 MeV.

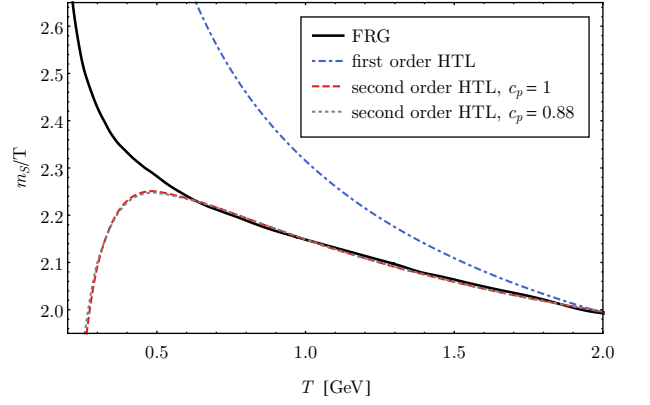
In conclusion a good semi-quantitative approximation to the thermal propagator (in particular the chromo-magnetic one) is the perturbative propagator with a temperature-dependent mass term. It goes beyond the scope of the present lecture notes to present a full computation, here we simply investigate the qualitative effect of such a mass gap, first done in [28], for a full, comprehensive analysis see [29]. We revisit (IV.71) for simple massive propagators

$$G_A \propto \frac{1}{(2\pi T)^2 (n + \varphi)^2 + \vec{p}^2 + m_T^2}, \quad (\text{IV.84})$$

even dropping the perturbative running. While the latter is important for the correct scaling (fixing Λ_{QCD} and hence

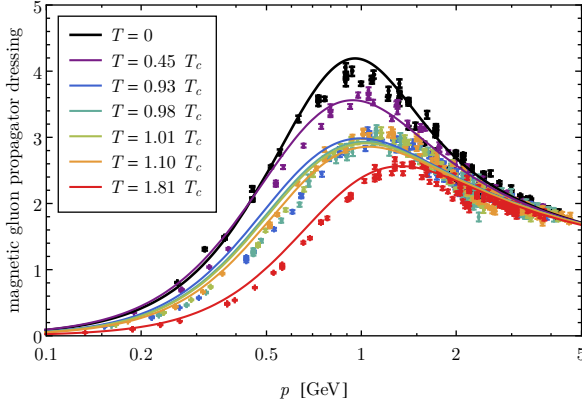


(a) Screening mass m_s in units of GeV at low temperatures. In the limit $T \rightarrow 0$ the screening mass smoothly tends towards its finite $T = 0$ value, see back curve in Fig. 14.

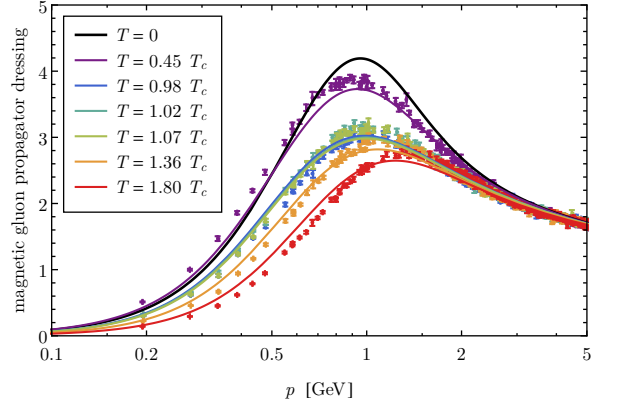


(b) Dimensionless Debye screening m_s/T mass at high temperatures in comparison with leading order perturbation theory (IV.82) and the Arnold-Yaffe prescription (IV.83) for accommodating beyond leading order effects [24].

FIG. 13: Debye screening mass m_s , plot taken from [23], for more details see there.



(a) Magnetic gluon dressing in $SU(2)$ from [23] in comparison with $SU(2)$ lattice results from [25, 26].



(b) Magnetic gluon dressing in $SU(2)$ from [23] in comparison with $SU(3)$ lattice results from [27].

FIG. 14: Magnetic gluon propagator dressing (IV.80).

for the correct T_c it is not important for the confining property. With the propagator (IV.84) we are led to

$$\begin{aligned}
 V_{\text{mode}}(\varphi, m) &= \frac{T}{4\pi^2} \sum_{\pm} \sum_{n=1}^{\infty} \frac{1}{n} (e^{\pm 2\pi i n \varphi} - 1) \int_0^{\infty} dp p^2 e^{-(\beta\sqrt{p^2+m^2})n} \\
 &= \frac{T^4}{4\pi^2} \sum_{\pm} \sum_{n=1}^{\infty} \frac{1}{n} (e^{\pm 2\pi i n \varphi} - 1) \int_0^{\infty} d\bar{p} \bar{p}^2 e^{-(\sqrt{\bar{p}^2+\beta^2 m^2})n}.
 \end{aligned} \tag{IV.85}$$

The momentum integration in (IV.86) cannot be performed analytically. However, in the zero temperature limit the terms in the sum decays with $e^{(-\beta m)n}$ up to polynomials. This is seen easily for the absolute value of the mode

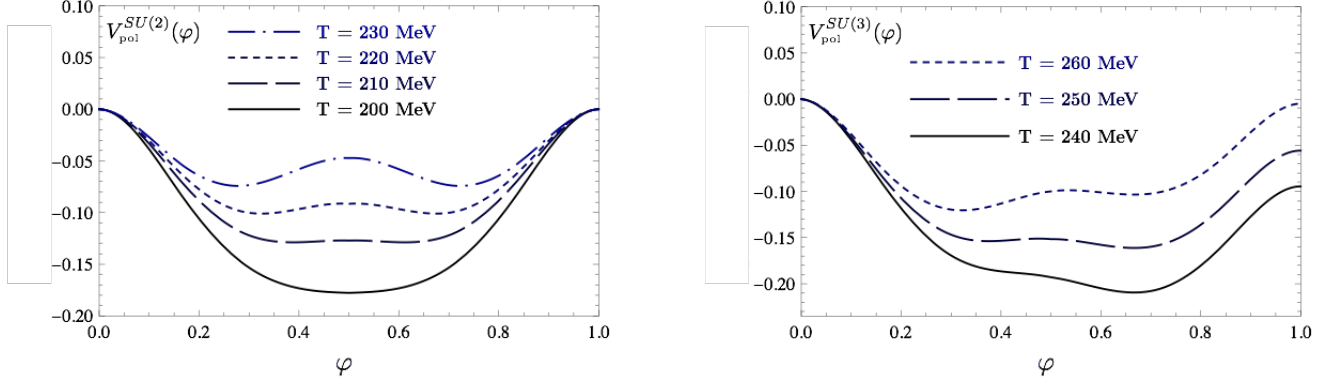
(a) $SU(2)$ Polyakov loop potential.(b) $SU(3)$ Polyakov loop potential

FIG. 15: $SU(2)$ and $SU(3)$ Polyakov loop potential taken from [29] for different temperatures across the phase transition. The potentials exhibits the second and first order of the $SU(2)$ and $SU(3)$ transitions respectively.

potential,

$$\begin{aligned}
 |V_{\text{mode}}(\varphi, m)| &\leq \frac{T^4}{4\pi^2} \sum_{n=1}^{\infty} \frac{1}{n} \int_0^{\infty} d\bar{p} \bar{p}^2 e^{-(\sqrt{\bar{p}^2 + \beta^2 m^2})n} \\
 &\leq \frac{T^4}{4\pi^2} \sum_{n=1}^{\infty} \frac{1}{n} \left[\int_0^{\beta m} d\bar{p} \bar{p}^2 e^{-(\beta m)n} + \int_0^{\beta m} d\bar{p} \bar{p}^2 e^{-\bar{p}n} \right] \\
 &\xrightarrow{\beta m \rightarrow \infty} T^4 \text{Pol}(\beta m) e^{-\beta m}, \tag{IV.86}
 \end{aligned}$$

with a polynomial $\text{Pol}(\beta m)$. In summary the mode potential decays exponentially for gapped propagators. This entails that for sufficiently small temperatures the contributions of the chromo-electro and the two chromo-magnetic modes decay exponentially. The longitudinal gauge mode stays trivial and gives the contribution $2V_{\text{mode}}(\varphi)$. Now we use that the ghost propagator keeps it $1/(-D^2)$ behaviour it already has perturbatively. In a covariant gauge this is already suggested from the ghost-gluon vertex which is linear in the anti-ghost momentum. Hence, all loop corrections to the inverse ghost propagator are proportional to p^2 from the onset. If no additional singularity is created from the propagators in the loops it stays this way. Since the gluon propagator is gapped this is only possible with a global non-trivial scaling.

Let us now study the case of a trivial ghost propagator and a gapped gluon propagator. In this case we conclude that

$$\begin{aligned}
 \lim_{T \rightarrow 0} V_{\text{Pol}}(A_0) &\simeq \frac{1}{2} \lim_{T \rightarrow 0} \text{Tr} \ln G_A^{-1}(A_0) - \lim_{T \rightarrow 0} \text{Tr} G_c^{-1}(A_0) \\
 &\simeq \frac{1}{2} \text{Tr} \ln (-D_\rho^2)(A_0) - \text{Tr} \ln (-D_\rho^2)(A_0) \tag{IV.87}
 \end{aligned}$$

$$= -\text{Tr} \ln (-D_\rho^2)(A_0) = \sum_i V_{\text{mode}}(\varphi_i). \tag{IV.88}$$

With the mode potential (IV.68), see Fig. 12 this gives confinement. The present qualitative study can be extended to a fully non-perturbative one with the help of functional methods, leading to the $SU(2)$ and $SU(3)$ potentials depicted in Fig. 15 taken from [29]. The respective Polyakov loop expectation values $L[\langle A_0 \rangle]$ are shown in Fig. 16.

The above considerations also hold in full Yang-Mills theory without approximations. This allows us to formulate a confinement criterion in Yang-Mills theory with (IV.55), (IV.73) and (IV.86):

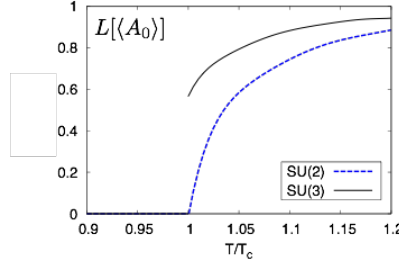


FIG. 16: Polyakov loop expectation values $L[\langle A_0 \rangle]$ for $SU(2)$ and $SU(3)$ taken from [28].

Confinement criterion: *'In covariant gauges the gluon propagator has to be gapped relative to the ghost at low temperatures'*

put forward in [28]. Note that we have been led to this criterion in the one-loop resummed approximation with (IV.55). However, it can be proven in Yang-Mills theory without approximations on the basis of the functional renormalisation group, [28, 29], as well as Dyson-Schwinger equations and the two-particle irreducible (2PI) formalism [29]. It also extends beyond the covariant gauges, e.g. to the Coulomb gauge. In QCD with dynamical QCD—as expected—the quark contributions spoil the applicability of the confinement criterion as they introduce center-breaking terms to the potential, for a detailed discussion see [29].

We close this chapter with some remarks on the order parameter we introduced. We started with the Polyakov loop variable $\langle L[A_0] \rangle$, but computed the Polyakov loop potential $V_{\text{pol}}[A_0]$ with the order parameter $\langle A_0 \rangle$ or $L[\langle A_0 \rangle]$. As both are order parameters for the same symmetry, this is not relevant for us. Still, one can investigate their relation: evidently they are not the same but only agree in a Gaussian approximation,

$$\langle L[A_0] \rangle \neq L[\langle A_0 \rangle], \quad (\text{IV.89})$$

Dropping for the moment the necessary renormalisation of $\langle A_0 \rangle$, they satisfy the Jensen inequality,

$$\langle L[A_0] \rangle \leq L[\langle A_0 \rangle], \quad (\text{IV.90})$$

see [28]. We conclude that if $L[\langle A_0 \rangle] = 0$, so is $\langle L[A_0] \rangle$. In turn, one can show that $L[\langle A_0 \rangle]$ vanishes if $\langle L[A_0] \rangle$ does, see [31]. While $L[\langle A_0 \rangle]$ has so far only been computed with functional methods, we have solid results for $\langle L[A_0] \rangle$ from the lattice, both in Yang-Mills theory and in QCD. More recently, $\langle L[A_0] \rangle$ has been also computed with the FRG on the basis of $L[\langle A_0 \rangle]$ in quantitative agreement with the lattice results [30], see Fig. 18. Seemingly, their relation is rather non-trivial but it has been shown in [30] that most of the difference between $\langle L[A_0] \rangle$ and $L[\langle A_0 \rangle]$ comes from

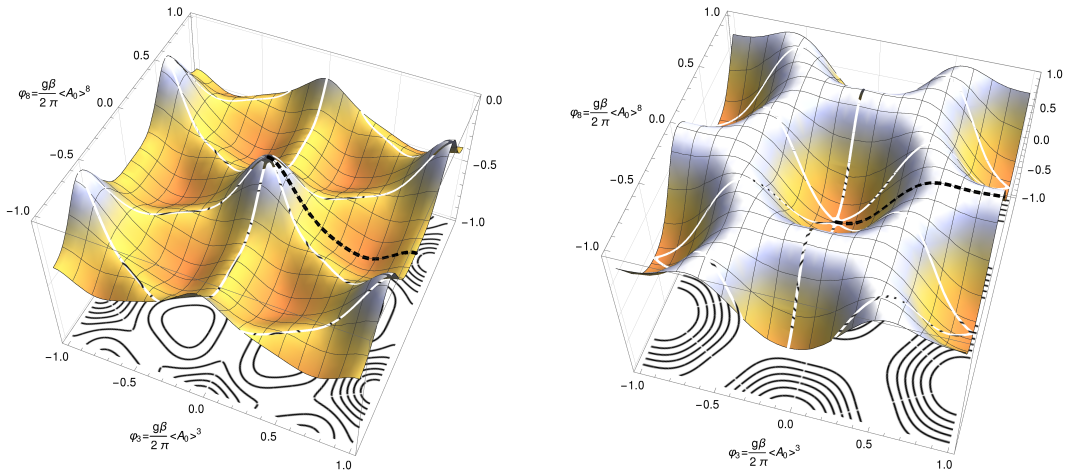


FIG. 17: The infrared glue potential, $V(\varphi_3, \varphi_8)$, is shown in the confined phase (left, $T = 236$ MeV) and in the deconfined phase (right, $T = 384$ MeV). We restrict ourselves to the line $\varphi_8 = 0$ and $\varphi_3 \geq 0$ (indicated by the black, dashed line), where one of the equivalent minima is always found, and where $L[\langle A_0 \rangle]$ is real and positive semi-definite.

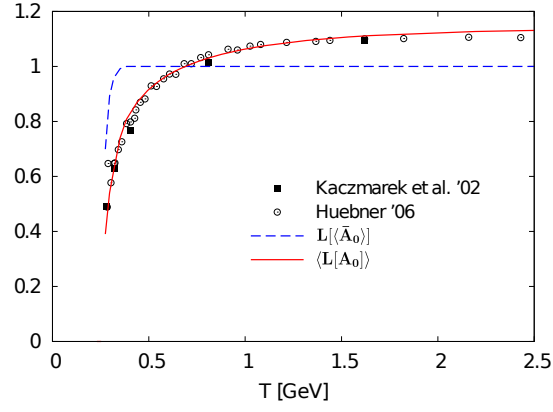


FIG. 18: Expectation value of $\langle L[A_0] \rangle$ versus $L[\langle \bar{A}_0 \rangle]$ from [30]. Both observables are order parameters for the confinement-deconfinement phase transition. Moreover, $L[\langle \bar{A}_0 \rangle] = 1$ entails $\langle \bar{A}_0 \rangle = 0$.

a temperature dependent normalisation of the former. In any case there is a relation

$$\langle L[A_0] \rangle(\varphi) \tag{IV.91}$$

that maps $\varphi = \beta g / (2\pi) \langle A_0 \rangle$ to the Polyakov loop expectation value in a given background.

V. PHASE STRUCTURE OF QCD

In this final chapter of the low energy part of the QCD lecture notes we discuss the phase structure of QCD at finite temperature and density. Here we shall study this in a combination of the low energy model for chiral symmetry breaking discussed in the chapters II and III and the confinement physics of the Polyakov loop potential discussed in the previous chapter IV. This class of low energy EFTs is called *Polyakov loop augmented/enhanced low energy EFTs*. They are based on the following observation that can be made already on a one-loop level (with resummed propagators). The full one loop resummed effective action of $N_f = 2$ flavour QCD including effective mesonic degrees of freedom is given by

$$\Gamma_{\text{QCD}}[\Phi] = S_{\text{QCD}}[\Phi] + \frac{1}{2} \text{Tr} \ln G_A^{-1}[\Phi] - \text{Tr} \ln G_c^{-1}[\Phi] - \text{Tr} \ln G_q^{-1}[\Phi] + \frac{1}{2} \text{Tr} \ln G_\phi^{-1}[\Phi], \quad \Phi = (A_\mu, c, \bar{c}, \psi, \bar{\psi}, \sigma, \vec{\pi}), \quad (\text{V.1})$$

with the gluon and ghost propagators G_A, G_c carrying the physics and fluctuations of the glue sector of QCD, and the quark and meson propagators carrying the physics and fluctuations of the matter sector of QCD. Note that (V.1) with the full propagators is a complicated non-perturbative equation where all different loops feed into each other. For example, taking the derivative of (V.1) w.r.t. the gauge field, we get

$$\frac{\delta \Gamma - S}{\delta A_0} = \frac{1}{2} \text{Tr} [\Gamma^{(3)} G]_{AA} - \text{Tr} G_c^{-1}[\Phi] [\Gamma^{(3)} G]_{c\bar{c}} - \text{Tr} [\Gamma^{(3)} G]_{q\bar{q}} + \frac{1}{2} \text{Tr} [\Gamma^{(3)} G]_{\phi^* \phi}, \quad (\text{V.2})$$

where the mesonic part has been dropped and G is the full matrix propagator of all modes. This has to be compared with the A_0 -DSE

$$\frac{\delta \Gamma}{\delta A_0} = \left\langle \frac{\delta S}{\delta A_0} \right\rangle, \quad (\text{V.3})$$

the QCD-version of (II.15). It is derived analogously from the path integral representation of the QCD effective action Γ , see (C.1), by taking an A_0 -derivative. It is depicted in Fig. 19. The vertices in the DSE (V.3) are the classical ones while in (V.2) they are the full quantum vertices. The other difference is the two-loop term in Fig. 19 that is not present in (V.2) but can be understood as part of the dressed vertices, see e.g. [29]. In any case, the two-loop term in the DSE is typically dropped in explicit computations for technical reasons, and modern applications often use 2PI and 3PI (three-particle irreducible) approximations that feature dressed vertices.

Note also that the Wegner-Houghton RG, or more generally functional renormalisation group equations for QCD, are one loop exact, see chapter IIF 3. Hence, they are given by a sum of gluon, ghost, quark and optionally meson diagrams, see Fig. 20. Note that the equation in Fig. 20 is exact, no two-loop or higher loop terms are missing.

1. Glue Sector

We conclude that (V.1) provides a good qualitative approximation to full QCD, and the following formal arguments also go through beyond the current approximation: we are interested in the low energy limit of QCD, in which the gapped gluons do not drive the matter dynamics anymore. Since the ghost terms only couple to matter through the gluons, they also decouple even though they are massless. Hence, in a first qualitative approximation we can drop the dynamics of the glue sector. Still, the gluons, i.e. $\langle A_0 \rangle$ serve as a background for the matter fluctuations. Its value is determined by the Polyakov loop potential in QCD, obtained by evaluating (V.1) for constant A_0 -background. The

$$\frac{\delta(\Gamma - S)}{\delta A_0} = \frac{1}{2} \text{Tr} \left[\text{Diagram 1} - \text{Diagram 2} - \text{Diagram 3} - \frac{1}{6} \text{Diagram 4} \right]$$

FIG. 19: Functional A_0 -Dyson-Schwinger equation for QCD.

glue part of the potential,

$$V_{\text{glue}}(A_0) = \frac{1}{2} \text{Tr} \ln G_A^{-1}[A_0] - \text{Tr} \ln G_c^{-1}[A_0], \quad (\text{V.4})$$

The definition of V_{glue} is identical to that in pure Yang-Mills theory, (IV.55). In (V.4), however, the QCD gluon and ghost propagator enter. A common procedure is now to use lattice results on the pressure and the Polyakov loop expectation value in pure Yang-Mills theory for an estimate of V_{glue} . From the perspective of the correlation functions approaches discussed here this is justified if the Yang-Mills gluon and ghost propagators in an A_0 -background are similar to those in QCD. This is indeed the case, the biggest difference coming from the RG-scaling that is reflected in the momentum-dependence at large and medium momenta $p^2 \gtrsim 2-5 \text{ GeV}^2$. This can be made even more quantitative if simply comparing the two glue potentials (in terms of A_0) in QCD and Yang-Mills theory, see [32]. Apart from the different absolute temperature scale and the different RG-running the two potentials agree semi-quantitatively.

These results support in retrospect the low energy EFT approach with lattice-induced Polyakov loop potentials $V(L, \bar{L})$. On the lattice the Polyakov loop variables

$$L = \langle L[A_0] \rangle, \quad \bar{L} = \langle L^*[A_0] \rangle, \quad (\text{V.5})$$

are computed. At vanishing density we have $\bar{L} = L^*$. At non-vanishing density this relation is not valid anymore as the chemical potential leads to a complex action in the path integral, and hence $\langle L[A_0] \rangle^* \neq \langle L[A_0] \rangle$. The respective potential is $U_{\text{pol}}(L, \bar{L})$. We emphasise that the potential $V_{\text{pol}}(\varphi)$ is not simply $U(L(\varphi), \bar{L}(\varphi))$ due to (IV.89).

These potentials are derived as follows:

- (1a) Compute the Yang-Mills pressure (zero-point function) and the Polyakov loop expectation value (one-point function)

$$p_A(T) =, \quad L = \langle L[A_0] \rangle(T), \quad \bar{L} = \langle L[A_0] \rangle(T). \quad (\text{V.6})$$

- (1b) Further correlation functions of the Polyakov loop variable are computed. At present this approach only extends to the two-point functions of the Polyakov loop, [33]. The two-point function of the Polyakov loop is nothing but its propagator at large distances, which is given by the inverse of the second derivative of the Polyakov loop potential. We write schematically

$$\begin{pmatrix} \langle LL \rangle & \langle L\bar{L} \rangle \\ \langle \bar{L}L \rangle & \langle \bar{L}\bar{L} \rangle \end{pmatrix} \propto \begin{pmatrix} \partial_L^2 U_{\text{pol}} & \partial_L \partial_{\bar{L}} U_{\text{pol}} \\ \partial_{\bar{L}} \partial_L U_{\text{pol}} & \partial_{\bar{L}}^2 U_{\text{pol}} \end{pmatrix}^{-1}. \quad (\text{V.7})$$

- (2) Construct a potential $V_{\text{YM}}(L, \bar{L})$ that leads to all the observables under (1a) and potentially (1b). We have

$$p_A = -V(L_{\text{EoM}}, \bar{L}_{\text{EoM}}), \quad \left. \frac{\partial U(L, \bar{L})}{\partial L} \right|_{\substack{L = L_{\text{EoM}} \\ \bar{L} = \bar{L}_{\text{EoM}}}} = 0, \quad \left. \frac{\partial U(L, \bar{L})}{\partial \bar{L}} \right|_{\substack{L = L_{\text{EoM}} \\ \bar{L} = \bar{L}_{\text{EoM}}}} = 0, \quad (\text{V.8})$$

and (V.7), evaluated on the equations of motion.

Here we quote the standard form of the Polyakov loop potential. It reads

$$U(L, \bar{L}) = \frac{1}{2} a(T) \bar{L} L + b(T) \ln M_H(L, \bar{L}) + \frac{1}{2} c(T) (L^3 + \bar{L}^3) + d(T) (\bar{L} L)^2, \quad (\text{V.9})$$

$$\Lambda \partial_\Lambda \Gamma_{\text{QCD}} = \frac{1}{2} \left[\text{Diagram 1} - \text{Diagram 2} - \text{Diagram 3} + \frac{1}{2} \text{Diagram 4} \right]$$

FIG. 20: Functional renormalisation group equation for QCD. In the Wegner-Houghton case the cross stands for the restriction of the loop integration to $p^2 = \Lambda^2$.

where M_H comes from the Haar measure of the gauge group

$$M_H = 1 - 6\bar{L}L + 4(L^3 + \bar{L}^3) - 3(\bar{L}L)^2. \quad (\text{V.10})$$

Eq.(V.9) is a variation of a Landau-Ginsburg-type ϕ^4 -potential commonly used for describing phase transitions. The cubic terms proportional to $c(T)$ and in M_H carry the center symmetry $L \rightarrow zL$ where the cubic roots $z \in Z_3$ has the property $z^3 = 1$. These terms drives the phase transition. The parameters $a(T), b(T), c(T)$ are now adjusted to the temperature-dependent observables in (1). Examples can be found e.g. in [33–35]. The latter work also contains a detailed study of various model potentials. We close this discussion with a few remarks. Firstly, as it is not possible to compute the glue potential in QCD on the lattice, we have to rely on Yang-Mills potentials on the lattice extrapolated to the glue potential. Secondly, the direct computation of the Polyakov loop potential in Yang-Mills theory proves to be very costly and has not fully been resolved yet. For that reason one has to rely on potentials that only match a few but important observables. Thirdly, the Polyakov loop potential U_{pol} is not the natural input in the low energy EFTs, it is V_{pol} and the two only agree in the Gaussian approximations.

Alternatively one computes the glue potential directly in the continuum, but at present neither U_{pol} nor V_{pol} has been computed to a quantitative satisfactory precision. This task is left for future work.

2. Matter sector

It is left to discuss the matter sector. In (V.1) it looks identical to the low energy EFT or the DSE/FRG in QCD we have discussed in the context of strong chiral symmetry breaking. However, now we have to consider also the glue background A_0 or L, \bar{L} depending on the treatment of the glue sector. Since the mesons are color-neutral, they do not couple to the gluon and hence the meson loop stays the same as before.

However, the quark loop has to be taken in an A_0 background. We recall the one-loop expression in (III.28), now in the presence of an A_0 background as well as a chemical potential μ . It reads

$$\begin{aligned} \Omega_{q,T} - \Omega_{q,T,\mu=0} &= -4T \sum_{n \in \mathbb{Z}} \int \frac{d^3p}{(2\pi)^3} \text{tr}_f \ln \frac{(2\pi T)^2 (n + \frac{1}{2} + \hat{\varphi} + i\mu)^2 + \vec{p}^2 + m_q^2}{(2\pi T)^2 (n + \frac{1}{2})^2 + \vec{p}^2 + m_q^2} - p_{q,\text{thermal}} \\ &= -\frac{2}{\pi^2} T \sum_{n \in \mathbb{Z}} \int_0^\infty dp p^2 \text{tr}_f \left\{ \ln \left(1 + P e^{-\beta(\epsilon_p^q - \mu)} \right) + \ln \left(1 + P^\dagger e^{-\beta(\epsilon_p^q + \mu)} \right) \right\}, \end{aligned} \quad (\text{V.11})$$

where $P(\vec{x}) = P(\beta, \vec{x})$ is the untraced Polyakov loop, see (IV.28), and we recall the quark dispersion and the thermal distribution function from (III.27)

$$\epsilon_p^q = \sqrt{\vec{p}^2 + m_q^2}, \quad n_F(\omega) = \frac{1}{e^{\beta\omega} + 1}. \quad (\text{V.12})$$

In the present approximation P, P^\dagger are \vec{x} -independent. The combinations $P e^{\beta\mu}$ and $P e^{-\beta\mu}$ reflect the relation of L and \bar{L} to the creation operator of quark and anti-quark states respectively. The final expression in (V.11) reduces to the quark contribution of the grand potential (III.38) discussed in chapter III for $P = \mathbb{1}$. Due to the subtraction of the $T = 0$ grand potential hidden in $p_{q,\text{thermal}}$ is nothing but the negative thermal pressure in a given background. On the EoM for all fields it is the physical quark pressure of the system. The color trace in (V.11) can be rewritten as a determinant with $\text{tr}_f \ln \mathcal{O} = \ln \det_f \mathcal{O}$, and we are led to

$$\begin{aligned} \Omega_{q,T} - \Omega_{q,T,\mu=0} &= -\frac{2}{\pi^2} T \int_0^\infty dp p^2 \left\{ \ln \left[1 + 3(L + \bar{L} e^{-\beta(\epsilon_p^q - \mu)}) e^{-\beta(\epsilon_p^q - \mu)} + e^{-3\beta(\epsilon_p^q - \mu)} \right] \right. \\ &\quad \left. + \ln \left[1 + 3(\bar{L} + L e^{-\beta(\epsilon_p^q + \mu)}) e^{-\beta(\epsilon_p^q + \mu)} + e^{-3\beta(\epsilon_p^q + \mu)} \right] \right\}. \end{aligned} \quad (\text{V.13})$$

For $L = \bar{L} = 1$ and $\mu = 0$ (V.13) reduces to the one in (III.38) in chapter III. This happens for large temperatures, $T/T_{\text{conf}} \rightarrow \infty$ deep in the perturbative regime. Then we simply see the thermal distribution of single quarks. Note

that (V.13) only vanishes for $T \rightarrow 0$ if $\epsilon_p > |\mu|$ for all p . For $\mu^2 > m_q^2$ we have

$$\lim_{T \rightarrow 0} (\Omega_{q,T} - \Omega_{q,T,\mu=0}) = -\frac{6}{\pi^2} \int_0^{\sqrt{\mu^2 - m_q^2}} dp p^2 (|\mu| - \epsilon_p^q), \quad (\text{V.14})$$

reflecting the fact that for $\mu^2 > m_q^2$ the level of the Fermi sea is rising accordingly and the part of the quark fluctuations below disappear from the fluctuation spectrum. As we have subtracted the grand potential at $T = 0$ and $\mu = 0$, this term is left in the $T \rightarrow 0$ limit.

For $T/T_{\text{conf}} \rightarrow 0$ the Polyakov loop expectation value tends towards one, $L = \bar{L} = 0$. Interestingly, for these values we have

$$\Omega_{q,T} - \Omega_{q,T,\mu=0} = -\frac{2}{\pi^2} T \int_0^\infty dp p^2 \left\{ \ln \left[1 + e^{-3\beta(\epsilon_p^q - \mu)} \right] + \ln \left[1 + e^{-3\beta(\epsilon_p^q + \mu)} \right] \right\}, \quad (\text{V.15})$$

the grand potential (or negative thermal pressure) of a gas of three-quark states, in our case the nucleons. This observation has been called *statistical confinement* as the confining value of the background Polyakov loop gives the thermal distribution of nucleons. If this property is investigated more carefully, the related distribution functions are given by

$$n_F(x, L, \bar{L}) = \frac{1 + 2\bar{L}e^{\beta x} + Le^{2\beta x}}{1 + 3\bar{L}e^{2\beta x} + 3Le^{2\beta x} + e^{3\beta x}}, \quad x = \sqrt{p^2 + m_q^2} - \mu, \quad \bar{x} = \sqrt{p^2 + m_q^2} + \mu, \quad (\text{V.16})$$

for the quark and $n_F(\bar{x}, \bar{L}, L)$ for the anti-quark. As for the grand potential, the Polyakov-loop enhanced thermal distribution functions tend towards the quark and anti-quark distribution functions for $L, \bar{L} \rightarrow 1$. For $L, \bar{L} \rightarrow 0$ (V.16) gives the nucleon distribution function. However, this only happens if

$$\lim_{T/T_{\text{conf}} \rightarrow 0} Le^{2\beta x} \rightarrow 0. \quad (\text{V.17})$$

It can be shown that the limit (V.17) is not present in QCD, see [36]. This does not invalidate the above picture as the failure of (V.17) originates in mesonic contributions that indeed should be present. Moreover, the grand potential is that of nucleons.

This concludes our derivation of the low energy EFT that governs the phase structure of QCD. This specific type of low energy EFT has been constructed in [34]. On the one loop level its grand potential in $N_f = 2$ flavor QCD is given by the sum of the quark contribution (V.13), the mesonic contribution and the Polyakov loop potential. This combination gives access to the two basic phenomena that governs the phase structure, confinement and chiral symmetry breaking.

A. RG for the phase structure*

Here we simply repeat the steps for the derivation of the Wegner-Houghton equation done in chapter III C for finite temperature at finite temperature and density. The mesonic part is the same as in (III.40) and we can just take it over here. The thermal quark part at finite density can be read off from (V.15) while the vacuum part (at $\mu = 0$) of the integral is the same as before. In summary we get

$$\begin{aligned} \Lambda \partial_\Lambda \Omega_\Lambda(\psi, \bar{\psi}, \phi) = & -\frac{\Lambda^3}{2\pi^2} \left\{ \frac{1}{2} \left[\epsilon_\Lambda^\phi(m_\sigma) + \frac{3}{2} \epsilon_\Lambda^\phi(m_\pi) \right] - 12 \epsilon_\Lambda^q \right. \\ & + T \left[\ln \left(1 - e^{-\beta \epsilon_\Lambda^\phi(m_\sigma)} \right) + \ln \left(1 - e^{-\beta \epsilon_\Lambda^\phi(m_\pi)} \right) \right] \\ & - 4T \left\{ \ln \left[1 + 3(L + \bar{L}e^{-\beta(\epsilon_\Lambda^q - \mu)}) e^{-\beta(\epsilon_\Lambda^q - \mu)} + e^{-3\beta(\epsilon_\Lambda^q - \mu)} \right] \right. \\ & \left. \left. + \ln \left[1 + 3(\bar{L} + Le^{-\beta(\epsilon_\Lambda^q + \mu)}) e^{-\beta(\epsilon_\Lambda^q + \mu)} + e^{-3\beta(\epsilon_\Lambda^q + \mu)} \right] \right\} \right\}. \quad (\text{V.18}) \end{aligned}$$

In (V.18) the first line is the $T, \mu = 0$ part of the flow, the second line comprises the thermal part of the meson fluctuations, while the last two lines comprise the thermal and density fluctuations of the quarks. As has been

discussed above, this term does not vanish in the limit $T \rightarrow 0$ but removes the infrared part of the vacuum fluctuations of the quark above the onset chemical potential $\mu^2 = m_q^2$, see (V.14).

Appendix A: Feynman rules for QCD in the covariant gauge

In this Appendix we depict the Feynman rules for QCD in the general covariant gauge.

$$\begin{array}{c} a \\ \text{-----} \\ p_\mu \end{array} \begin{array}{c} b \\ \text{-----} \\ k_\nu \end{array} = \delta^{ab} \delta^{(4)}(p+k) \left(\delta_{\mu\nu} - (1-\xi) \frac{p_\mu p_\nu}{p^2} \right) \frac{1}{p^2}$$

$$\begin{array}{c} a \\ \text{-----} \\ p \end{array} \begin{array}{c} b \\ \text{-----} \\ k \end{array} = -\delta^{ab} \delta^{(4)}(p+k) \frac{1}{p^2}$$

$$\begin{array}{c} \text{-----} \\ p \end{array} \begin{array}{c} \text{-----} \\ k \end{array} = \delta^{(4)}(p+k) \frac{1}{i \not{p} + m}$$

$$\begin{array}{c} a \\ \text{-----} \\ k_{1,\mu} \\ \downarrow \\ \text{-----} \\ c \end{array} \begin{array}{c} k_{3,\rho} \\ \nearrow \\ \text{-----} \\ b \end{array} \begin{array}{c} k_{2,\nu} \\ \searrow \\ \text{-----} \\ b \end{array} = i g f^{abc} (2\pi)^4 \delta^{(4)}(k_1 + k_2 + k_3) \left[(k_2 - k_1)_\rho \delta_{\mu\nu} + (k_1 - k_3)_\nu \delta_{\mu\rho} + (k_3 - k_2)_\mu \delta_{\nu\rho} \right]$$

$$\begin{array}{c} a \\ \text{-----} \\ k_{1,\mu} \\ \searrow \\ \text{-----} \\ d \end{array} \begin{array}{c} k_{4,\sigma} \\ \nearrow \\ \text{-----} \\ c \end{array} \begin{array}{c} b \\ \text{-----} \\ k_{2,\nu} \\ \nearrow \\ \text{-----} \\ c \end{array} \begin{array}{c} k_{3,\rho} \\ \searrow \\ \text{-----} \\ c \end{array} = g^2 (2\pi)^4 \delta^{(4)} \left(\sum_{i=1}^4 k_i \right) \left[f^{iab} f^{icd} (\delta_{\mu\rho} \delta_{\nu\sigma} - \delta_{\mu\sigma} \delta_{\nu\rho}) + f^{iac} f^{ibd} (\delta_{\mu\nu} \delta_{\rho\sigma} - \delta_{\mu\sigma} \delta_{\nu\rho}) + f^{iad} f^{ibc} (\delta_{\mu\nu} \delta_{\rho\sigma} - \delta_{\mu\rho} \delta_{\nu\sigma}) \right]$$

$$\begin{array}{c} a \\ \text{-----} \\ k_\mu \\ \downarrow \\ \text{-----} \\ b \end{array} \begin{array}{c} q \\ \nearrow \\ \text{-----} \\ c \end{array} \begin{array}{c} p \\ \searrow \\ \text{-----} \\ c \end{array} = -i g f^{abc} p_\mu (2\pi)^4 \delta^{(4)}(p - q - k)$$

$$\begin{array}{c} a \\ \text{-----} \\ k_\mu \\ \downarrow \\ \text{-----} \\ q \end{array} \begin{array}{c} p \\ \searrow \\ \text{-----} \\ p \end{array} = -i g \gamma_\mu T^a (2\pi)^4 \delta^{(4)}(p - q - k)$$

FIG. 21: Feynman rules.

Appendix B: Gribov copies

In Chapter IA we have derived the gauge-fixed path integral under the assumption that there is only one representative of the gauge orbit that satisfies the gauge fixing condition. However, there might be several (Gribov) copies, i.e. several physically equivalent solutions to the gauge fixing condition that are related by gauge transformations not yet fixed by the gauge fixing condition $\mathcal{F} = 0$. Indeed, any sufficiently smooth gauge exhibits (infinite many) Gribov copies, $\sum_{\text{Gribov copies}} = \#_{\text{Gr}}$. As for the integration over the gauge group, $\#_{\text{Gr}}$ occurs in the numerator as well as the denominator in (I.18) and hence cancels. It is left to compute the Jacobian $J[A] = \Delta_{\mathcal{F}}[A]$. To that end we use the

representation of the Dirac δ -function

$$\delta[\mathcal{F}[A^{\mathcal{U}}]] = \sum_{i=1}^{\#\text{Gr}} \frac{1}{|\det \frac{\delta \mathcal{F}}{\delta \omega}|} \delta[\omega - \omega_i] \quad \text{with} \quad \mathcal{U} = e^{i\omega}. \quad (\text{B.1})$$

which leads to

$$\Delta_{\mathcal{F}}[A] = \left(\sum_{i=1}^{\#\text{Gr}} \frac{1}{|\det \mathcal{M}_{\mathcal{F}}[A^{e^{i\omega_i}}]|} \right)^{-1} \quad \text{with} \quad \mathcal{M}_{\mathcal{F}}[A] = \left. \frac{\delta \mathcal{F}}{\delta \omega} \right|_{\omega=0} [A^{e^{i\omega}}]. \quad (\text{B.2})$$

In the QFTII lecture notes in chapter IV, Appendix A the occurrence of the Gribov copies in gauge field reparameterisations due to gauge fixing is elucidated at the simple example of the reparameterisation of a two-dimensional integral.

Appendix C: Some important fact of the background field approach

In the background field approach the effective action has the following integro-differential path integral representation which facilitates the access to important properties,

$$e^{-\Gamma[\bar{A}, a]} = \int D\hat{a} \Delta_{\mathcal{F}}[\bar{A}, \hat{a} + a] \delta[\bar{D}_{\mu}(\hat{a}_{\mu} + a)] e^{-S_{\text{YM}}[A + \hat{a}] + \int_x \frac{\delta \Gamma[\bar{A}, a]}{\delta a_{\mu}} \hat{a}_{\mu}}, \quad J = \frac{\delta \Gamma[\bar{A}, a]}{\delta a} \quad a = \langle \hat{a} \rangle. \quad (\text{C.1})$$

where $\hat{A} = \bar{A} + \hat{a}$, $\bar{D} = D(\bar{A})$, $D = D(A)$ and we restricted ourselves to *Landau-deWitt gauge* ($\xi = 0$) with the background gauge fixing condition

$$\bar{D}_{\mu} \hat{a}_{\mu} = 0, \quad \longrightarrow \quad \mathcal{M}[\bar{A}, \hat{a} + a] = -\bar{D}_{\mu} D_{\mu}, \quad \Delta_{\mathcal{F}}[\bar{A}, \hat{a} + a] = \det \mathcal{M}[\bar{A}, \hat{a} + a]. \quad (\text{C.2})$$

see (IV.48). Inserting the relation between the a -derivative of Γ and the current J in (C.1) as well as using $\Gamma = \int_x J_{\mu} a_{\mu} - \log Z$ we arrive at the standard path integral expression for $Z[J]$ in the gauge (C.2). First we note that the effective action, evaluated on the equation of motion for the fluctuation field a ,

$$\left. \frac{\delta \Gamma[\bar{A}, a]}{\delta a_{\mu}} \right|_{a=a_{\text{EoM}}} = 0 \quad (\text{C.3})$$

does not depend on the background field: the effective action $\Gamma[\bar{A}, a_{\text{EoM}}]$ is given by (C.1) without the source term. Then the path integral in (C.1) reduces to

$$e^{-\Gamma[\bar{A}, a_{\text{EoM}}]} = \int D\hat{a}_{\text{gf}} e^{-S_{\text{YM}}[A + \hat{a}_{\text{gf}}]}. \quad (\text{C.4})$$

Even though the measure depends on the background field via the gauge fixing, the intergration leads to \bar{A} -independent result as the action S_{YM} is gauge invariant. Accordingly we have

$$\frac{\delta \Gamma[\bar{A}, a_{\text{EoM}}]}{\delta \bar{A}} = \left. \frac{\delta}{\delta \bar{A}} \right|_{a_{\text{EoM}}} \Gamma[\bar{A}, a_{\text{EoM}}] = 0. \quad (\text{C.5})$$

The first relation in (C.5) follows with (C.3), the second from the \bar{A} -independence of the integration in (C.4). In conclusion, a solution to the EoM of a also is one of \bar{A} . Eq.(C.4) also entails that

$$\Gamma[\bar{A}, a_{\text{EoM}}(\bar{A})] = \Gamma[\bar{A} + a_{\text{EoM}}(\bar{A})], \quad (\text{C.6})$$

it only depends on the full gauge field A .

[1] W. Tung, *Group Theory in Physics* (World Scientific, 1985).

- [2] L. Faddeev and V. Popov, Phys.Lett. **B25**, 29 (1967).
- [3] S. Bethke, Progress in Particle and Nuclear Physics **58**, 351 (2007), arXiv:hep-ex/0606035.
- [4] J. C. Collins, (1984).
- [5] R. Alkofer and L. von Smekal, Phys. Rept. **353**, 281 (2001), hep-ph/0007355.
- [6] M. Buballa, Phys.Rept. **407**, 205 (2005), hep-ph/0402234.
- [7] J. Braun, (2011), 1108.4449.
- [8] A. K. Cyrol, M. Mitter, J. M. Pawłowski, and N. Strodthoff, (2017), 1706.06326.
- [9] S. Klevansky, Rev.Mod.Phys. **64**, 649 (1992).
- [10] F. J. Wegner and A. Houghton, Phys. Rev. **A8**, 401 (1973).
- [11] K. Symanzik, Commun. Math. Phys. **18**, 227 (1970).
- [12] C. G. Callan, Phys. Rev. D **2**, 1541 (1970).
- [13] K. G. Wilson, Phys.Rev. **B4**, 3184 (1971).
- [14] K. G. Wilson, Phys.Rev. **B4**, 3174 (1971).
- [15] L. P. Kadanoff, Physics **2**, 263 (1966).
- [16] E. C. G. Stueckelberg and A. Petermann, Helv. Phys. Acta **26**, 499 (1953).
- [17] M. Gell-Mann and F. E. Low, Phys. Rev. **95**, 1300 (1954).
- [18] Particle Data Group, C. Patrignani *et al.*, Chin. Phys. **C40**, 100001 (2016).
- [19] J. R. Pelaez, Phys. Rept. **658**, 1 (2016), 1510.00653.
- [20] L. Fister and J. M. Pawłowski, Phys. Rev. **D92**, 076009 (2015), 1504.05166.
- [21] D. J. Gross, R. D. Pisarski, and L. G. Yaffe, Rev.Mod.Phys. **53**, 43 (1981).
- [22] N. Weiss, Phys.Rev. **D24**, 475 (1981).
- [23] A. K. Cyrol, M. Mitter, J. M. Pawłowski, and N. Strodthoff, (2017), 1708.03482.
- [24] P. B. Arnold and L. G. Yaffe, Phys. Rev. **D52**, 7208 (1995), hep-ph/9508280.
- [25] A. Maas, J. M. Pawłowski, L. von Smekal, and D. Spielmann, Phys.Rev. **D85**, 034037 (2012), 1110.6340.
- [26] A. Maas, private communication.
- [27] P. J. Silva, O. Oliveira, P. Bicudo, and N. Cardoso, Phys. Rev. **D89**, 074503 (2014), 1310.5629.
- [28] J. Braun, H. Gies, and J. M. Pawłowski, Phys.Lett. **B684**, 262 (2010), 0708.2413.
- [29] L. Fister and J. M. Pawłowski, (2013), 1302.1373.
- [30] T. K. Herbst, J. Luecker, and J. M. Pawłowski, (2015), 1510.03830.
- [31] F. Marhauser and J. M. Pawłowski, (2008), 0812.1144.
- [32] L. M. Haas, R. Stiele, J. Braun, J. M. Pawłowski, and J. Schaffner-Bielich, (2013), 1302.1993.
- [33] P. M. Lo, B. Friman, O. Kaczmarek, K. Redlich, and C. Sasaki, Phys. Rev. **D88**, 074502 (2013), 1307.5958.
- [34] B.-J. Schaefer, J. M. Pawłowski, and J. Wambach, Phys.Rev. **D76**, 074023 (2007), 0704.3234.
- [35] B.-J. Schaefer, M. Wagner, and J. Wambach, Phys.Rev. **D81**, 074013 (2010), 0910.5628.
- [36] W.-j. Fu and J. M. Pawłowski, Phys. Rev. **D92**, 116006 (2015), 1508.06504.